LABORATOIRE DE PHYSIQUE THEORIQUE
UNITE MIXTE DE RECHERCHE n° 7085
UNIVERSITE LOUIS PASTEUR
CENTRE NATIONAL DE LA RECHERCHE SCIENTIFIQUE
Institut de Physique - 3 rue de l'Université- 67084 Strasbourg Cedex
Tél : 03 90 24 07 38 / Fax : 03 90 24 06 54

Dimensional reduction of Hilbert space and renormalization. Application to quantum spin ladders

Thèse

pour l'obtention du grade de DOCTEUR DE L'UNIVERSITÉ LOUIS PASTEUR STRASBOURG I

Discipline : Physique Théorique

Présentée par

Tarek KHALIL

Le 23 Mars 2007 à Strasbourg

Directeur de thèse

Jean RICHERT, Directeur de Recherche *CNRS*

Jury

Rapporteur interne	:	Janos POLONYI, Professeur
Rapporteur externe	:	Claire LHUILLIER, Professeur
Rapporteur externe	:	Didier POILBLANC, Directeur de Recherche *CNRS*
Examinateur	:	Jean-Yves FORTIN, Chargé de Recherche *CNRS*
Examinateur	:	Andreas HONECKER, Docteur Habilité

Abstract

We propose a specific non-perturbative algorithm to study the energies of low-lying bound states of quantum strongly interacting systems at zero temperature in a reduced Hilbert space. We use a projection technique which allows to generate effective Hamiltonians in reduced Hilbert spaces by the renormalization of the coupling strengths which enter the Hamiltonian, e.g. the coupling parameters. We test the procedure by working out and analyzing the spectral properties of antiferromagnetic two-leg frustrated spin ladder systems for which perturbation approaches break down. The role and importance of symmetries are investigated. We also develop an approach which identifies exceptional points in the energy spectrum of systems which exhibit quantum phase transitions. These transitions are related to fixed points in Hilbert space in the framework of the renormalization theory mentioned above. We test this approach at first order transitions and avoided crossing points.

Résumé

On propose un algorithme non perturbatif pour étudier les états de basse énergie des spectres de systèmes quantiques fortement corrélés à température nulle dans un espace de Hilbert réduit. On utilise une technique de projection qui permet de générer des Hamiltoniens effectifs dans des espaces de Hilbert réduits en renormalisant les constantes de couplage qui caractérisent l'Hamiltonien. On teste la procédure en calculant et analysant les propriétés spectrales des systèmes antiferromagnétiques, échelles de spins à deux montants dans lesquels une approche de perturbation n'est pas valide. Le rôle et l'importance des symétries sont étudiés. On développe une approche qui identifie les points exceptionnels dans le spectre d'énergie des systèmes qui présentent des transitions de phase quantiques. Ces transitions sont liées aux points fixes dans l'espace de Hilbert dans le cadre de la théorie de renormalisation. On examine cette approche dans le cadre de l'étude des transitions du premier ordre et des croisements évités.

to my parents Khalil, Alia

and my brother Hicham . . .

Acknowledgements

First and foremost I would like to thank and express my gratitude to my supervisor Jean Richert for having been so considerate and motivating in all aspects of my research during these three years. I am greatly honored to have had the opportunity to work with him.

I am grateful to the members of my Ph.D. jury : Prof. Janos Polonyi, Prof. Didier Poilblanc, Prof. Claire Lhuillier, Dr. Andreas Honecker and Dr. Jean Yves Fortin for finding time to participate to the jury and also for helping me to improve the manuscript.

I would like to thank all people with whom I had discussions about physics subjects, especially Teimuraz Vekua, Raoul Dillenschneider, Franck Stauffer and Raoul Santachiara.

Last but not the least I owe a lot to my parents Khalil and Alia for their education, guidance and support.

Finally, I dedicate this modest work to the memory of the martyrs who lost their life during the last war in Lebanon, in August 2006.

Résumé

Introduction

L'étude des systèmes microscopiques et mésoscopiques quantiques est confrontée aux difficultés liées au grand nombre de degrés de liberté mis en jeu et à la nature des interactions qui agissent entre leurs composants. Ces interactions de courte ou de longue portée sont souvent fortes et mettent en question la validité des méthodes de traitement approchées telle que les développements perturbatifs.

La description de ces systèmes exige une modélisation adéquate et l'introduction de concepts physiques théoriques adaptés qui décrivent de manière réaliste les interactions entre les constituants et permettent de réaliser des calculs effectifs. Il en est ainsi du concept de quasi-particule introduit par Landau [49, 75]. Cette approche est physiquement justifiée si l'interaction entre les quasi-particules est faible et permet par conséquent un traitement perturbatif de cette interaction. Dans le même esprit le concept de champ moyen et d'interaction résiduelle traitée perturbativement a un sens dans la description de systèmes tels que les atomes et les molécules [5, 10, 40].

Ces approches ne sont cependant pas utilisables si la dynamique des systèmes est de nature collective, autrement ne peut se concevoir comme une dynamique d'objets individuels faiblement en interaction les uns avec les autres. Ceci est le cas pour beaucoup de systèmes microscopiques, des sytèmes dont les parties sont en interaction forte et pour lesquelles la notion de champ moyen n'a pas de sens. Il en est ainsi de beaucoup de systèmes tels que les noyaux d'atomes et de nombreux matériaux magnétiques ce qui exige d'autres

méthodes d'approche pour leur description.

En général il n'y a pas de méthodes analytiques qui traitent exactement des systèmes fortement correlés mis à part l'introduction de fonctions d'ondes d'essai capables de diagonaliser l'hamiltonien des systèmes intégrables comme le Bethe Ansatz (BA) pour des systèmes spécifiques unidimensionnels ($1D$) [9], l'hypothèse BCS qui explique la supraconductivité [81] et autres comme les états de Néel, l'état liquide de spins " **R**esonant **V**alence **B**ond" (**RVB**) proposé par Anderson [1], l'état " **V**alence **B**ond **C**rystal" (**VBC**)... Ces états ont pour but de décrire des systèmes $2D$ mais il reste le problème de leurs degrés de réalisme, c'est à dire leur capacité d'inclure les effets essentiels de l'interaction dans des systèmes fortement corrélés [52]. La complexité de la structure de tels systèmes conduisent à la diagonalisation numérique de l'hamiltonien qui doit être réaliser dans un espace de Hilbert N très grand. Comme exemple, un système de spins quantiques avec r particules de spin s a une dimension $N = (2s + 1)^r$ dont r peut devenir très grand. Ceci conduit à la conclusion que des difficultés apparaissent dans les deux approches analytiques et numériques. Ces problèmes qui sont aussi reliés à la compréhension des phénomènes critiques dans lesquels les particules sont fortement corrélées ont conduit au développement d'un outil efficace, la méthode de groupe de renormalisation appliquée en physique des hautes et basses énergies. Le succés de cette approche en matière condensée à débuté avec les travaux de Wilson [93].

Le concept de groupe de renormalisation redéfinit l'Hamiltonien initial (action), le nouveau Hamiltonien (action) devient une quantité efficace. Dans la pratique les degrés de liberté inessentiels sont éliminés. La renormalisation met des contraintes sur l'Hamiltonien afin de préserver les propriétés physiques du système à l'étude. Par exemple l'état fondamental et la fonction de partition dans le temps imaginaire (fonction génératrice) devraient être préservés pendant le processus d'élimination. Les contraintes imposées mènent à la renormalisation des intensités des interactions qui sont fixées par les paramètres de couplage. Le groupe de renormalisation dans la matière condensée permet généralement l'étude des propriétés de basse énergie des systèmes à basse dimentionalité et fortement

corrélés, et montre des lois d'échelle à proximité des points critiques des systèmes complexes liés aux transitions de phase. Le grand nombre d'applications relié à des approches du groupe de renormalisation montre son universalité [17, 69, 93].

Procédure de réduction de la dimension de l'espace de Hilbert et renormalisation d'un Hamiltonien des systèmes fortement corrélés

Dans ce présent travail on introduit une version du concept de renormalisation sous la forme d'un algorithme de réduction de l'espace de Hilbert des états qui caractérisent des systèmes physiques quantiques dont les composants interagissent fortement à température nulle tels que les systèmes de spins quantiques.

Généralement la taille de l'espace des états d'un système microscopique quantique est très grand et nécessite des moyens de calcul importants pour diagonaliser la matrice permettant d'obtenir le spectre et les états propres alors que l'intérêt physique porte sur l'état fondamental et les premiers états excités.

L'algorithme introduit permet de réduire la dimension de l'espace de Hilbert des états que l'on essaie de réduire à un espace beaucoup plus petit dans lequel les propriétés physiques des états de basse énergie sont reproduites pour un système fini à spectre discret. A partir du choix d'une base réaliste étendue la procédure élimine séquentiellement les états générant des énergies élevées pour réduire la description à celle des états physiques de basse énergie.

Cette élimination entraine néceessairement une renormalisation des quantités qui définissent l'Hamiltonien, les constantes de couplage dans le cas de systèmes de spins. La renormalisation est en effet imposé par les contraintes fixées par les propriétés physiques du système

qui doivent être préservées.

En pratique la procédure de réduction des dimensions de l'espace des états est réalisé à l'aide d'une méthode de projection basée sur le formalisme de Feshbach [27]. Pendant la réduction de l'espace de Hilbert, les paramètres de couplage de l'Hamiltonien qui évoluent en conservant l'énergie de l'état fondamental d'énergie évoluent en suivant des équations de flot à la limite d'une description continue [43].

La méthode est universelle dans le sens qu'elle n'est pas reliée à la structure de l'espace réel (resp. espace réciproque). Cette propriété permet son application à des systèmes fortement corrélés dans des réseaux et encore à tous les systèmes microscopiques quantiques comme les atomes, les molécules, les agrégats, les noyaux, les points quantiques et autres.

Applications aux systèmes antiferromagnétique d'échelle de spins frustrés

L'algorithme de réduction a été appliqué à des modèles d'interaction forte (tight-binding) et des systèmes de spins quantiques, en pratique des échelles de spins frustrés à deux montants [19, 20, 53]. Dans ce dernier cas la base des états a été développée dans le cadre d'une symétrie $SU(2)$ et $SO(4)$ [41, 44, 45]. La comparaison des deux approches montre comment le choix de l'une ou l'autre symétrie mène à un spectre d'états de basse énergie différents qui approxime plus ou moins bien le spectre initial dans un espace réduit de dimensions différentes. Ce phénomène est intimement corrélé à la structure de la fonction d'onde de l'état fondamental et traduit la structure intriquée de cette fonction d'onde qui est différente dans différentes représentations. En ce sens la procédure de réduction constitue un test de sa structure.

L'algorithme de la procédure de réduction nécessite d'une part la connaissance du fonda-

mental d'énergie du système et l'état propre correspondant. Ces quantités sont déterminées à chaque étape de la réduction à l'aide de la technique de Lanczos [18, 48] qui permet de les déterminer sans avoir recours à une diagonalisation dans l'espace initial complet. Il est ainsi possible de réduire systématiquement la dimension de l'espace de Hilbert en éliminant les états de base du haut de spectre étape par étape et en renormalisant à chaque étape les constantes de couplage qui se réduisent à une seule dans le cas traité en pratique.

Points exceptionnels et transitions de phase quantique dans l'espace de Hilbert

Pour certaines valeurs des paramètres de couplage le système considéré peut passer par une transition de phase continue ou discontinue. Ce phénomène apparait dans le présent contexte à des points dits exceptionnels correspondant à des croisements d'états physiques du spectre pour des valeurs complexes (croisements évités, transitions continues) ou réelles (transitions discontinues) de ces paramètres de couplage [35, 36, 74, 77]. On montre que ces croisements sont des points fixes de transition dans la procédure décrite ci-dessus [42, 43].

Nous avons étudié le comportement de ces systèmes d'échelles à proximité de transitions de phase. Nous avons pu montrer qu'aux points fixes on observe bien la constance des paramètres de couplage comme le prévoit l'étude théorique. Suivant le cas (choix du groupe de symétrie, transition continue ou discontinue) le spectre est plus ou moins stable. Il s'avère que la procédure de réduction permet de localiser une transition et de déterminer sa nature en utilisant l'entropie du système correspondant à l'état fondamental.

Conclusion et perspectives

Conclusion

Dans ce travail, nous avons proposé un algorithme qui génère une procédure de réduction dimensionnelle de l'espace de Hilbert dans le but d'étudier les propriétés spectrales correspondant aux énergies basses des systèmes fortement corrélés dans l'espace de Hilbert réduit. Nous avons examiné cette méthode sur les systèmes antiferromagnétiques d'échelles de spins quantique frustrés à deux montants pour lesquels les approches de perturbation échouent. Nous avons prouvé que l'algorithme proposé tient compte de la détermination des propriétés spectrales des énergies basses de tels systèmes. Nous avons analysé les propriétés spectrales d'énergie pour le système mentionné ci-dessus dans deux schémas de symétrie, $SU(2)$ et $SO(4)$. Pour les différentes valeurs des constantes de couplage nous avons montré à quel point les états excités peuvent être reproduits dans un espace réduit jusqu'à une valeur minimum N_{min} de l'espace de Hilbert où la procédure de réduction doit s'arrêter parce que le spectre de basse énergie devient instable.

Nous avons noté que dans la pratique et d'une manière générale un algorithme significatif de troncation n'est pas nécessairement basé sur l'élimination systématique des états dont les éléments diagonaux de la matrice de l'Hamiltonien sont ceux qui correspondent aux énergies les plus grandes. Les états physiques de basse énergie sont les états qui présentent un intérêt physique. Les états qui ont les composantes les plus fortes sur les états de basse énergie dus aux éléments non-diagonaux forts de la matrice devraient être maintenus dans l'espace final des états. La symétrie et le choix de l'arrangement des éléments de matrice peuvent aider à améliorer la description des propriétés des états bas physiques d'un système dans l'espace de Hilbert réduit. Dans ce travail, nous avons choisi d'arranger les éléments diagonaux dans l'ordre croissant en énergie et étudier à quel point la renormalisation peut maintenir le spectre de basse énergie pour différents domaines de valeurs des paramètres de couplage.

Nous avons prouvé que des points exceptionnels qui peuvent apparaî tre dans des spectres

physiques sont liés aux points fixes dans l'espace de Hilbert caractérisent l'existence des transitions de phase et correspondent aux valeurs des paramètres de couplage qui restent constants pendant la procédure de réduction.

Nous avons étudié l'effet de la procédure de réduction dans l'espace de Hilbert aux croisements des niveaux dans le spectre de l'énergie pour des valeurs réelles et à proximité des croisements évités pour des valeurs complexes de la constante de couplage. Suivant l'évolution du paramètre de couplage et le bas du spectre de l'énergie nous avons noté qu'aux croisements des niveaux qui correspondent à une dégénérescence des états d'énergie le paramètre de couplage reste constant jusqu'à une petite dimension de l'espace de Hilbert. Cette stabilité remarquable peut être expliquée par le fait que la fonction d'onde de l'état fondamental est fortement dominé par un nombre restreint d'états. La stabilité est plus grande dans le cas d'une représentation de symétrie-$SO(4)$ où le nombre de grands composants est réduit.

Les investigations actuelles montrent que des points de transition du premier ordre dans des systèmes de spins quantiques peuvent être corrélés avec des fluctuations fortes dans les énergies des premiers états excités. La présence de ces points est prévue par des considérations théoriques et signalée numériquement dans quelques cas spécifiques par la constance de la constante de couplage qui entre dans l'Hamiltonien le long de la procédure dimensionnelle de réduction de l'espace de Hilbert. C'est le cas au moins jusqu'au point auquel la stabilité numérique n'est plus assurée. Ceci peut se produire à différentes étapes de la procédure de réduction puisque ce point dépend de la structure de la fonction d'onde de l'état fondamental.

On peut encore mentionner que la constance de l'intensité des paramètres de couplage pendant la procédure de réduction n'est pas toujours un signal numérique suffisant de l'existence d'un point fixe dans l'espace de Hilbert. Nous commentons les résultats dans le cadre du modèle étudié en confrontant deux choix différents de ces paramètres. Dans les deux cas, l'état fondamental de l'énergie est dominé par des énergies de dimère et

pour le même schéma de symétrie la structure du vecteur propre de l'état fondamental est presque semblable. Dans les deux cas nous observons une forte stabilité du paramètre de couplage et dans l'énergie de l'état fondamental. Ceci est lié au mécanisme de la méthode de réduction. En effet le critère de stabilité d'énergie de l'état fondamental et la propriété de *l'état fondamental* à un point fixe peuvent dans certains cas se recouvrir, à savoir sur le même fait la constance du paramètre de couplage. Par conséquent, il est nécessaire d'analyser dans le détail les conclusions (indications) liées au degré de stabilité du paramètre de couplage et l'énergie des états excités dans l'espace de Hilbert réduit. Un autre signal lié à ce point peut être donné par le comportement de l'entropie d'état fondamental qui peut sauter au point fixe et signaler un croisement de niveau.

En conclusion, il est nécessaire d'étudier différents domaines de valeurs des paramètres de couplage dans le cas où les conclusions peuvent être ambiguës. Il en est ainsi dans les cas expliqués ci-dessus, dans lequel l'une d'entre elles reflète la structure de dimère de l'état fondamental et l'autre qui correspond à une transition quantique de premier ordre entre la phase de dimère et la phase de Haldane. Souvent l'utilisation de la procédure de réduction ne permet de conclure quant aux niveaux des états physiques qui se croisent. Malgré la difficulté pour localiser les points fixes avec précision la procédure de réduction peut montrer dans certains cas leur existence et fournir un signal pour leur relation avec des transitions de phase quantique induites à des points exceptionnels (PEs).

Perspectives

- Dans la présente approche la séquence de réduction de la dimension de l'espace de Hilbert suivait une critère d'énergie. Il peut être judicieux de classer la séquence des états à éliminer en commençant par ceux qui ont la plus petite amplitude dans la fonction d'onde du fondamental d'énergie. Les deux procédures doivent être corrélés sinon équivalents.

- Il peut être intéressant d'étudier l'évolution des observables physiques dans des es-

paces de Hilbert réduits tels l'aimantation et la fonction de corrélation des systèmes de spins quantiques.

- L'étude peut être étendu à des systèmes bidimensionnels avec champ magnétique.
- Le concept de réduction peut ultérieurement être étendu à des systèmes à température finie [13, 71].

Contents

Chapter 1

Introduction

The study of quantum microscopic and mesoscopic systems is confronted with difficulties related to the large number of degrees of freedom which are present and the nature of the interactions which act between the components. These interactions of short or long range are often strong and put the validity of methods with treatments like perturbative developments under question [10, 40, 60].

The description of these systems requires an adequate modeling and the introduction of adapted theoretical physical concepts which describe the interaction between the constituents in a realistic way and allow effective calculations. Landau introduced the quasi-particle concept [49, 75]. This approach is justified when the interaction between the particles is weak and allows a perturbative treatment of the interaction. In the same spirit the mean field and residual interaction concepts were introduced in perturbative treatments of systems like atoms and molecules. The mean field approach is a method which allows to describe different phenomena related to the many-body problem, by assuming that residual contributions of the interaction in the system are small. This means that the problem of many-body system is essentially a problem of weakly interacting quasi-particles [5, 10].

In general, there exist no analytical methods to treat exactly strongly interacting systems apart from the assumption of trial wave functions able to diagonalize the Hamiltonian

of integrable models, like the Bethe Ansatz (BA) for specific one dimensional systems ($1D$) [9], the BCS hypothesis which explains the supraconductivity [81] and others like the Néel state, the **R**esonant **V**alence **B**ond **(RVB)** spin liquid states proposed by Anderson [1], the **V**alence **B**ond **C**rystal states (**VBC**)... They are aimed to describe $2D$ systems but there remains the problem of their degree of realism, i.e. their ability to include the essentials of the interaction in strongly interacting systems [52]. The complexity of the structure of such systems leads to the diagonalization of the Hamiltonian numerically which must in general be performed in very large Hilbert space of dimension N. As an example, a quantum spin system with r particles of spin s has dimension $N = (2s+1)^r$ where r can get very large. This leads to the conclusion that difficulties appear in both analytical and numerical approaches. These problems and others related to the understanding of critical phenomena in which the particles are strongly correlated led to the development of a powerful mathematical tool, the renormalization group method applied in high-energy and low-energy physics. The success of this approach method in condensed matter physics began with Wilson [93].

The Renormalization group concept redefines the initial Hamiltonian (action), the new Hamiltonian (action) becomes an effective quantity. In practice the inessential degrees of freedom are integrated out. The renormalization puts constraints on the Hamiltonian in order to preserve the physical properties of the system under study. For instance the ground state and the partition function in imaginary time(generating function) should be preserved during the elimination process. The imposed constraints lead to the renormalization of the strengths of the interactions which are set by the coupling parameters. The renormalization group in condensed matter generally allows the study of the low energy properties of low dimensional strongly interacting systems and shows scaling laws in the neighbourhood of critical points of complex systems related to phase transitions. The large number of applications related to renormalization group approaches shows its universality [17, 69, 93].

Materials in which the particles are strongly interacting and exhibit collective physical

properties at low energy, are f.i. low dimensional systems like the quantum spin systems. They have been under intensive scrutiny during the last decades. These systems were studied by means of many different methods and led to the development of different algorithms relying on renormalization group methods, among them the real space renormalization group of quantum systems on the lattice. There one integrates out the degrees of freedom corresponding to the high energy contributions of the systems.

A basic idea behind this type of methods is concerned with the enlargement of the size of the lattice system without increasing the size of Hilbert space, i.e. a way to truncate the Hilbert space by eliminating the inessential basis states without touching the low-lying state properties which are essential for the understanding of the phase diagram of the physical system at low energy and low or zero temperature T.

Many different methods were proposed for quantum systems on lattices and based on the modeling of these systems as sets of blocks of sites diagonalized exactly and linked to each other through the lowest-lying eigenstates of the block Hamiltonian in different approaches. In this way one may construct a new effective Hamiltonian which keeps the relevant states playing an important role in the low-lying states properties of the whole physical lattice system [87]. Wilson was the first to propose a renormalization approach effective for the Kondo model [93], but it could not treat strongly correlated systems like Hubbard, Heisenberg models and others [59]. Then White proposed the *Density Matrix Renormalization Group* ($DMRG$) to treat lattice systems [88, 89]. This method led to a good description of the low-lying properties of one and quasi-one dimensional lattice systems [25, 90]. In some specific cases, the $DMRG$ and other real space renormalization group ($RSRG$) methods can describe two dimensional systems [12, 91]. Among renormalization methods one may quote the Real Space Renormalization Group with Effective Interactions (RSRG-EI) [58, 87], the Contractor Renormalization group technology (CORE) [62], the Entanglement Renormalization [83] and the Energy Renormalization Group [4].

In the present work we introduce another approach which relies on a reduction procedure aimed to describe the low lying properties of strongly interacting systems. It works in Hilbert space and we shall try to show that it is flexible and simple in its principles.

This reduction procedure acts directly in Hilbert space by eliminating the basis states belonging to a defined Hilbert space $\mathcal{H}$ in which they are estimated inessential in view of some criteria concerning the stability of the low-lying states of strongly interacting systems at $T = 0$. During the reduction of Hilbert space dimension, the method is meant to compensate the elimination of states by the renormalization of the strength of the interactions like the coupling parameters of the Hamiltonian in order to keep the low energy states stable. The method requires the knowledge of the ground state properties, therefore it is useful to understand how far the properties of excited states can be reproduced in this framework.

The method is universal in the sense that it does not rely on the structure of the real (resp. reciprocal) space. This property allows its application not just to strongly interacting systems on lattices but in principle also to all microscopic quantum systems like atoms, molecules, agregates, nuclei, quantum dots and others.

Studying quantum phase transitions is an intriguing fundamental problem in physics. Phase transitions appear in all physical fields in high as well as in low energy physics. In condensed matter physics they signalize the change of the low physical state properties especially the ground and first excited ones for systems at low or zero temperature T. These changes of behaviour lead to new physical properties in systems like for instance those which show superconductivity and superfluidity phenomena [81]. Crossings between two energy levels can be a signal of degeneracy in the spectrum and the existence of underlying symmetry in the Hamitonian of the system. We shall show that quantum phase transitions corresponding to level crossing points are fixed points in Hilbert space in the sense of the renormalization idea mentioned above.

In Chapter 2 we introduce the mathematical tools used to develop our theory concerning the dimensional reduction procedure in Hilbert space ($DRHS$) by renormalizing the coupling parameter which enters the Hamiltonian at $T = 0$. This reduction procedure is based on a projection method introduced by *H. Feshbach* [27] which leads to the construction of an effective Hamiltonian in projected space. Normally, one uses this effective Hamiltonian as a starting point of perturbation study. But in the present work it will be used in order to generate the flow equation in Hilbert space of a renormalized coupling parameter which enters the Hamiltonian of strongly interacting systems. The procedure is aimed to assure the conservation of the ground and the low excited state energies. We develop a formal framework for Hamiltonians with one coupling parameter and the algorithm applicable numerically to realistic physical systems. Work on these points can be found in [43]. Further we propose an approach which tackles the Hamiltonians with more than one coupling parameter.

In Chapter 3 we apply and test the algorithm of the $DRHS$ procedure in an application to two-leg frustrated antiferromagnetic quantum spin ladder systems for which the perturbation and mean field approaches break down. We study the evolution of this system in $SU(2)$ and $SO(4)$ symmetry-schemes which correspond to a different structures of the ground state eigenvector. The $DRHS$ procedure is sensitive to the choice of the symmetry-scheme. We show by means of numerical applications that in different domains of coupling parameters the $DRHS$ procedure works differently from one symmetry to other. Work on these points can be found in [41].

In Chapter 4 we develop an approach which identifies exceptional points (EPs) in the spectrum of energy of systems which exhibit quantum phase transitions. These transitions are related to fixed points in Hilbert space in the framework of the renormalization theory developed in chapter 2. We show that in the frustrated quantum spin ladder system the coupling parameter which exhibits a first order transition from a Haldane phase to a dimer phase is a fixed point in Hilbert space. We study the system in the vicinity of avoided crossing in the spectrum of energy. Work on this point can be found in [42].

In Chapter 5 we present the numerical implementation developed to test the reduction procedure on realistic systems.

In Chapter 6 we summarize and comment the results of this work and the possibility to perform further investigations in the spirit of these approaches.

Chapter 2

Dimensional reduction procedure in Hilbert space and Renormalization of strongly interacting system Hamiltonians

Contents

In 1958 *H. Feshbach* proposed an original projection method which allows to describe the physical properties of a quantum system in a reduced Hilbert space of states [27]. It divides Hilbert space into two subspaces and generates effective Hamiltonians which are aimed to act in one of these subspaces. The method has been applied in many fields of many-body physics like optics [16], nuclear [39] and recently condensed matter physics [58].

In this work, we take advantage of this method in order to develop a non-perturbative renormalization procedure which allows to study the spectral properties of low-lying bound states of low dimensional systems at $T = 0$, especially strongly correlated systems like quantum frustrated systems, quantum dots, nuclei, atoms, aggregates and molecules, whatever the explicit form of the Hamiltonian.

2.1 Effective Hamiltonian

2.1.1 Introduction

The study of the physical properties of quantum many-body systems has very often relied on perturbation theoretical procedures [40]. This approach works very well as far as, for example, the residual interaction acting beyond a mean field description is weak. But perturbation theory is unable to tackle the description of many systems such as quantum spin systems in condensed matter physics. Hence other tools are needed in order to describe these systems.

The main technical problem in the treatment of quantum many-body systems concerns the diagonalization of the many-body Hamiltonian in Hilbert space which leads to the energy spectra of these systems. The complete set of basis states in this space may be of infinite dimension or at least generally very large. We introduce and discuss below a method which is aimed to overcome the problem of large dimension of Hilbert space. This method relies on the *projection method* introduced by *H. Feshbach* [27].

We recall first the *Feshbach formalism* and explain how this method works when the Hilbert space is divided into two subspaces. At this point it may become the starting point of perturbation expansions in the projected Hilbert space for systems like for example of atoms and photons [16]. In the present work, we show how the formalism can be implemented in the framework of a non-perturbative renormalization procedure in Hilbert space.

2.1.2 Projection formalism

In general, the Hamiltonian can be written in the form :

$$H^{(N)} = \sum_{k=0}^{p} g_k^{(N)} H_k \tag{2.1}$$

where H_k are different contributions which describe the interaction between the constituents of the quantum system.

The Hamiltonian $H^{(N)}$ characterizes the system in Hilbert space $\mathcal{H}^{(N)}$, where N denotes the dimension of this space in which it acts. N is generally very large. H_0 describes the motion of independent objects f.i. a mean field contribution and $H_{(k=1,\ldots,p)}$ the interactions between the quantum objects beyond the mean-field. The pertinence of their treatment as residual parts in a perturbation treatment depends on the intensity of the coupling constants $g_k^{(N)}$, $(k = 1, \ldots, p)$ which characterize the interaction between the constituents.

We consider a complete basis of states which spans the Hilbert space $\{|\Phi_i\rangle,\ i = 1, \cdots, N\}$. These states can for instance be chosen to be the eigenstates of a mean-field Hamiltonian H_0.

$$H_0|\Phi_i\rangle = \epsilon_i|\Phi_i\rangle \tag{2.2}$$

where $\{\epsilon_i\}$ are the corresponding eigenvalues. Other choices of $\{|\Phi_i\rangle\}$ are of course possible.

The eigenvectors of $H^{(N)}$, $\{|\Psi_i^{(N)}(g^{(N)})\rangle,\ i = 1, \cdots, N\}$ obey the Schroedinger equation

$$H^{(N)}(g^{(N)})|\Psi_i^{(N)}(g^{(N)})\rangle = \lambda_i(g^{(N)})|\Psi_i^{(N)}(g^{(N)})\rangle \tag{2.3}$$

where $g^{(N)} \equiv \{g_k^{(N)}, k = 1, \ldots, p\}$ and $\{\lambda_i(g^{(N)}), i = 1, \ldots, N\}$ are the eigenvalues of $H^{(N)}(g^{(N)})$.

Each eigenvector can be written as a linear combination of a complete set of basis states

$$|\Psi_i^{(N)}\rangle = \sum_{j=1}^{N} a_{ij}^{(N)}(g^{(N)})|\Phi_j^{(N)}\rangle \tag{2.4}$$

The Feshbach formalism introduces the definition of projectors in Hilbert space. If this space is divided into two subspaces the projection operators P and Q act in the subspaces $\mathcal{P}\mathcal{H}^{(N)}$, $\dim\mathcal{P}\mathcal{H}^{(N)} = M$ and $\mathcal{Q}\mathcal{H}^{(N)}$, $\dim\mathcal{Q}\mathcal{H}^{(N)} = N - M$ of the Hilbert space $\mathcal{H}^{(N)}$.

We introduce :

$$P = \sum_{i=1}^{M} |\Phi_i^{(N)}\rangle\langle\Phi_i^{(N)}| \tag{2.5}$$

$$Q = \sum_{i=M+1}^{N} |\Phi_i^{(N)}\rangle\langle\Phi_i^{(N)}| \tag{2.6}$$

The subspaces $\mathcal{PH}^{(N)}$ and $\mathcal{QH}^{(N)}$ are orthogonal to each other

$$PQ = QP = 0 \tag{2.7}$$

if $\{|\Phi_i^{(N)}\rangle\}$ are orthonormalized basis states.

Furthermore they obey the general properties of projection operators

$$P + Q = 1 \tag{2.8}$$

$$P^+ = P \tag{2.9}$$

$$Q^+ = Q \tag{2.10}$$

$$P^2 = P \tag{2.11}$$

$$Q^2 = Q \tag{2.12}$$

Where P^+ and Q^+ are the hermitic conjugates of P and Q.

Using these projectors any Hamiltonian H can be written in the generic matrix form

$$(H) = \begin{pmatrix} PHP & PHQ \\ \\ QHP & QHQ \end{pmatrix} \tag{2.13}$$

The procedure leads to an effective Hamiltonian $H_{eff}(\lambda_{i=(1,...,M)}(g^{(N)}))$ which acts in the projected subspace $\mathcal{PH}^{(N)}$ and obeys the equation

$$H_{eff}(\lambda_{i=(1,...,M)}(g^{(N)}))P|\Psi^{(N)}_{(i=1,...,M)}\rangle = \lambda_{i=(1,...,M)}(g^{(N)})P|\Psi^{(N)}_{i=(1,...,M)}\rangle \tag{2.14}$$

where

$$P|\Psi^{(N)}_{i=(1,...,M)}\rangle = \sum_{j=1}^{M} a^{(N)}_{ij}(g^{(N)})|\Phi^{(N)}_{j}\rangle \tag{2.15}$$

is the projection on $P\mathcal{H}^{(N)}$ of the eigenvector $|\Psi^{(N)}_{i}\rangle$ given by Eq. (2.4) and $\lambda_{i=(1,...,M)}(g^{(N)})$ are the corresponding eigenvalues, equal to the physical eigenvalues defined in Eq. (2.3)

The explicit derivation of H_{eff} acting in the projected subspace $P\mathcal{H}^{(N)}$ is given in *Appendix B*.

Explicitly one finds

$$H_{eff}(\lambda_{i=(1,...,M)}) = PHP + PHQ(\lambda_i - QHQ)^{-1}QHP \tag{2.16}$$

We notice that $H_{eff}(\lambda_i)$ is a non-local energy-dependent operator which contains the local operator H given by Eq. (2.16) [27]. This point has been considered recently [97]. We shall develop it in the next sections.

Eq. (2.16) can be used as the starting point of perturbation developments in the projected $P-$subspace [10, 77] f.i. in nuclear physics for the study of resonance theory for elastic and inelastic scattering [26, 27], the introduction of the resolvent method for the study of the coherence and the population of particles in optics. [16]. It can be used in order to generate a *Heisenberg Hamiltonian* from a *Hubbard Hamiltonian* [63].

The projection method, which allows to work in a defined finite subspace, is formally interesting in the framework of perturbation approaches but raises problems when the virtual part PHQ of Eq. (2.16) which relates the two subspaces $P\mathcal{H}^{(N)}$ and $Q\mathcal{H}^{(N)}$ be-

comes strong or when eigenstates in QHQ come close to λ_i. This contribution plays a crucial role since then perturbation expansions generally break down.

Many groups developed non-perturbative methods in physics in order to try to overcome the problem of the large size of space in real, reciprocal or in zero-dimensional Hilbert space. *Wilson* [93] was the first to propose to use the renormalization concept in real space (resp. reciprocal space) in order to describe continuous phase transition phenomena in low dimensional systems avoiding the use of perturbation theory and going beyond mean field approximation which neglects the fluctuations in the physical system.

In the next section, we shall proceed differently by using the Feshbach formalism in order to work out a non-perturbative reduction approach in Hilbert space. This approach is useful in order to study the spectral properties of low dimensional systems at $T = 0$ in which the quantum objects are strongly interacting or are subject to quantum phase transitions [74].

2.2 Renormalization in Hilbert space at Temperature T= 0

The interest in physical properties of a microscopic quantum many-body system of particles is in many cases restricted to the knowledge of a few spectral properties of the system which involve the ground state and low excited states.

We present now a formal framework in which we develop a dimensional reduction procedure of the space of states in Hilbert space. We work out a method designed for many-body quantum systems at $T = 0$ which leads to the generation of effective Hamiltonians in reduced space. These Hamiltonians act in these new spaces under the constraint that they reproduce low spectral properties corresponding to those obtained in the original space.

2.2.1 Formal framework

Consider a system with a fixed but arbitrary number of bound quantum objects in a Hilbert space $\mathcal{H}^{(\mathcal{N})}$ of dimension N governed by a Hamiltonian $H^{(N)}\left(g_0^{(N)},\cdots,g_p^{(N)}\right)$ where $\left\{g_0^{(N)},\cdots,g_p^{(N)}\mapsto g^{(N)}\right\}$ are a set of parameters (coupling constants) which characterize $H^{(N)}$ as defined in Eq. (2.1). The eigenvectors $|\Psi_i^{(N)}(g^{(N)})\rangle$ $\{i=1,\cdots,N\}$ of $H^{(N)}$ span the Hilbert space and are the solutions of the Schrödinger equation Eq. (2.3).

The diagonalization of $H^{(N)}$ delivers both the eigenvalues $\{\lambda_i(g^{(N)}),\, i=1,\ldots,N\}$ and eigenvectors $\left\{|\Psi_i^{(N)}(g^{(N)})\rangle,\, i=1,\ldots,N\right\}$ in terms of a linear combination of orthogonal basis states $\left\{|\Phi_i^{(N)}\rangle,\, i=1,\ldots,N\right\}$. Since dim $\mathcal{H}^{(N)}=N$ is generally very large if not infinite and the information needed reduces to a finite part of the spectrum it makes sense to try to restrict the space dimensions. If the relevant quantities of interest are for instance M eigenvalues out of the set $\left\{\lambda_i(g^{(N)})\right\}$, generally but not necessarily the lowest energy states, then one may define a new effective Hamiltonian $H^{(M)}(g^{(M)})$ such that

$$H^{(M)}(g^{(M)})|\Psi_i^{(M)}(g^{(M)})\rangle=\lambda_i(g^{(M)})|\Psi_i^{(M)}(g^{(M)})\rangle \tag{2.17}$$

with the constraints

$$\lambda_i(g^{(M)})=\lambda_i(g^{(N)}) \tag{2.18}$$

for $i=1,...,M$. Eq. (2.18) implies relations between the sets of coupling constants $g^{(M)}$ and $g^{(N)}$

$$g_k^{(M)}=f_k(g_0^{(N)},g_1^{(N)},...g_p^{(N)}) \tag{2.19}$$

with $k=0,\ldots,p$. The solution of these equations generates new coupling constants which allow to define a new Hamiltonian in the corresponding reduced space. Such an effective Hamiltonian $H^{(M)}(g^{(M)})$ may not be unique. It should be constructed in such a way that

it best preserves the eigenenergies and the physical observables which characterize the system.

2.2.2 General space reduction procedure and renormalization algorithm for systems at temperature T = 0

We develop here an explicit and general approach called *Dimensional Reduction Procedure in Hilbert Space (DRHS)*. We start from the complete Hilbert space $\mathcal{H}^{(\mathcal{N})}$ in which the system is described by the Hamiltonian $H^{(N)}$. Since we want to reduce the dimensions of the space but describe the same physical system as in the original space the Hamiltonian changes and gets an effective operator. One may try to achieve these changes by means of the renormalization of quantities which characterize it, in practice interaction strengths, coupling parameters. The evolution of these quantities with the reduction of space is determined by means of constraints which fix physical quantities like energies or other physical observables corresponding to those obtained in the complete space and (or) experimentally known. In this way the physical properties such as the energies of the low-energy part of the spectrum can be determined in the reduced space and are hopefully close to those which are generated in the complete space. In the sequel we consider a Hamiltonian with one parameter g so that one needs one constraint to fix its value at each step of the reduction procedure. The quantity we consider to be fixed here is the ground state energy of the system. Constraints on the energies of other states can be implemented as we shall show below.

Following the procedure sketched above we reduce the dimensions of the space by means of a projection technique. Using the Feshbach formalism [27] we divide the Hilbert space $\mathcal{H}^{(N)}$ into two subspaces, $P\mathcal{H}^{(N)}$ and $Q\mathcal{H}^{(N)}$ by means of the projection operators P and Q,

$$\mathcal{H}^{(N)} = P\mathcal{H}^{(N)} + Q\mathcal{H}^{(N)}$$

In the present case the dimensions of the subspaces are chosen such that

$$\dim P\mathcal{H}^{(N)} = N-1, \quad \dim Q\mathcal{H}^{(N)} = 1 \tag{2.20}$$

In the projected subspace $P\mathcal{H}^{(N)}$ the system with energy E is described by the effective Hamiltonian [7, 27]

$$H_{eff}(E) = PHP + PHQ(E - QHQ)^{-1}QHP \tag{2.21}$$

The Hamiltonian H characterizes the system in Hilbert space $\mathcal{H}^{(\mathcal{N})}$. We suppose that H depends on one parameter g and write it in the form

$$H^{(N)} = H_0 + g^{(N)}H_1 \tag{2.22}$$

where H_0 and H_1 are Hamiltonian operators and $g^{(N)}$ (coupling constant) is the strength of the interaction between the constituents. We consider an arbitrary complete set of basis states which spans $\mathcal{H}^{(N)}$ $\{|\Phi_i\rangle,\, i = 1, \cdots, N\}$. As already mentioned it may be chosen as the eigenvectors of H_0 with the corresponding eigenvalues $\{\epsilon_i = \langle\Phi_i|H_0|\Phi_i\rangle,\, i = 1, \cdots, N\}$.

We consider the projected eigenvector

$$P|\Psi_1^{(N)}\rangle = \sum_{i=1}^{N-1} a_{1i}^{(N)}(g^{(N)})|\Phi_i\rangle \tag{2.23}$$

which is the projection on $P\mathcal{H}^{(N)}$ of an eigenvector

$$|\Psi_1^{(N)}\rangle = \sum_{i=1}^{N} a_{1i}^{(N)}(g^{(N)})|\Phi_i\rangle \tag{2.24}$$

of $\mathcal{H}^{(N)}$. If $E = \lambda_1^{(N)}$ is the eigenvalue corresponding to $|\Psi_1^{(N)}\rangle$ we look for the solution of

$$H_{eff}(\lambda_1^{(N)})P|\Psi_1^{(N)}\rangle = \lambda_1^{(N)}P|\Psi_1^{(N)}\rangle \tag{2.25}$$

In the present applications $|\Psi_1^{(N)}\rangle$ will be the lowest energy eigenstate. The one-dimensional subspace $Q\mathcal{H}^{(N)}$ can correspond to any other state, f.i. a state which lies in the high energy sector of the spectrum of H_0.

The expression given by Eq. (2.25) may be projected on $\langle\Phi_1|$ which may be chosen as the eigenvector of H_0 with lowest energy. Then

$$\langle\Phi_1|H_{eff}(\lambda_1^{(N)})|P\Psi_1^{(N)}\rangle = \lambda_1^{(N)}(g^{(N)})a_{11}^{(N)}(g^{(N)}) \tag{2.26}$$

At this point we start the reduction procedure to go over from the complete Hilbert space $\mathcal{H}^{(N)}$ to the reduced one $\mathcal{H}^{(N-1)}$. The coupling $g^{(N)}$ which characterizes the Hamiltonian $H^{(N)}$ in $\mathcal{H}^{(N)}$ is now aimed to be changed in such a way that the eigenvalue in the new space $\mathcal{H}^{(N-1)}$ is the same as the one in the complete space $\mathcal{H}^{(N)}$

$$\lambda_1^{(N-1)} = \lambda_1^{(N)} \tag{2.27}$$

We develop the l.h.s. of Eq. (2.26) with the definition and introduction of $H^{(N-1)} = H_0 + gH_1$, $g = g^{(N-1)}$ acting in the space $\mathcal{H}^{(N-1)}$. These implementations lead to the scalar equation

$$\langle\Phi_1|H_{eff}(\lambda_1^{(N)})|P\Psi_1^{(N)}\rangle = \mathcal{F}(g^{(N-1)}) \tag{2.28}$$

where

$$\mathcal{F}(g^{(N-1)}) = \overline{H_{1N}^{(N-1)}} + H_{1N}^{(N-1)}(\lambda_1^{(N)} - H_{NN}^{(N-1)})^{-1}\overline{H_{N1}^{(N-1)}} \tag{2.29}$$

with

$$\begin{aligned} H_{ij}^{(N-1)} &= \langle\Phi_i|H^{(N-1)}|\Phi_j\rangle \\ &= \langle\Phi_i|H_0 + g^{(N-1)}H_1|\Phi_j\rangle \\ &= \langle\Phi_i|H_0|\Phi_j\rangle + g^{(N-1)}\langle\Phi_i|H_1|\Phi_j\rangle \end{aligned} \tag{2.30}$$

if $i = j$, $H_{ii}^{(N-1)} = \epsilon_i + g^{(N-1)}\langle\Phi_i|H_1|\Phi_i\rangle$, else $H_{ij}^{(N-1)} = g^{(N-1)}\langle\Phi_i|H_1|\Phi_j\rangle$

and

$$\begin{aligned} \overline{H_{1N}^{(N-1)}} &= \langle\Phi_1|H^{(N-1)}|P\Psi_1^{(N)}\rangle \\ &= \langle\Phi_1|H_0 + g^{(N-1)}H_1|P\Psi_1^{(N)}\rangle \\ &= a_{11}^{(N)}\epsilon_1 + g^{(N-1)}\sum_{i=1}^{N-1} a_{1i}^{(N)}\langle\Phi_1|H_1|\Phi_i\rangle \end{aligned} \tag{2.31}$$

$\overline{H_{N1}^{(N-1)}}$ is the matrix element as $\overline{H_{1N}^{(N-1)}}$ with $\langle\Phi_1|$ replaced by $\langle\Phi_N|$.

Eq. (2.29) can be worked out explicitly. The denominator in the second term of $H_{eff}(\lambda_1^{(N)})$ is a scalar quantity since $\dim Q\mathcal{H}^{(N)} = 1$.

Developing Eq. (2.29) leads to a relation which fixes the renormalized coupling constant $g^{(N-1)}$. One gets explicitly a discrete quadratic equation

$$a^{(N-1)}{g^{(N-1)}}^2 + b^{(N-1)}g^{(N-1)} + c^{(N-1)} = 0 \tag{2.32}$$

where

$$a^{(N-1)} = G_{1N} - H_{NN}F_{1N} \tag{2.33}$$

$$H_{ij} = \langle \Phi_i | H_1 | \Phi_j \rangle \tag{2.34}$$

$$b^{(N-1)} = a_{11}^{(N)} H_{NN} (\lambda_1^{(N)} - \epsilon_1) + F_{1N} (\lambda_1^{(N)} - \epsilon_N) \tag{2.35}$$

$$c^{(N-1)} = -a_{11}^{(N)} (\lambda_1^{(N)} - \epsilon_1)(\lambda_1^{(N)} - \epsilon_N) \tag{2.36}$$

with

$$F_{1N} = \sum_{i=1}^{N-1} a_{1i}^{(N)} \langle \Phi_1 | H_1 | \Phi_i \rangle \tag{2.37}$$

and

$$G_{1N} = H_{1N} \sum_{i=1}^{N-1} a_{1i}^{(N)} \langle \Phi_N | H_1 | \Phi_i \rangle \tag{2.38}$$

The two solutions of Eq. (2.32) are

$$g_{1,2}^{(N-1)} = \frac{-b^{(N-1)} \pm \sqrt{\delta^{(N-1)}}}{2a^{(N-1)}} \tag{2.39}$$

with

$$\begin{aligned} \delta^{(N-1)} &= [a_{11}^{(N)} H_{NN} (\lambda_1^{(N)} - \epsilon_1) + F_{1N} (\lambda_1^{(N)} - \epsilon_N)]^2 \\ &\quad + 4a_{11}^{(N)} (G_{1N} - H_{NN} F_{1N}) (\lambda_1^{(N)} - \epsilon_1)(\lambda_1^{(N)} - \epsilon_N) \end{aligned}$$

$$\begin{aligned} \Rightarrow \delta^{(N-1)} &= \{a_{11}^{(N)} H_{NN} (\lambda_1^{(N)} - \epsilon_1) - F_{1N} (\lambda_1^{(N)} - \epsilon_N)\}^2 \\ &\quad + G_{1N} \{4a_{11}^{(N)} (\lambda_1^{(N)} - \epsilon_1)(\lambda_1^{(N)} - \epsilon_N)\} \end{aligned} \tag{2.40}$$

$\delta^{(N-1)}$ can in principle take negative or positive values. Consequently the parameter $g_{1,2}^{(N-1)} \in$ the real $\mathcal{R}$ or the complex $\mathcal{C}$ ensembles [15] .

The terms $a^{(N-1)}$, $b^{(N-1)}$ and $c^{(N-1)}$ in Eq. (2.32) depend on $g^{(N)}$ through the presence of the coefficients $a_{1i}^{(N)}, i = 1, \ldots, N-1$. Since Eq. (2.32) is non-linear in $g^{(N-1)}$ and has two solutions, $g^{(N-1)}$ is chosen as the one closest to $g^{(N)}$ by continuity. The Hamiltonian $H^{(N-1)} = H_0 + g^{(N-1)}H_1$ defines now the system in the reduced space $\mathcal{H}^{(N-1)}$ as a new space.

The reduction process inferred above can now be iterated step by step by projection from the space of dimension $N-1$ to $N-2$ and further, keeping at each step λ_1 equal to its initial value $\lambda_1^{(N)}$. One generates subsequently a succession of values of the strength parameter (coupling constant) $g^{(N-k)}$ after k iterations. At each step the projected wave-function $|P\Psi_1^{(N-k)}\rangle$ is obtained from $|\Psi_1^{(N-k)}\rangle$ by elimination of a basis state $|\Phi_{(N-k)}\rangle$.

The evolution of the coupling constant g can be written in the continuum limit. For large N one goes over from $(k, k-1)$ to $(x, x-dx)$. Writing out Eq. (2.32) for two successive steps k to $k-1$ and $k-1$ to $k-2$, subtracting and going over to the continuum formulation x leads to the flow equation (see *Appendix C*)

$$\frac{dg}{dx} = -\frac{1}{2a(x)g(x) + b(x)}\left(\frac{dc}{dx} + \frac{db}{dx}g(x) + \frac{da}{dx}g(x)^2\right) \tag{2.41}$$

where $a(x), b(x), c(x)$ and $g(x)$ are the continuous extensions of the corresponding discrete quantities which depend on the dimension x of the space. Eq. (2.41) is a non-linear differential equation which a priori can only be solved numerically [43].

In the following, we propose another reduction procedure in Hilbert space as an approximation of the one above. It takes into account the fact that $H_{eff}(E = \lambda_1^{(N)})$ is a non-local energy-dependent operator containing the local operator H. The advantage of this approach is that it leads to a discrete linear equation of $g^{(N-1)}$.

Some remarks

- The procedure is aimed to generate the energies and other physical properties of the ground state and low-energy excited states of strongly interacting systems.

- In practice the reduction of the vector space from N to $N-1$ results in a renormalization of the coupling constant from $g^{(N)}$ to $g^{(N-1)}$ preserving the physical eigenenergy $\lambda_1^{(N)}$, i.e. $\lambda_1^{(N)} = \lambda_1^{(N-1)} = \lambda_1$. The determination of $g^{(N-1)}$ by means of the constraint expressed by Eq. (2.27) is the central point of the procedure.

- The process does not guarantee a rigorous stability of the eigenvalue λ_1. Indeed one notices that $|\Psi_1^{(k-1)}\rangle$ which is the eigenvector in the space $\mathcal{H}^{(k-1)}$ and the projected state $P|\Psi_1^{(k)}\rangle$ of $|\Psi_1^{(k)}\rangle$ into $\mathcal{H}^{(k-1)}$ differ from each other. As a consequence it may not be possible to keep $\lambda_1^{(k-1)}$ rigorously equal to $\lambda_1^{(N)} = \lambda_1$. In practice the degree of accuracy depends on the relative size of the eliminated amplitudes $a_{1k}^{(k)}(g^{(k)})$. This difficulty will appear in the implementation of the numerical tests developed later.

- The reduction procedure needs a fixed ordering of the sequentially eliminated basis states. This ordering may be chosen by following different criteria. Here the states are arranged according to increasing energies $\langle\Phi_i^{(N)}|H|\Phi_i^{(N)}\rangle$ and eliminated starting from the one which corresponds to the highest energy at each step of the procedure.

- In Eq. (2.26) we choose to project on $\langle\Phi_1|$ because the expected large amplitude $\{a_{11}^{(N)}\}$ is related to the lower diagonal energy on the Hamiltonian matrix.

- If in these reduction procedures applied to Hamiltonians of the form $H = H_0 + gH_1$ H_0 is diagonal and H_1 contains only off-diagonal elements of the Hamiltonian matrix, the renormalization of $g(x)$ becomes trivial in the sense that the flow equation evolves with $dg/dx = 0$.

- The reduction procedure developed above can in principle be generalized to Hamiltonians taking the form $H = H_0 + H_1(g)$ with a flow equation of g which will be different from the one given by Eq. (2.41).

2.2.3 Linear Dimensional Reduction procedure in Hilbert Space

The correspondence between energy-dependent and energy-independent operators has been considered recently in a recent work [97]. Energy-dependent Hamiltonians are in general non-linear operators, like the effective Hamiltonians generated in the Feshbach formalism. Znojil [97] exhibits a linear representation of energy-dependent Hamiltonians. Following the spirit of this work, we develop here a *Linear Dimensional Reduction procedure in Hilbert Space (LDRHS)* by renormalizing the coupling strength parameter like in the former procedure.

At this stage, the non-local operator $H_{eff}(E = \lambda_1^{(N)})$ can be related to the local operator H by constraining H_{eff} in the l.h.s. of Eq. (2.26) to be equal to a local operator H given by Eq. (2.22) with the introduction of $H^{(N-1)} = H_0 + gH_1$, $g = g^{(N-1)}$, acting in the space $\mathcal{H}^{(N-1)}$ and by maintaining the constraint (2.27).

$$\langle \Phi_1 | H^{(N-1)} | P\Psi_1^{(N)} \rangle = \langle \Phi_1 | H_{eff}(\lambda_1^{(N)}) | P\Psi_1^{(N)} \rangle \tag{2.42}$$

This implies that

$$\langle \Phi_1 | H^{(N-1)} | P\Psi_1^{(N)} \rangle = \lambda_1^{(N)}(g^{(N)}) a_{11}^{(N)}(g^{(N)}) \tag{2.43}$$

Developing the left-hand member of Eq (2.43) one gets a discrete linear equation which fixes a renormalized coupling constant $g^{(N-1)}$

$$b^{(N-1)} g^{(N-1)} = a^{(N-1)} \tag{2.44}$$

where

$$a^{(N-1)} = (\lambda_1^{(N)} - \epsilon_1) a_{11}^{(N)}(g^{(N)}) \tag{2.45}$$

and

$$b^{(N-1)} = F_{1N} = \sum_{i=1}^{N-1} a_{1i}^{(N)} \langle \Phi_1 | H_1 | \Phi_i \rangle \tag{2.46}$$

The terms $a^{(N-1)}$ and $b^{(N-1)}$ in Eq. (2.44) depend on $g^{(N)}$ through the presence of the coefficients $a_{1i}^{(N)}$, $\{i = 1, ..., N-1\}$.

One should notice that if in Eq. (2.45) $a_{11}^{(N)}(g^{(N)}) = 0$, this reduction procedure will not be applicable because $g^{(N-1)} = 0$.

The evolution of the coupling constant g can be worked out in the continuum limit. For large N one goes over from $(k, k-1)$ to $(x, x-dx)$. Writing out Eq. (2.44) for two successive steps k to $k-1$ and $k-1$ to $k-2$, subtracting and going over to the continuum formulation x leads to the flow equation

$$\frac{dg}{dx} = -\frac{1}{a(x)}\left(\frac{da}{dx} g(x) - \frac{db}{dx}\right) \tag{2.47}$$

where $a(x)$, $b(x)$ and $g(x)$ are the continuous extensions of the corresponding discrete quantities which depend on the dimension x of the space. Eq. (2.47) is a non-linear differential equation which a priori can only be solved numerically.

Comparison between the two reduction procedure approaches

The advantages of the $LDRHS$ compared to the $DRHS$ are the following:

- $g^{(N-1)}$ obeys a linear equation which makes step by step the reduction procedure easier.

- There is no matrix inversion in $LDRHS$ like it is the case in the general $DRHS$ procedure, see Eq. (2.16).

- In Eq. (2.45) the efficiency of the linear presentation is seen by observing that the non-local operator H_{eff} is replaced by the local operator H.

- One should notice that by using the effective Hamiltonian, it is necessary to normalize the projected eigenvector in $\mathcal{PH}^{(\mathcal{N})}$(see appendix B), but the mathematical structure of Eqs. (2.26) and (2.43) of the reduction procedure eliminates the constant of normalization.

Discussion about the validity of $LDRHS$

In Eq. (2.39), G_{1N} depends on the off-diagonal elements of the line of the Hamiltonian matrix $H(N \times N)$ which correspond to the eliminated state N. If H_{1N} is small or (and) the sum over $(i = 1, \ldots, N-1)$ stays small then G_{1N} gets small in the reduction procedure developed in the section (2.2.2) ($G_{1N} \longrightarrow 0$) Eq. (2.39) reduces to

$$g_1^{(N-1)} = \frac{(\lambda_1^{(N)} - \epsilon_1^{(N)}) a_{11}^{(N)}(g^{(N)})}{F_{1N}} \tag{2.48}$$

and

$$g_2^{(N-1)} = \frac{(\lambda_1^{(N)} - \epsilon_N^{(N)})}{H_{NN}} \tag{2.49}$$

with $H_{NN} = \langle \Phi_N | H_1 | \Phi_N \rangle$.

The expression $g_1^{(N-1)}$ in Eq. (2.48) is the same as the one shown in Eq. (2.44) of the $LDRHS$. The equation expresses the couplings between $|\Phi_1\rangle$ and the remains states $|\Phi_i\rangle$ through the presence of F_{1N}. The off-diagonal elements $\langle \Phi_i | H | \Phi_j \rangle$ couple the basis states $\langle \Phi_i |$ and $|\Phi_j\rangle$ through H. They play a crucial role in the stability of the renormalization

procedure. Hence one should keep the states $|\Phi_i\rangle$ for which the matrix elements are strong. This leads to the conclusion that $g_1^{(N-1)}$ which takes into account the role of the off-diagonal elements through F_{1N} may be a better solution than $g_2^{(N-1)}$ in the implementation of linearized the reduction procedure ($LDRHS$).

2.2.4 Reduction procedure in Hilbert space with more than one coupling strength

We can generalize the previous reduction procedure ($DRHS$) which is restricted to Hamiltonians depending on one parameter to Hamiltonians depending on several parameters $\{g_i^{(N)}\}$.

We take the case of Hamiltonians depend on two coupling parameters, $H^{(N)} = H_0 + g_1^{(N)}H_1 + g_2^{(N)}H_2$. To renormalize $g_1^{(N)}$ and $g_2^{(N)}$, we need to fix two constraints, f.i. the ground and first excited state energies $\lambda_1^{(N)}$ and $\lambda_2^{(N)}$.

$$\lambda_1^{(N-k)} = \lambda_1^{(N-1)} = \lambda_1^{(N)}$$
$$\lambda_2^{(N-k)} = \lambda_2^{(N-1)} = \lambda_2^{(N)}$$

Proceeding like in the case where Hamiltonians depend on one coupling parameter only by using the Feshbach formalism of the effective Hamiltonians H_{eff},

$$H_{eff}(\lambda_1^{(N)})P|\Psi_1^{(N)}\rangle = \lambda_1^{(N)}P|\Psi_1^{(N)}\rangle$$
$$H_{eff}(\lambda_2^{(N)})P|\Psi_2^{(N)}\rangle = \lambda_2^{(N)}P|\Psi_2^{(N)}\rangle$$

Projecting these Schroedinger equations on $\langle\Phi_1|$ and $\langle\Phi_2|$ respectively

$$\langle \Phi_1 | H_{eff}(\lambda_1^{(N)}) | P\Psi_1^{(N)} \rangle = \mathcal{F}_1(g_1^{(N-1)}, g_2^{(N-1)})$$
$$\langle \Phi_2 | H_{eff}(\lambda_2^{(N)}) | P\Psi_2^{(N)} \rangle = \mathcal{F}_2(g_1^{(N-1)}, g_2^{(N-1)})$$

Developing these two scalar equations, one gets a system of two coupled equations for $g_1^{(N-1)}$ and $g_2^{(N-1)}$.

The reduction procedure can be generalized to Hamiltonians which depend on more than two coupling strengths.

But, it remains an open question whether this reduction procedure based on the knowledge of a set of eigenvalues can be an efficient method to treat physical problems for systems at $T = 0$. It may get a numerically cumbersome procedure.

2.3 Reduction algorithm for the Dimensional Reduction procedure in Hilbert Space $(DRHS)$

We summarize here the algorithm which governs the reduction:

1− Consider a quantum system described by an Hamiltonian $H^{(N)}$ which acts in a N-dimensional Hilbert space.

2− Compute the elements of the Hamiltonian matrix $H^{(N)}$ in a definite basis of states $\{|\Phi_i\rangle, i = 1, \ldots, N\}$. The diagonal matrix elements $\{\langle \Phi_i | H^{(N)} | \Phi_i \rangle\}$ are arranged in increasing order with the corresponding off-diagonal elements by taking into account that the discrete equation of $g^{(N-1)}$ (Eq. (2.32)) is constructed by assuming that the larger amplitude $\{a_{11}^{(N)}\}$ is related to the lower diagonal energy on the Hamiltonian matrix.

3− Use a numerical technique which allows to determine $\lambda_1^{(N)}$ and $|\Psi_1^{(N)}(g^{(N)})\rangle$, f.i. the Lanczos technique. $\lambda_1^{(N)}$ may be chosen as the experimental value λ_1 if known.

4− Fix $g^{(N-1)}$ as described in *section* 2.2.2. Take the solution of the algebraic second order equation closest to $g^{(N)}$ (Eq. (2.32)) of the $DRHS$.

5− Construct $H^{(N-1)} = H_0 + g^{(N-1)}H_1$ by elimination of the matrix elements of $H^{(N)}$ involving the state $|\Phi_N\rangle$.

6− Repeat the procedures 2, 3, 4 and 5 by fixing at each step k $\lambda_1^{(N-k)} = \lambda_1^{(N)} = \lambda_1$.

7− The iterations may be stopped at $N = N_{min}$ corresponding to the limit of space dimensions for which the spectrum gets unstable.

If $LDRHS$ is applied Eq. (2.44) is used in order to fix $g^{(N-1)}$.

The next chapter is devoted to the applications of the theory to the study of strongly interacting frustrated quantum spin ladder systems. The role and importance of representations corresponding to different symmetries are investigated by using different bases of states.

Chapter 3

Applications to antiferromagnetic frustrated quantum spin ladder systems

Contents

3.1 Introduction

In this part we will apply the reduction procedure introduced in the previous chapter in order to test the role of matrix element ordering, symmetry properties which play an important role in the structure of the ground state eigenvector, and finally the size of the system. The method has been tested on tight-binding models (see *Appendix F*).

3.2 Symmetries in quantum mechanics

Symmetry is a fundamental concept which characterizes physical systems. Its elegance and efficiency appears in all fields of physics, in particular microscopic physics (point-groups in crystallography, orbital symmetries in atoms, molecules, and quantum solid state physics). It provides a fundamental framework in the study of quantum many-body systems.

The study of the physical properties of quantum many-body particles is related to symmetries of the model describing the system which are induced by the structure of the Hamiltonian. A quantum system is group-symmetry invariant when its Hamiltonian, like the one shown in Eq. (2.1), possesses group-symmetry invariance. Practically, in the case of discrete quantum spin systems with one spin-1/2 fermion per site, the Hamiltonian is $SU(2)$ (rotationally, translationally) invariant and may obey other symmetries like time-reversal symmetry, $\mathcal{Z}_2$ symmetry which allows the reduction of the Hilbert space into a product of disconnected subspaces.

The commutation properties of physical operators signal symmetry properties of the Hamiltonian. It allows to define the quantum numbers attached to the basis states in Hilbert space $\mathcal{H}$, $[H, \Omega] = 0$ where Ω is a definite operator [3, 52, 59]. Generally speaking the effective Hamiltonian of Eq. (2.14) may break the commutation relation, $[H_{eff}, \Omega] \neq 0$.

An interesting aspect of symmetry apart from the one related to the Hamiltonian is

the concept of dynamical symmetry [8, 45, 73] like $SO(n)$ of low energy excitations whose generators are constructed via Hubbard operators. The operators of this symmetry are generated in terms of Dirac brakets which introduce transitions between states belonging to different irreducible representations of symmetry groups. They reveal new symmetries which appear in the Casimir operator and are used to rewrite the Hamiltonian.

A simple non-trivial Hamiltonian associated with dynamical symmetry is governed by a pair of electron spins coupled by an exchange interaction J_t. This system is a spin dimer which is related to the dynamical symmetry $SO(4)$ of a spin rotator. The generators are constructed via a singlet state $|S_iM_i\rangle = |00\rangle$ with a singlet energy (E_S) and a triplet state $|S_iM_i\rangle = |1\{+1, 0, -1\}\rangle$ with a triplet energy (E_T), the gap of energy is $J_t = E_T - E_S$. These states belong to different irreducible representations of the non-Abelian Lie group $SO(4)$. The spin dimers characterize more complex systems, e.g. quantum dots, spin ladders and others. This symmetry has been recently investigated in interesting developments in nanophysics [44, 46]. We shall introduce it below.

3.3 Symmetry-schemes of the two-leg spin ladder $s = 1/2$

3.3.1 Introduction

The antiferromagnetic frustrated quantum spin ladder has been exhaustively studied during the last decades from a both experimental and theoretical point of view. This arrangement could provide a clue for the study and understanding of high critical-temperature (T_c) superconductors. These systems are related to the experimental realization of ladder compounds, like the family of cuprates $Sr_{14-x}Ca_xCu_{24}O_{41}$ where x is the hole doping, and the vanadyl pyrophosphate $(VO)_2P_2O_7, \ldots$, in which several recent experiments have revealed additional close analogies between superconducting ladder compounds and high-T_c superconductors. Furthermore these systems show a rich phase diagram in terms of the coupling strengths which characterize their Hamiltonians [19, 20, 86]. As an example one

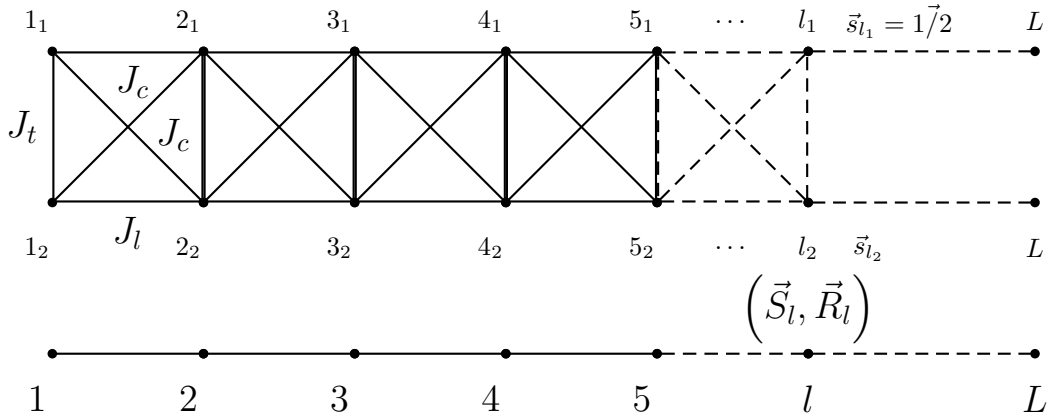

Figure 3.1: Top: the original spin ladder. The coupling strengths are indicated as given in the text. Bottom: The ladder in the SO(4) representation. See the text.

can quote frustrated quantum magnets in magnetic fields which show phase transitions and magnetization plateaux, see references [11, 23, 61, 82].

We aim to use the spin ladder model as a test system of the reduction procedure developed in *chapter* 2. The application of the algorithm will show some interesting aspects concerning the properties of the low energy spectrum in particular as far as symmetry properties and transition points are concerned [41, 42].

In the following our study will be restricted to the case of spin ladders with two legs.

3.3.2 The model

SU(2)-symmetry framework.

Consider antiferromagnetic spin ladders in which each site is occupied by a spin-1/2 [54, 55] with open boundary conditions described by Hamiltonians of the following type shown in Fig.(3.1) .

$$\begin{aligned} H^{(s,s)} &= J_t \sum_{i=1}^{L} s_{i_1} s_{i_2} + J_l \sum_{<ij>} s_{i_1} s_{j_1} + J_l \sum_{<ij>} s_{i_2} s_{j_2} + J_{1c} \sum_{(ij)} s_{i_1} s_{j_2} \\ &\quad + J_{2c} \sum_{(ij)} s_{i_2} s_{j_1} \end{aligned} \tag{3.1}$$

The indices 1 or 2 label the spin 1/2 vector operators s_{i_k} acting on the sites i on both ends of a rung, in the second and third term i and j label nearest neighbours, here $j = i + 1$ along the legs of the ladder. The fourth and fifth term correspond to diagonal interactions between sites located on different legs, $j = i + 1$. L is the number of sites on a leg (Fig.(3.1)). We fix $J_{1c} = J_{2c} = J_c$ in the coming applications. The antiferromagnetic exchange coupling parameters J_t, J_l, J_c are positive [3, 19].

As stated in *section* 2.2.2 the renormalization induced by the reduction procedure is restricted to a unique coupling strength, see Eq. (2.22). It is implemented here by putting $H_0 = 0$ and $H^{(N)} = g^{(N)} H_1$ where $g^{(N)} = J_t$ and

$$H_1 = \sum_{i=1}^{L} s_{i_1} s_{i_2} + \gamma_{tl} \sum_{<ij>} (s_{i_1} s_{j_1} + s_{i_2} s_{j_2}) + \gamma_c \sum_{<ij>} (s_{i_1} s_{j_2} + s_{i_2} s_{j_1}) \ . \tag{3.2}$$

where $\gamma_{tl} = J_l/J_t$, and $\gamma_c = J_c/J_t$. These quantities are kept constant and $g^{(N)} = J_t$ will be subject to renormalization in the reduction process.

The basis of states for a system with $2L$ sites $\{|\Phi_k\rangle \ , k = 1, \ldots, N\}$ is chosen as

$$|\Phi_k\rangle = |1/2 \ \ m_1, ..., 1/2 \ \ m_i, ..., 1/2 \ \ m_{2L}, \sum_{i=1}^{2L} m_i = M_{tot}\rangle$$

with $\{m_i = +1/2, -1/2\}$.

SO(4)-symmetry framework.

Different choices of bases may induce a more or less efficient reduction procedure depending on the strength of the coupling constants J_t, J_l, J_c. This point is investigated here by choosing also a basis of states which is written in an $SO(4)$-symmetry scheme

By means of a spin rotation [45]

$$s_{i_1} = \frac{1}{2}(S_i + R_i) \tag{3.3}$$

$$s_{i_2} = \frac{1}{2}(S_i - R_i) \tag{3.4}$$

The Hamiltonian Eq. (3.1) can be expressed in the form

$$H^{(S,R)} = \frac{J_t}{4}\sum_{i=1}^{L}(S_i^2 - R_i^2) + J_1\sum_{<ij>} S_iS_j + J_2\sum_{<ij>} R_iR_j \tag{3.5}$$

The structure of the corresponding system is shown in the lower part of Fig.(3.1). Here $J_1 = (J_l + J_c)/2$, $J_2 = (J_l - J_c)/2$ and as before $J_{1c} = J_{2c} = J_c$. The components $S_i^{(+)}, S_i^{(-)}, S_i^{(z)}$ and $R_i^{(+)}, R_i^{(-)}, R_i^{(z)}$ of the vector operators S_i and R_i are the $SO(4)$ group generators which act on the same site i and $< ij >$ denotes nearest neighbour indices. The generators of the $SO(4)$ group via Hubbard operators can be written as

$$S_i^{(+)} = \sqrt{2}(X_i^{(11)(10)} + X_i^{(10)(1-1)}) = S_i^{(-)*}$$

$$S_i^{(z)} = X_i^{(11)(11)} - X_i^{(1-1)(1-1)}$$

$$R_i^{(+)} = \sqrt{2}(X_i^{(11)(00)} - X_i^{(00)(1-1)}) = R_i^{(-)*}$$

$$R_i^{(z)} = -(X_i^{(10)(00)} + X_i^{(00)(10)})$$

where

$$X_i^{(S_iM_i)(S_i'M_i')} = |S_iM_i\rangle\langle S_i'M_i'|$$

In this framework the states $\{|S_iM_i\rangle\}$ are generated by tensor coupling a couple of site states by means of Clebsh-Gordan coefficients

$$|S_iM_i\rangle = \sum_{m_1,m_2} \langle 1/2 \;\; m_1 \;\; 1/2 \;\; m_2|S_iM_i\rangle |1/2 \;\; m_1\rangle_i |1/2 \;\; m_2\rangle_i$$

Along a rung the spin states $|1/2 \;\; m_{1,2}\rangle_i$ are coupled either to a singlet state $|S_iM_i\rangle = |00\rangle$ or a triplet state $|S_iM_i\rangle = |1\{+1, 0, -1\}\rangle$ (see *Appendix A*). Spectra are constructed in this representation as well as in the $SU(2)$ representation and the basis of states $\{|\Phi_k\rangle\}$ takes the form

$$|\Phi_k\rangle = |S_1M_1, ..., S_iM_i, ..., S_LM_L, \sum_{i=1}^{L} M_i = M_{tot}\rangle$$

Remarks

- The vector operator S_i is an effective spin-1 operator in which the eigenvalue of S_i^2 acting in a triplet state is 2 and R_i is a pseudospin which describes the singlet-triplet transition.

- The vector operators S_i and R_i are characterized by the commutation algebra: $[S_i^x, S_i^y] = iS_i^z$, $[R_i^x, R_i^y] = iS_i^z$ and $[R_i^x, S_i^y] = iR_i^z$.

- S_i and R_i are orthogonal operators $S_i \times R_i = 0$ and the Casimir operator is $S_i^2 + R_i^2 = 3$.

3.4 Reduction algorithm for quantum spin ladder systems

Consider a two-leg quantum spin ladder with open boundary conditions (OBC), and L sites along each leg.

The reduction procedure applied to the spin ladders goes along the following steps:

1− Generate the matrix elements of the Hamiltonian matrix $H^{(N)}$ in a definite basis of states $\{|\Phi_i\rangle, i = 1, \ldots, N\}$, here basis of states coupled to $M_{tot} = 0$.

2− Use the Lanczos technique to determine $\lambda_1^{(N)}$ and $|\Psi_1^{(N)}(g^{(N)})\rangle$ (see *Appendix E*).

3− Take $g^{(N)} = J_t$, $J_l = \gamma_{tl} J_t$ and $J_c = \gamma_{tc} J_t$ by keeping the ratios γ_i constants at their initial values. This implies that the coupling parameters J_i evolve in the same way. Fix $g^{(N-1)}$ as described in *section* 2.2.2. Take the solution of the algebraic second order equation closest to $g^{(N)}$ Eq. (2.32) of the $DRHS$.

4− Construct $H^{(N-1)} = g^{(N-1)} H_1$ by elimination of the matrix elements of $H^{(N)}$ involving the state $|\Phi_N\rangle$ which corresponds to the highest energy of the diagonal matrix element. Repeat the procedure by fixing at each step k, $\lambda_1^{(N-k)} = \lambda_1^{(N)} = \lambda_1$.

One should point out that the renormalization does not change if one chooses another coupling parameter as a renormalizable parameter, here J_l or J_c, because they are related to each other at the beginning of the reduction procedure by the ratios $\gamma_{tl} = J_l/J_t$ and $\gamma_c = J_c/J_t$.

This can be seen by considering for instance $J_l^{(N-1)}$ as the renormalized coupling parameter. The coefficients $a^{(N-1)}$, $b^{(N-1)}$(Eq. (2.32)) and $J_l^{(N-1)}$ in the case of $H^{(N)} = J_l^{(N)} H_1$ are related through the relations

$a^{(N-1)} \sim 1/(\gamma_{tl} J_t^{(N)})^2$, $b^{(N-1)} \sim 1/\gamma_{tl} J_t^{(N)}$ and $J_l^{(N)} = \gamma_{tl} J_t^{(N)}$. It is clear that one retrieves the discrete equation of $J_t^{(N-1)}$. This shows that numerical results are independent of the choice of the renormalized coupling parameter.

Remarks

- The basis states of the considered ladder systems are characterized by a fixed total magnetic magnetization M_{tot}. We shall work in subspaces which correspond to fixed M_{tot}. The total spin S_{tot} is also a good quantum number which defines smaller subspaces for fixed M_{tot}. We shall not introduce them here because projection procedures on S_{tot} are time consuming. Furthermore we want to test the algorithm in large enough spaces although not necessarily the largest possible ones in this preliminary tests considered here.

- The eigenvalue $\lambda_1 = \lambda_1^{(N)}$ is chosen as the physical ground state energy of the system. Eigenvalue and eigenvector can be obtained by means of the Lanczos algorithm which is particularly well adapted to very large vector space dimensions. This algorithm is used here in order to fix λ_1 and $|\Psi_1^{(N-k)}\rangle$.

3.5 Test observables

3.5.1 Accuracy of the low energy spectrum

In order to quantify the accuracy of the procedure we introduce different test quantities in order to estimate quantitatively deviations between ground state and low excited state energies in Hilbert spaces of different dimensions. The stability of low-lying states can be investigated by means of

$$p(i) = |\frac{(e_i^{(N)} - e_i^{(N-k)})}{e_i^{(N)}}| \times 100 \quad with \quad i = 1, \ldots, (N-k) \tag{3.6}$$

where $e_i^{(N-k)} = \lambda_i^{(N-k)}/2L$ corresponds to the energy per site at the ith physical state starting from the ground state at the kth iteration in Hilbert space. These quantities provide a percentage of loss of accuracy of the eigenenergies in the different reduced spaces.

3.5.2 Entropy

A global characterization of the ground state wavefunction in different symmetry schemes can also be given by the entropy [56, 65] per site s in a space of dimension n

$$s = -\frac{1}{2L}\sum_{i=1}^{n} P_i ln P_i \quad with \quad P_i = |\langle \Phi_i^{(n)} | \Psi_1^{(n)} \rangle|^2 = |a_{1i}^{(n)}|^2 \tag{3.7}$$

which works as a global measure of the distribution of the amplitudes $\{a_{1i}^{(n)}\}$ in the physical ground state [80]. This quantity is stable as long as the renormalization does not affect J_t in the course of space dimension reduction. The same behaviour should be observed where one uses a correlation function $\langle \Psi_1 | S_k S_l | \Psi_1 \rangle$, where k and l are the sites. Both entropy and correlation function are strongly sensitive to the structure of the ground state eigenvector $|\Psi_1\rangle$.

3.6 Numerical applications

3.6.1 Energy spectrum

We work out energies of the low-lying states of quantum spin ladder systems described above in the subspace in which the basis states are coupled to $M_{tot} = 0$ (see Fig.(3.2)). The energy spectrum is of course the same in the $SU(2)$ and $SO(4)$ symmetry schemes.

3.6.2 Spectra in the SU(2)-symmetry framework

We apply the reduction algorithm to ladders with different numbers of sites and different values of the coupling strengths. Results obtained with an $SU(2)$-symmetry basis of states are shown in Figs.(3.3-3.4-3.5-3.6) and Fig.(3.7)

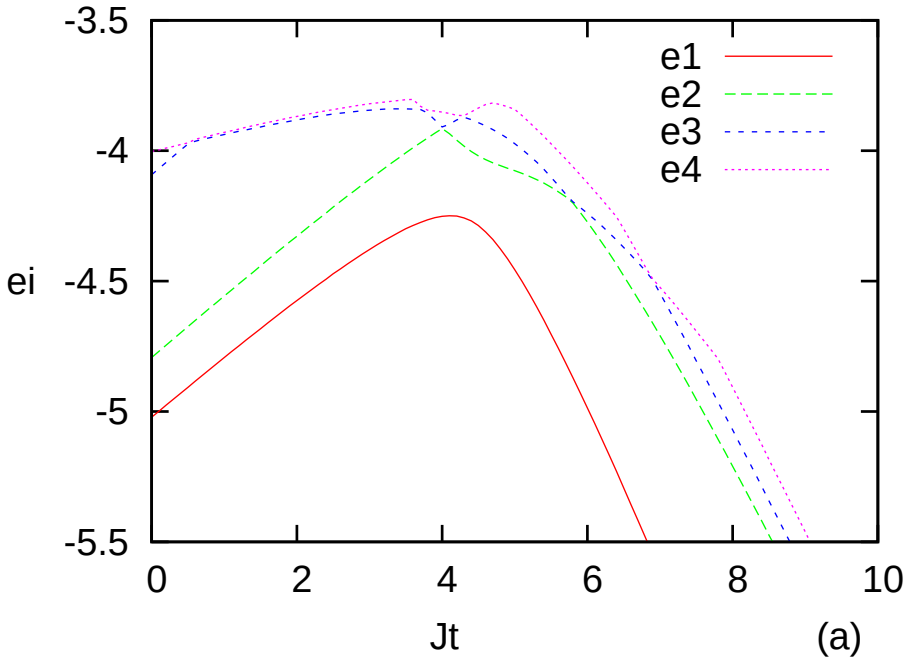

Figure 3.2: The $\{e_i, i = 1, 2, 3, 4\}$ are the energies of the ground and lowest excited states per site. The number of sites is $L = 6$ along the chain, $J_l = 5$ and $J_c = 3$

First case: L= 6, J_t=15, J_l=5, J_c=3

The number of basis states in the framework of the M-scheme corresponding to subspaces with fixed values of the projection of the spin of the $\{|\Phi_i\rangle\}$, $M_{tot} = 0$ is $N = 924$.

In the present case $J_t > J_l, J_c$. The dimension of the subspace is reduced step by step as explained above starting from $N = 924$. As stated in *section* 2.3 the basis states $\{|\Phi_i\rangle\}$ are ordered with increasing energy of their diagonal matrix elements $\langle\Phi_i|H^{(N)}|\Phi_i\rangle$ and eliminated starting from the state with highest energy $\langle\Phi_N|H^{(N)}|\Phi_N\rangle$.

As seen in Fig.(3.3a) the ground state of the system stays stable down to $n \sim 50$ where n is the dimension of the reduced space. The coupling constant J_t does not move either down to $n \sim 300$. Figs.(3.3a-b) show the evolution of the first excited states which follows the same trend as the ground state. Deviations from their initial value at $N = 924$ can be seen in Figs.(3.3c-d) where the $p(i)$ defined above represent these deviations in terms of percentages.

For $n \leq 50$ the spectrum gets unstable, the renormalization of the coupling constant can no longer correct for the energy of the lowest state. Indeed the coupling constant J_t increases drastically as seen in Fig.(3.3e). The reason for this behaviour can be found in the fact that at this stage the algorithm eliminates states which have an essential component in the state of lowest energy. The same message can be read in Fig.(3.3f), the fall-off in the entropy per site s is due to the elimination of sizable amplitudes $\{a_{1i}\}$.

Second case: L= 6, J_t=5.5, J_l=5, J_c=3

Contrary to the former case the coupling constant J_t along rungs is now of the same strength as J_l, J_c. Results are shown in Fig.(3.4). The lowest energy state is now stable down to $n \sim 100$. This is also reflected in the behaviour of the excited states which move now appreciably already for $n \leq 200$. Fig.(3.4e) shows that the coupling constant J_t starts to increase sharply between $n = 300$ and $n = 200$. It is able to stabilize the excited states down to about $n = 200$ and the ground state down to $n = 70$. The instability for $n \leq 70$ reflects in the evolution of the $p(i)$'s, Figs.(3.4c-d) which get of the order of a few percents. The entropy Fig.(3.4f) follows the same trend.

Comparing the two cases above and particularly the entropies Fig.(3.4f) and Fig.(3.3f) one sees that the stronger J_t the more the amplitude strength of the ground state wavefunction is concentrated in a smaller number of basis state components. The elimination of sizable components of the wavefunction leads to deviations which can be controlled down to a certain limit by means of the renormalization of J_t. One sees that large values of J_t favour a low number of significative components in the low energy part of the spectrum in a $SU(2)$ symmetry framework. The mixing is stronger for smaller values of J_t.

A confirmation of this trend can be observed in Figs.(3.5a-f) where $J_t = 2.5$. The rates of destabilisation of the excited states are higher than in the former cases as it can be seen in Figs.(3.5c-d). This point is also reflected in the behaviour of the entropy s which

is larger than in the former case for $n = N$ and decreases more rapidly with decreasing n, Fig.(3.5f).

Third case: L= 8, J_t=15, J_l=5, J_c=3

For $L = 8$ sites the Hilbert space is spanned by $N = 12870$ basis states with $M_{tot} = 0$. The results are shown in Figs.(3.6a-f). The stability of the spectrum with decreasing space dimension is relatively stronger than the stability observed for $L = 6$. Indeed if n/N defines the ratio of the number of states in the reduced space over the total number of states one finds for n around 200 and 65 $p(1)$ jumps from $\sim 10^{-6}$ % , 10^{-3} % to 0.8% and $p(2), p(3), p(4)$ jump from $\sim$ 0.1% to 0.8% where $n/N \sim 65/924 \sim 0.07$ for $L = 6$. For $L = 8$ $p(1)$ jumps from $\sim 10^{-7}$ % to $\sim$ 0.8% where n is around 500 and 90 ($n/N \sim 0.038$ and 0.007) and $p(2), p(3), p(4)$ jump from $\sim$ 0.1% to $\sim$ 0.5% where $n/N \sim 280/12870 \sim 0.023$.

Fourth case: L= 9, J_t=15, J_l=5, J_c=3

For $L = 9$ sites the Hilbert space is spanned by $N = 48620$ basis states with $M_{tot} = 0$. The results are shown in Figs.(3.7). $p(1)$ jumps from $\sim 10^{-8}$ % to $\sim$ 0.8% where n is around 1000 and 100 ($n/N \sim 0.02$ and ~ 0.002), $p(2), p(3), p(4) \sim 0.1\%$, $p(5) \sim 0.08\%$, $p(6) \sim 0.07\%$ and $p(7) \sim 0.05\%$ where $n/N \sim 600/48620 \sim 0.012$.

The evolution of the spectrum and its stability with decreasing J_t follows the same trend as in the cases where $L = 6, 8$. But one notices that the instability falls off significantly by increasing the number of sites.

This shows a sizable improvement in the stability of the spectrum with an increasing size of the Hilbert space, at least in the specific domains where the coupling parameter J_t is large compared to the others.

By comparing the cases of $L = 6, 8$ and 9 sites one can conclude that in the domains in which the reduction procedure works well the percentage of relevant states to kept in the reduced Hilbert space after renormalization of the coupling parameter decreases by increasing the number of sites and reproduces more and less the low-lying energy states of the quantum spin ladder systems.

One should notice that one finds the same results by exchanging the values of J_l and J_c even when $J_{c1} \neq J_{c2}$ but close to each other. We can conclude that going from a larger J_t to a smaller one corresponds to a strong change of nature of the frustrated system. As a special case is the singlet state when $J_l = \frac{(J_{c1}+J_{c2})}{2}$ in which the frustrations cancel the effect of the interaction along the chains, and the change leads from a dimer state to another singlet state for $J_t \lesseqgtr J_l$ [55].

Remarks

In Fig.(3.3a) it is seen that the ground state shows "bunches" of energy fluctuations. The peaks are intermittent, they appear and disappear during the space dimension reduction process. They are small in the case where $J_t = 15$ but can grow with decreasing J_t as it can be observed for $J_t = 5.5, 2.5$. The subsequent stabilization of the ground state energy following such a bunch shows the effectiveness of the coupling constant renormalization which acts in a progressively reduced and hence incomplete basis of states.

These bunches of fluctuations are correlated with the change of the number of relevant amplitudes of the ground state eigenvector(i.e. amplitudes larger than some value ϵ as explained in the caption of Fig.(3.8)) during the reduction process.

One notices that in spite of the renormalization the elimination of a set of relevant amplitudes of the ground state eigenvector in reduced Hilbet space n leads to an energy spectrum in which even the ground state becomes unstable. This remark shows how far the structure of the ground state eigenvector contributes in the properties of the low en-

ergy spectrum, and it can be a sign about the appropriate number of basis states N_{min} defined in the *section* 2.3 at which the reduction process should stop.

Coming back to the case where $J_t > J_l, J_c$. One notices in the caption of Fig.(3.8a) that down to $n \sim 300$ the number of relevant amplitudes defined in Fig.(3.8) stays stable like the ratios $\{p(i)\}$ in Figs.(3.3c-d). For $158 < n < 300$ these ratios change quickly. A bunch of fluctuations appears in this domain of values of n as seen in Figs.(3.3c-d) and correspondingly the number of relevant amplitudes decreases steeply. For $60 < n \leq 158$ the ratios $\{p(i)\}$ stay again stable as well as the number of relevant amplitudes. The $\{p(i)\}$ in Fig.(3.3c-d) almost decrease back to their initial values. The same explanation is valid for $L = 8$ in Figs.(3.6,3.8d). For n around 240 the number of relevant amplitudes decreases steeply and the ratios $\{p(i)\}$ become strongly unstables. One should notice that the choice of the $\epsilon = 10^{-2}$ criterion is to some extent arbitrary. Indeed, one observes that the beginning of sizable renormalization effects appear at dimensions of the reduced space which can be much higher than the dimensions at which the defined relevant amplitudes start to be eliminated, see Figs.(3.6e,3.8d). In the case where $J_t \approx J_l, J_c$ shown in Fig.(3.8b), at n around 750 the number of relevant amplitudes decreases steeply down to a small number of states. But for n around 200 the ratios $\{p(i = 1, 2, 4)\}$ in Fig.(3.4c-d) almost decrease back to their initial values. The analysis shows that bunches of fluctuations may signal the local elimination of relevant contributions of basis states to the physical states in the spectrum. The stabilization of the spectra which follows during the elimination process shows that renormalization is able to cure these effects down to a certain point.

In the case where $J_t < J_l, J_c$ shown in Fig.(3.8c) the relevant and irrelevant amplitudes move continuously during the reduction process and the corresponding $\{p(i)\}$ do no longer decrease to the values they showed before the appearance of the bunch of energy fluctuations as seen in Figs.(3.5c-d). It signals the fact that the coupling renormalization is no longer able to compensate for the reduction of the Hilbert space dimensions.

3.6.3 Spectra in the SO(4)-symmetry framework

The reduction algorithm is now applied to the system described by the Hamiltonian $H^{(S,R)}$ given by Eq. (3.5) with a basis of states written in the $SO(4)$-symmetry framework. We consider two cases corresponding to large and small values of J_t relative to the strengths of the other coupling parameters.

Reduction test for $L = 6$, J_t = 15, 2.5 and J_l=5, J_c=3

Figs.(3.9) show the behaviour of the spectrum for a system of size $L = 6$. A large value of J_t ($J_t = 15$) favours the dimer structure along rungs in the lowest energy state and stabilizes the spectrum down to small Hilbert space dimensions. This effect is clearly seen in Fig.(3.9a), the ground state is very stable. The excited states are more affected, see Figs.(3.9b), although they do not move significantly, Figs.(3.9c-d). The renormalization of the coupling strength J_t starts to work for $n \simeq 50$.

The situation changes progressively with decreasing values of J_t. Figs.(3.10) show the case where $J_t = 2.5$. The ground state energy experiences sizable bunches of fluctuations like in the $SU(2)$-scheme, but much stronger than in this last case. The same is true for the excited states which is reflected through all the quantities shown in Figs.(3.10), in particular J_t, Fig.(3.10e). The arguments used in the $SU(2)$-scheme about relevant and irrelevant amplitudes are also valid here.

The result shows that the renormalization procedure is quite sensitive to the symmetry-scheme chosen in Hilbert space. It is expected that essential components of the ground state wavefunction get eliminated early during the process when the rung coupling gets of the order of magnitude or smaller than the other coupling strengths.

3.6.4 Summary

The present results lead to two correlated remarks. The efficiency of the algorithm is different in different sectors of the coupling parameter space. In the case of frustrated ladders considered here the algorithm is the more efficient the stronger the coupling between rung sites J_t. Second, this behaviour is strongly related to the symmetry representation in which the basis of states is defined. The $SU(2)$ representation leads to a structure of the wavefunctions (i.e. the size of the amplitudes of the basis states) which is very different from the one obtained in the $SO(4)$ representation. For large values of J_t the spectrum is more stable in the $SO(4)$ -scheme. For small values of J_t the stability is better realized in the $SU(2)$-scheme. Finally, in the regime where $J_t > J_l, J_c$, one observes that the reduction procedure is the more efficient the closer J_l to J_c. This effect can be understood and related to previous analytical work in the $SO(4)$ framework [72].

3.6.5 Conclusions

In the present applications we tested and analysed the outcome of an algorithm which aims to reduce the dimensions of the Hilbert space of states describing strongly interacting systems. The reduction is compensated by the renormalization of the coupling strengths which enter the Hamiltonians of the systems. By construction the algorithm works in any space dimension and may be applied to the study of any microscopic N-body quantum system. The robustness of the algorithm has been tested to frustrated quantum spin ladders.

The analysis of the numerical results obtained in applications to two-leg quantum spin ladders leads to the following conclusions :

- The evolution of the spectrum depends on the initial size of the Hilbert space. The larger the initial space the larger the ratio between the initial number of states and the number of states corresponding to the limit of stability of the spectrum.
- The efficiency of the reduction procedure depends on the symmetry frame in which the basis of states are defined. It appears clearly that the evolution of the spec-

trum described in an $SU(2) - scheme$ is significantly different from the evolution in an $SO(4)$-scheme. This is again understandable since different symmetry-schemes partition Hilbert space in different ways and favour one or the other symmetry depending on the relative strengths of the coupling constants. This observation can be related to other work developed in ref. [67] in which one observes the importance of the symmetry induced by a definitive basis, f.i. a plaquette basis to approximate low-lying exact eigenstates of Heisenberg ladders especially when the coupling along the rungs is much stronger than the coupling between the rungs.

- Local spectral instabilities appearing in the course of the reduction procedure are correlated with the elimination of basis states with sizable amplitudes in the ground state wavefunction. One or another representation can be more efficient for a given set of coupling parameters because it leads to physical states in which the weight on the basis states is concentrated in a different number of components. This point relates to the correlation between quantum entanglement and symmetry properties which are presently under intensive scrutiny, see f.i. [47] and refs. therein. In some sense the present algorithm works like a filter. It gives indications about the structure and number of states which contribute effectively to the content of the ground state wave function.

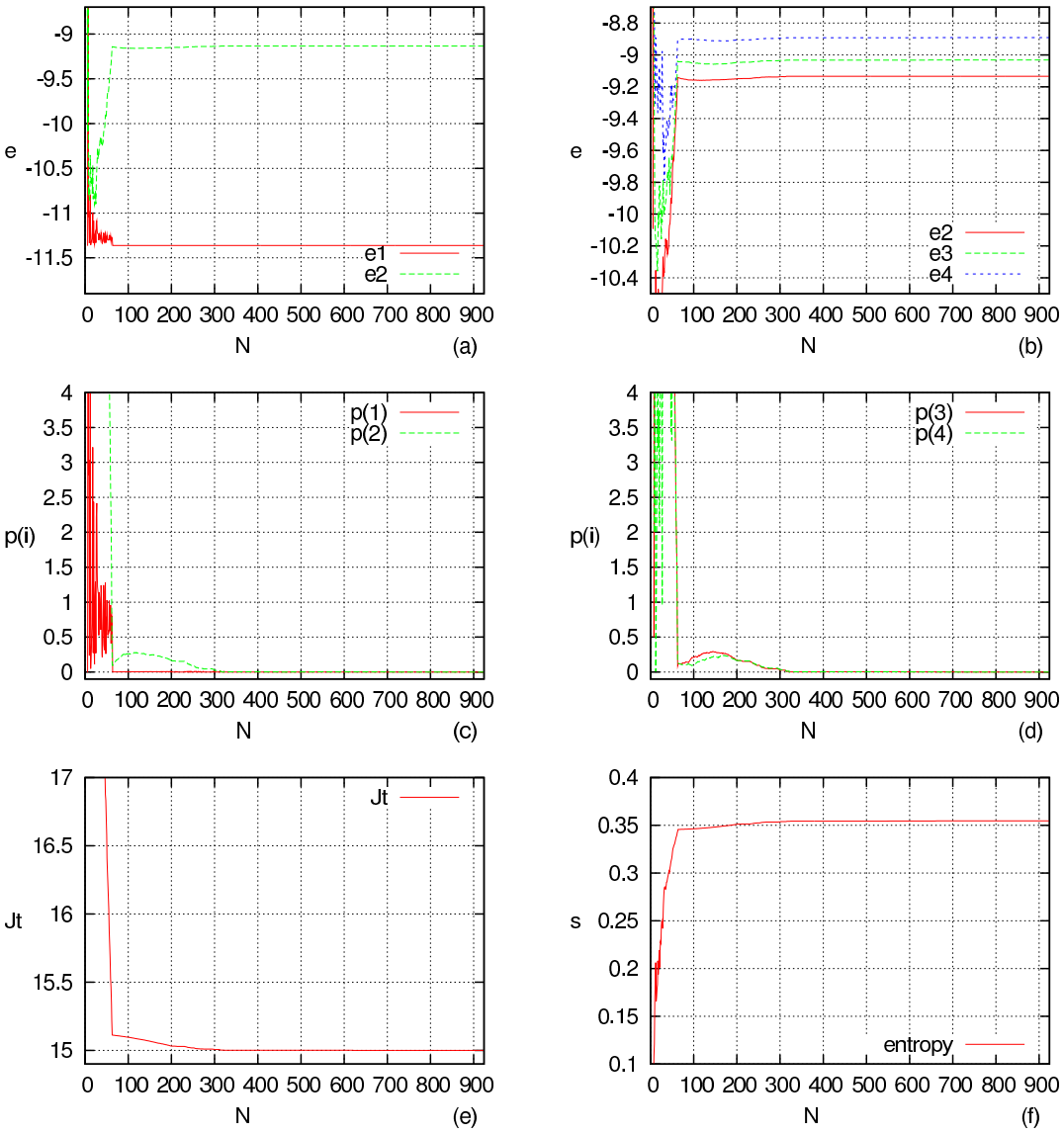

Figure 3.3: $SU(2) - scheme$. N is Hilbert space dimension. The $\{e_i, i = 1, 2, 3, 4\}$ are the energies of the ground and excited states per site. $L = 6$ sites along a leg. $J_t = 15$, $J_l = 5$, $J_c = 3$

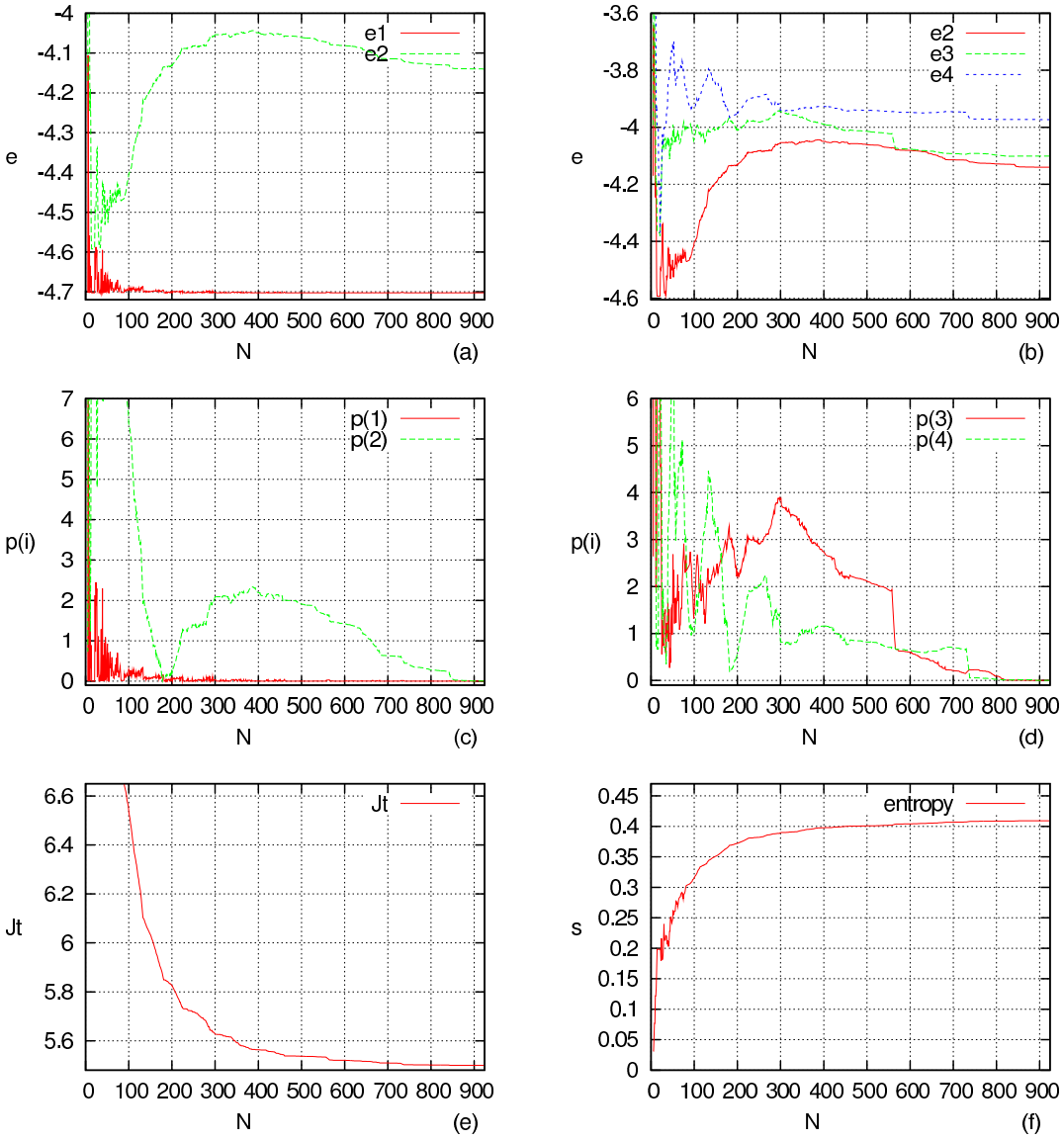

Figure 3.4: $SU(2) - scheme$. N is Hilbert space dimension. The $\{e_i, i = 1, 2, 3, 4\}$ are the energies of the ground and excited states per site. $L = 6$ sites along a leg. $J_t = 5.5$, $J_l = 5$, $J_c = 3$

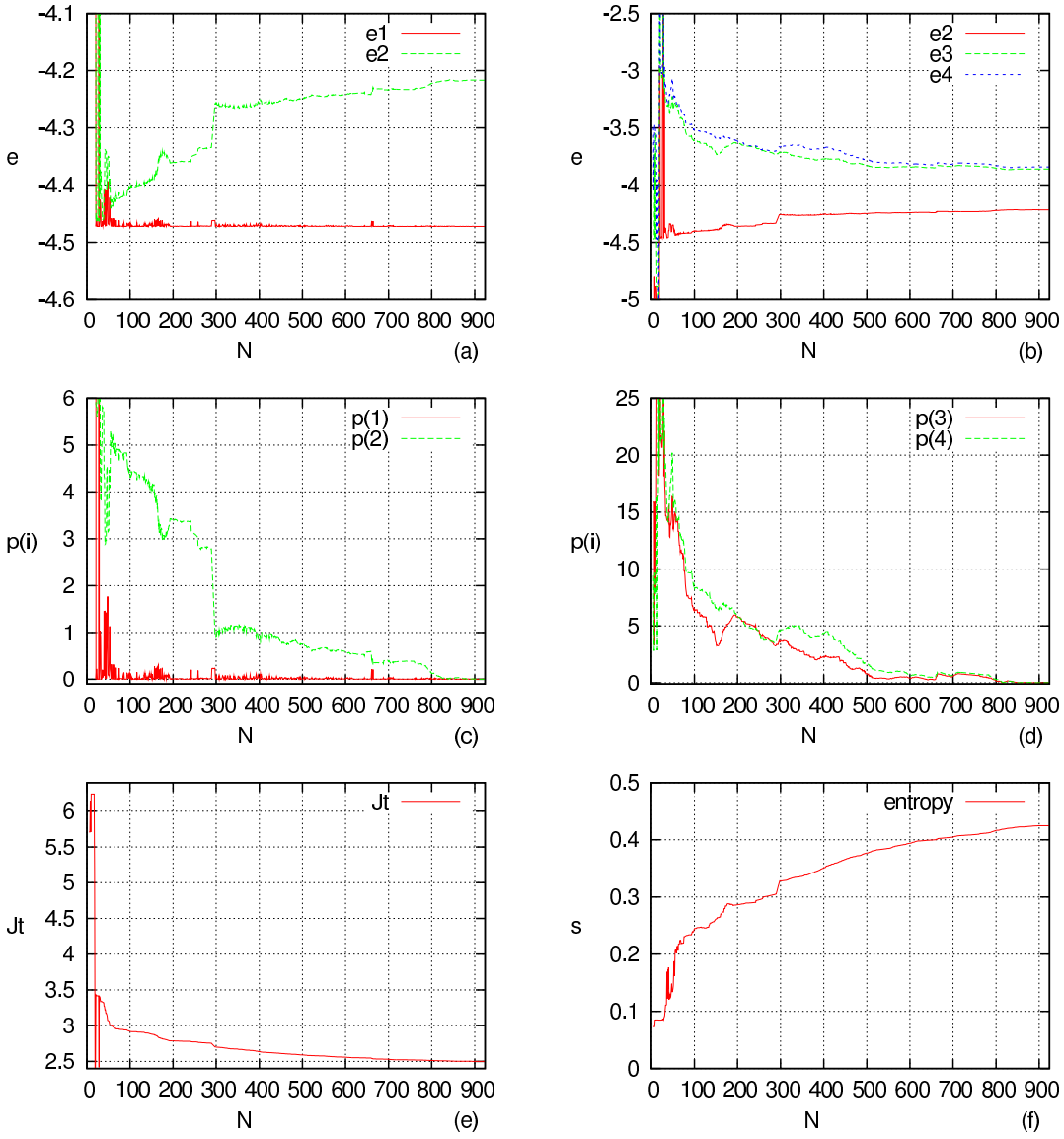

Figure 3.5: $SU(2) - scheme$. N is Hilbert space dimension. The $\{e_i, i = 1, 2, 3, 4\}$ are the energies per site. $L = 6$ sites along a leg. $J_t = 2.5$, $J_l = 5$, $J_c = 3$

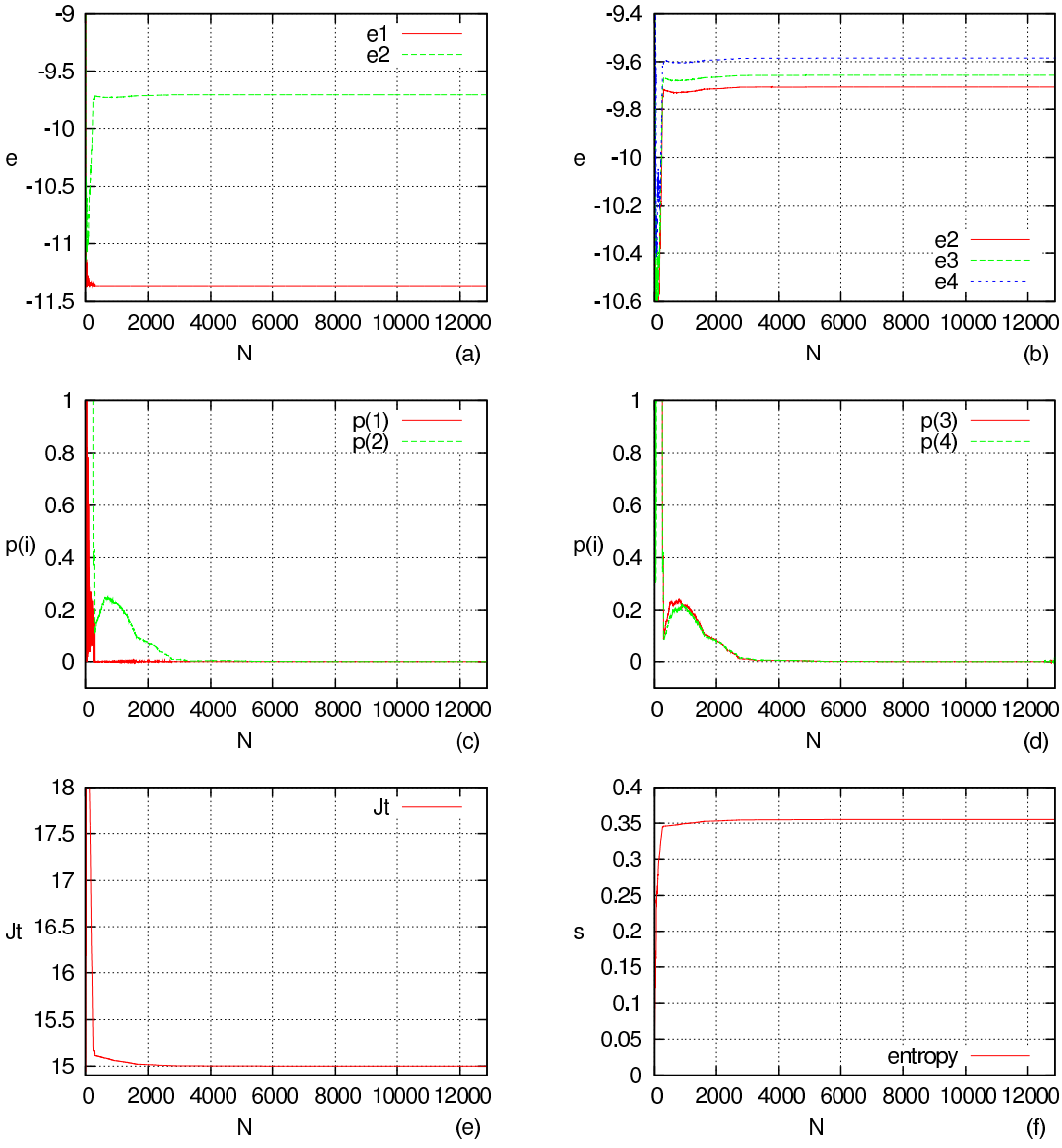

Figure 3.6: $SU(2) - scheme$. N is Hilbert space dimension. The $\{e_i, i = 1, 2, 3, 4\}$ are the energies per site. $L = 8$ sites along a leg. $J_t = 15$, $J_l = 5$, $J_c = 3$

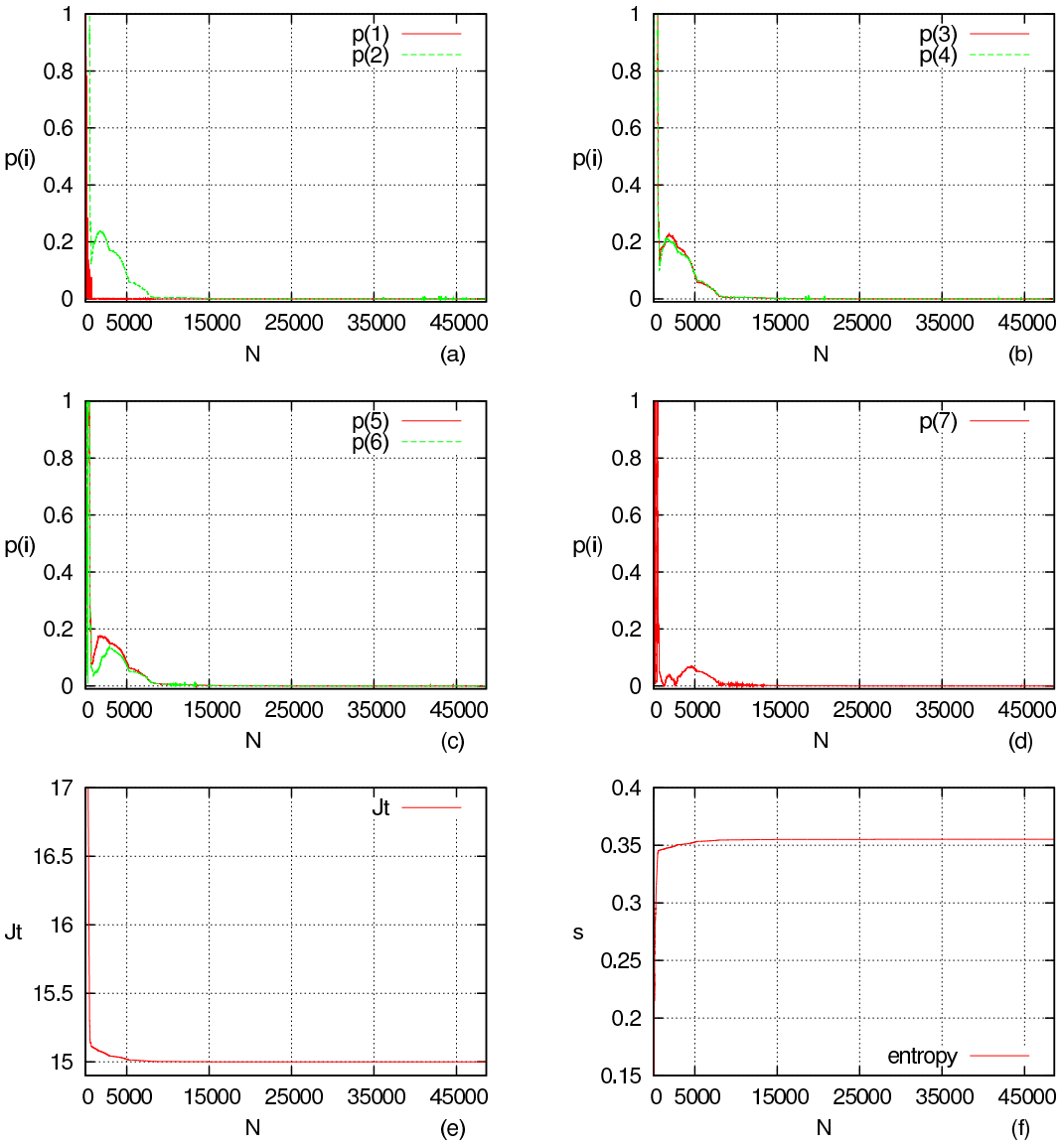

Figure 3.7: $SU(2) - scheme$. N is Hilbert space dimension. The $\{p(i), i = 1, \ldots, 7\}$ are the accuracies of the ground and excited states. $L = 9$ sites along a leg. $J_t = 15$, $J_l = 5$, $J_c = 3$

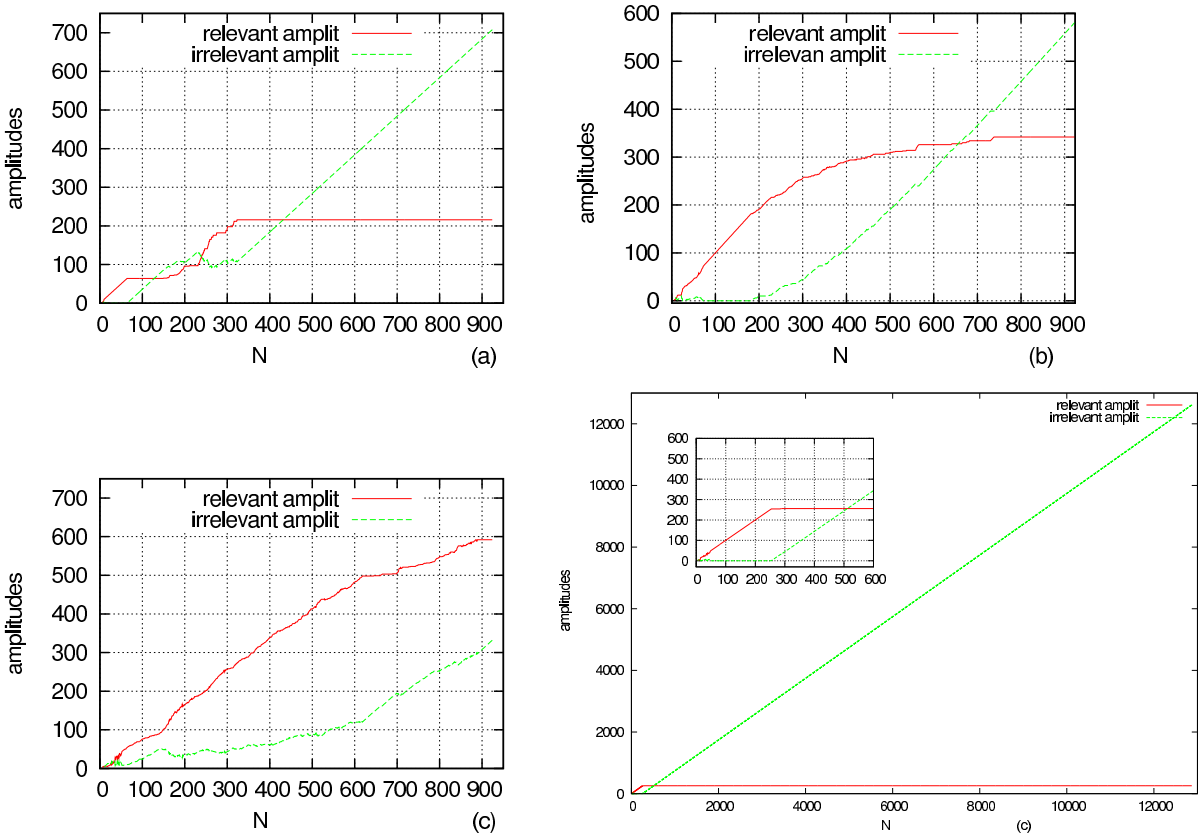

Figure 3.8: $SU(2) - scheme$. N is the dimension of the Hilbert space. *Amplitudes* show the number of relevant -irrelevant amplitudes in the ground state eigenfunction. Relevant amplitudes are those for which $\{a_{1i} > \epsilon$, (here $\epsilon = 10^{-2}$), $i = 1, \ldots, n\}$. For (a) corresponds to $J_t = 15$, (b) to $J_t = 5.5$ and (c) to $J_t = 2.5$, $J_l = 5$, $J_c = 3$ the number of sites along a leg is $L = 6$. For (d) corresponds to $J_t = 15$, $J_l = 5$, $J_c = 3$ the number of sites along a leg is $L = 8$.

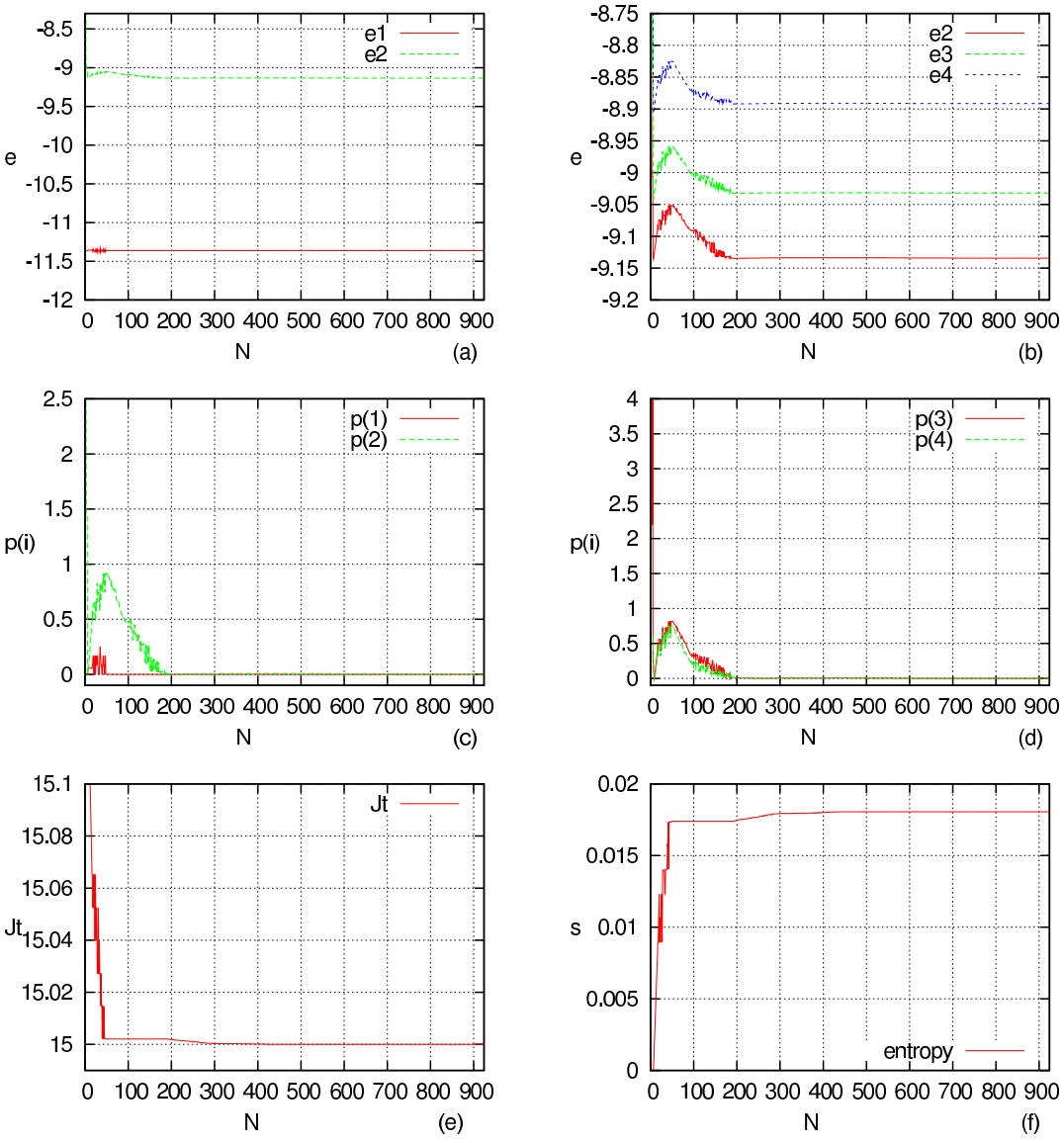

Figure 3.9: $SO(4) - scheme$. N is Hilbert space dimension. The $\{e_i, i = 1, 2, 3, 4\}$ are the energies per site. $L = 6$ sites along the chain. $J_t = 15$, $J_l = 5$, $J_c = 3$

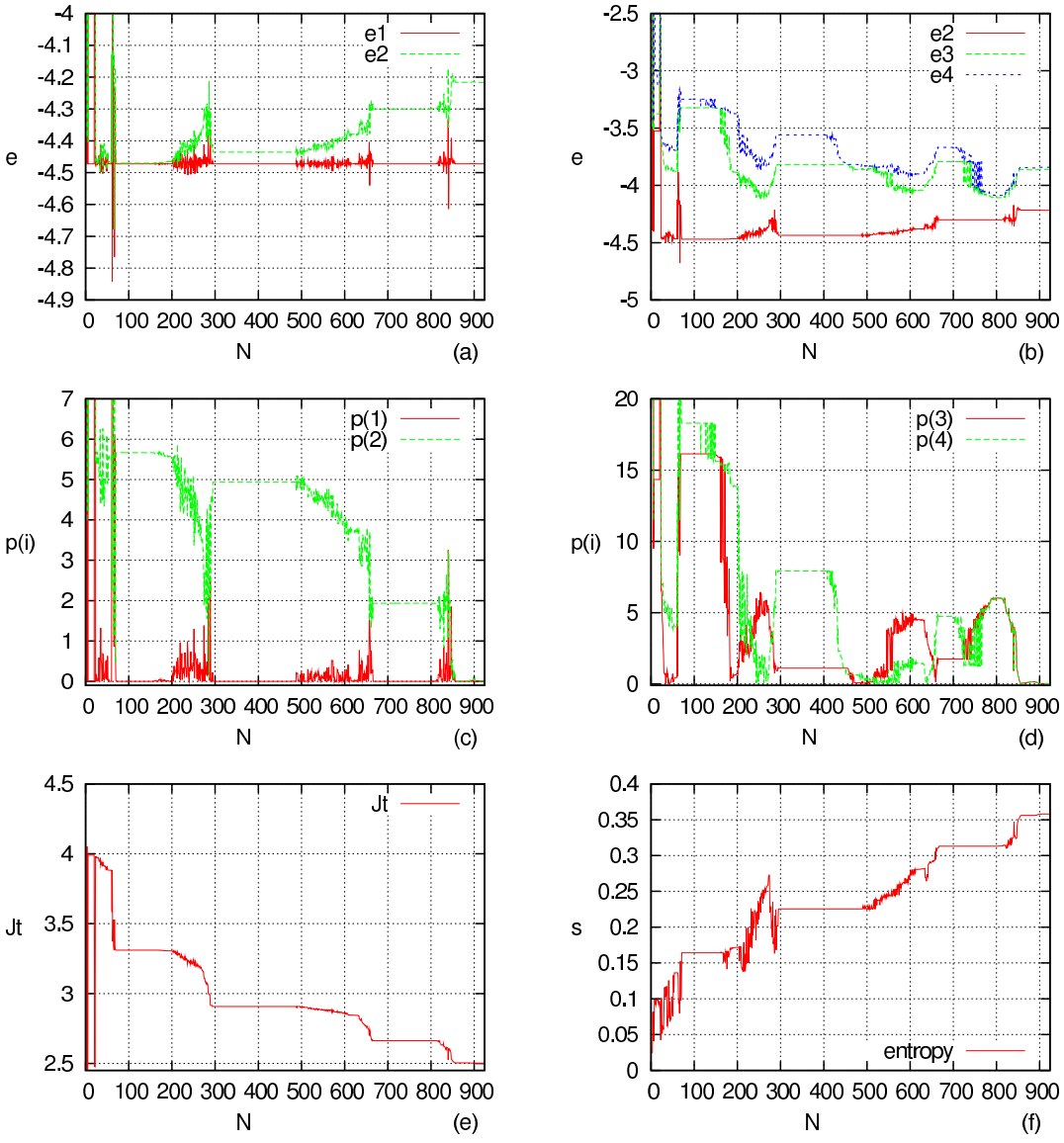

Figure 3.10: $SO(4) - scheme$. N is Hilbert space dimension.The $\{e_i, i = 1, 2, 3, 4\}$ are the energies per site. $L = 6$ sites along the chain. $J_t = 2.5$, $J_l = 5$, $J_c = 3$

Chapter 4

Exceptional points and quantum phase transitions in Hilbert space

Contents

4.1 Introduction

Exceptional points (EPs) are singularities which occur generically in the spectrum and eigenfunctions of operators (matrices) depending analytically on a parameter like the strength g of Hamiltonians of the form $H_0 + H_1(g)$ [33, 40]. They appear in many different fields of physics, at avoided crossings (resp. level crossings) in energy spectra of finite size systems [74]. At avoided crossings the levels cross in the complex plane of g [29, 36, 64]. Levels can also cross for real values of g [77]. The location of avoided crossings (resp. level crossings) is related to the subspaces, reducible and irreducible matrices, chosen and defined in a finite Hilbert space [35]. In a physical interpretation we shall show below that EPs which correspond to quantum phase transitions in the thermodynamic limit in the case of avoided crossings [14, 34] can be identified as *fixed points in Hilbert space* [42]. EPs were observed and detected recently in a microwave cavity experiment [22].

In the next section, we develop the relation between EP and level crossing (resp. avoided-level crossing) in the spectrum of energy which is under some constraints a fixed point in Hilbert space.

4.2 Exceptional points

The eigenvalues $\lambda_k(g)$ of $H(g) = H_0 + H_1(g)$ are analytic functions of g with possible algebraic singularities [32, 40, 77]. In general they get singular at so called exceptional points $g = g_e$ corresponding to avoided crossings of physical states in a finite Hilbert space. Exceptional points are first order branch points of the eigenvalues in the complex g - plane which appear if two (or more) eigenvalues get degenerate. This can happen if g takes values such that $H_{kk} = H_{ll}$ where $H_{kk} = \langle\Phi_k|H|\Phi_k\rangle$, see Fig.(4.1). As a consequence, if an energy level H_{kk} belonging to the $P\mathcal{H}$ subspace defined above crosses an energy level H_{ll} lying in the complementary $Q\mathcal{H}$ subspace the perturbation development constructed from $H_{eff}(E)$ diverges [33, 77] see Eq. (2.16).

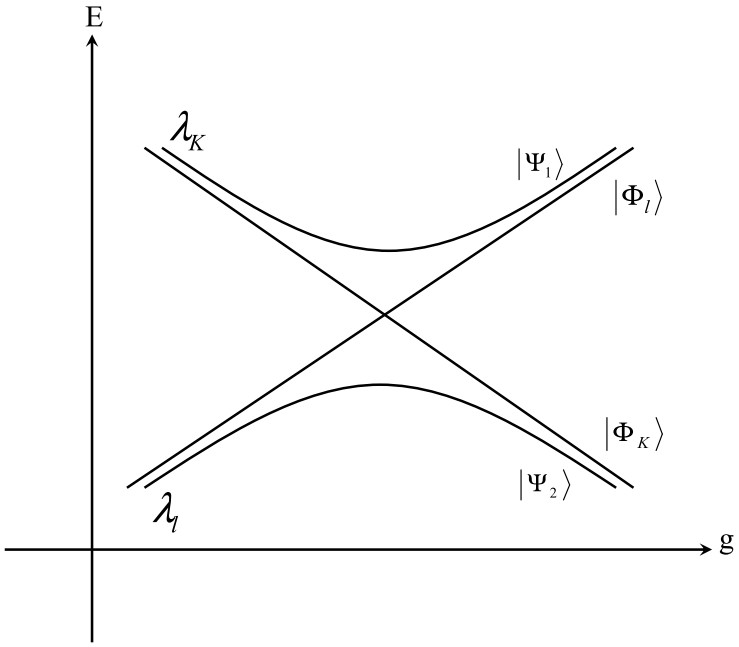

Figure 4.1: Level crossing (here avoided) in the spectrum of energy. g is a real coupling parameter. λ_k (resp. λ_l) and Ψ_1 (resp. Ψ_2) are the eigenvalues and the eigenvectors of the energy levels.

Exceptional points are mathematically defined as the solutions of [32]

$$f(\lambda(g_e)) = det[H(g_e) - \lambda(g_e)I] = 0 \tag{4.1}$$

and

$$\frac{df(\lambda(g_e))}{d\lambda}|_{\lambda=\lambda(g_e)} = 0 \tag{4.2}$$

We show now the correlation between exceptional points and fixed points in Hilbert space.

4.3 Fixed points

If $\{\lambda_i(g)\}$ are a complete set of eigenvalues the secular equation can be written as

$$\prod_{i=1}^{N} (\lambda - \lambda_i) = 0 \ . \tag{4.3}$$

Consider $\lambda = \lambda_p$ which satisfies Eq. (4.1). Eq. (4.2) can only be satisfied if there exists another eigenvalue $\lambda_q = \lambda_p$, hence if a degeneracy appears in the spectrum in the complex or real plane. This is the case at an exceptional point [40].

If the eigenvalue $\lambda_j^{(k)}, k = N, N-1, ...$ which is either constant or constrained to take the fixed value λ_j gets degenerate with some other eigenvalue $\lambda_i^{(k)}(g = g_e)$ in the space reduction process this eigenvalue must obey

$$\lambda_i^{(k)}(g_e) = \lambda_i^{(l)}(g_e') \tag{4.4}$$

which is realized in any projected space of dimensions k and l containing states $|\Phi_j\rangle$ and $|\Phi_i\rangle$. Going over to the continuum limit for large values of N as introduced above and considering the reduced spaces of dimension x and $x + dx$

$$\lambda_i(g_e(x), x) = \langle \Psi_i(g_e(x), x)|H(g_e(x))|\Psi_i(g_e(x), x)\rangle$$

verifies

$$\frac{d\lambda_j}{dx} = 0 = \frac{d\lambda_i(g_e(x), x)}{dx} \tag{4.5}$$

Consequently

$$\frac{\partial \lambda_i}{\partial x} + \frac{\partial \lambda_i}{\partial g_e}\frac{dg_e}{dx} = 0 \tag{4.6}$$

Since $\lambda_i(g_e(x), x)$ does not move with x under the constraint of Eq. (4.4) in the space dimension interval $(x, x + dx)$ the first term in Eq. (4.6) is equal to zero.

Due to the Wigner - Neumann avoided crossing rule the degeneracy of eigenvalues is generally not fulfilled for real values of the coupling constant and the derivative of λ_i with respect to g vanishes. There exist however specific situations, systems with symmetry properties [55, 77, 96] or infinitely large ones [78] for which degeneracy for real g can occur. Hence, for real g

$$\frac{\partial \lambda_i}{\partial g_e} \neq 0 \quad \text{and} \quad \frac{dg_e}{dx} = 0 \tag{4.7}$$

Avoided-level crossings related to EPs exhibit degeneracy for real g at the thermodynamic limit or in some specific symmetries for finite systems in the case of level crossings the energies of the physical states $\{|\Psi_i\rangle\}$ show a real degeneracy point, i.e. their energies cross at real values of $g = g_e$. These properties are a signature of quantum phase transitions [74] at zero temperature. In the framework of the present approach we can conclude that these points are fixed points in Hilbert space in the sense of renormalization theory as shown by the second relation of Eq.(4.7). Thus, we establish a connection between quantum phase transition and fixed points in Hilbert space through the existence of exceptional points.

If the Hamiltonian depends linearly on g, $H(g) = H_0 + gH_1$ a sufficient condition for possible level crossings is given by

$$[H_0, H_1] = 0 \tag{4.8}$$

i.e. H_0 and H_1 can be simultaneously diagonalized [31, 74]. In this case if H_0 is diagonal in the $\{|\Phi_i\rangle,\, i = 1, \cdots, N\}$ basis of states it is also an eigenbasis for H and

$$\frac{d\lambda_i(g_e(x), x)}{dx} = \frac{d\langle\Phi_i|H_0 + g_e(x)H_1|\Phi_i\rangle}{dx} \tag{4.9}$$

Since H_0 and H_1 do not depend on x, $d\lambda_i/dx = 0$ implies $dg_e/dx = 0$ for this specific form of the Hamiltonian which is consistent with the general result Eq. (4.7).

Remarks.

- The relation $[H_0, H_1] = 0$ is applied to Eqs (3.1,3.5) of the spin ladder system in both $SU(2)$ and $SO(4)$ symmetry schemes where H_0 and H_1 are the operators related to J_t and $J_l = J_c$ respectively [74, 86, 95].

- In the general case $H(g) = H_0 + H_1(g)$ $g(x) = g_e$ evolves through a flow equation which is different from the one obtained in Eq. (2.41). We shall restrict our numerical investigations to Hamiltonians which show a linear dependence on g.

- The energy level crossings can occur for any two energy eigenstates of the spectrum. Therefore it is worthwhile to emphasize that the result concerning the connection between exceptional points and fixed points is not restricted to the ground state, it is valid at any physical level crossing in which one of the eigenvalues stays or is constrained to stay constant for any value of the coupling constant. We have tested this property on several systems. We shall consider level crossings or avoided crossings between the ground state and an excited state as well as the case of crossings or avoided crossings of excited states.

4.3.1 Reduction procedure and fixed points

Following the results obtained above fixed points in Hilbert space may in principle be identified by means of an algorithm which allows to reduce the Hilbert space dimension. Here, the $DRHS$ procedure is the optimal method which allows to detect fixed points in the low energy spectrum. We analyze the behaviour of the reduction algorithm in the neighbourhood of fixed points and show its characteristic properties close to fixed points in an application to two-leg frustrated spin ladders for different choices of the basis of states.

For linear Hamiltonians $H^{(N)} = H_0 + g^{(N)}H_1$ (Eq. (2.41)) the flow equation of the renormalized coupling parameter in the Hilbert space continuum limit is

$$\frac{dg}{dx} = \frac{\frac{-1}{2ag+b}(\frac{\partial c}{\partial x} + \frac{\partial b}{\partial x}g + \frac{\partial a}{\partial x}g^2)}{1 + \frac{1}{2ag+b}(\frac{\partial c}{\partial g} + \frac{\partial b}{\partial g}g + \frac{\partial a}{\partial g}g^2)} \tag{4.10}$$

with $a(x, g(x)) = a$, $b(x, g(x)) = b$ and $c(x, g(x)) = c$.

At a fixed point $dg_e/dx = 0$, this implies that during the reduction procedure the relation

$$\frac{\partial c}{\partial x} + \frac{\partial b}{\partial x}g + \frac{\partial a}{\partial x}g^2 = 0 \tag{4.11}$$

is realized.

4.4 Application of the reduction procedure at phase transition points in quantum spin ladder systems

4.4.1 Introduction

As already mentioned above state degeneracy due to level crossings is indeed a signature for the existence of phase transitions [14, 30, 74], perturbation expansions break down at these points. The ground state wavefunction changes its properties when the coupling constant g crosses the exceptional point g_e. There the eigenstates exchange the main components of their projection on the set of basis states $|\Phi_i\rangle, i = 1, ...N$. These changes are accompanied by strong effects. They concern the order parameter related to a breaking of symmetry in Landau's theory, the correlation functions [74], the entropy of the ground state [51, 84] and the continuity (discontinuity) in the gap of energy between the ground and first excited states [54, 66, 95]. These studies have been developed further recently in order to establish an analogy between thermodynamic phase transitions and ground-state quantum phase transitions in systems with variable Hamiltonian parame-

ters, f.i. see [13] and references therein. It may be mentioned here that there exists other methods which are aimed to detect crossing and avoided crossing points. One of them relies on discontinuities in the entanglement properties of wavefunctions which have to be known at crossings or avoided crossings as a signal of a quantum phase transition [21, 94]. A second approach relies on an algebraic method which works very nicely in the case of small systems. This interesting mathematical tool based on matrix properties allows to detect avoided-level crossing in physical systems without looking at the spectrum [6]. It is not clear however whether its use can be easily applied to very large Hilbert spaces such as those which correspond to realistic quantum spin systems.

4.4.2 First order phase transitions of the two-leg spin ladder with level crossing for real g. Application of the reduction algorithm at fixed points

At first order transitions which happen at level crossings of states belonging to specific subspaces for real g the amplitudes of the wavefunctions are expected to acquire weights of the same order of magnitude over a large number of basis states. The analyses performed in *chapter* 2 show that the use of the algorithm at fixed points should work as a stringent test of the method to detect first order transitions in the low energy spetrum.

Fixed points in the SU(2)-symmetry framework.

As a first unrealistic but instructive application, we consider the quantum spin 1/2 ladder with $2L = 4$ sites $(1_1, 1_2, 2_1, 2_2)$ described in Fig.(3.1). Their antiferromagnetic interaction is described by the Hamiltonian [53] (see Eq. (3.1))

$$H^{(s,s)} = J_t[s_{1_1}s_{1_2} + s_{2_1}s_{2_2} + \gamma_{tl}(s_{1_1}s_{2_1} + s_{1_2}s_{2_2}) + \gamma_c(s_{1_1}s_{2_2} + s_{1_2}s_{2_1})] \quad (4.12)$$

where J_t is a positive coupling constant subject to renormalization, γ_{tl} and γ_c are

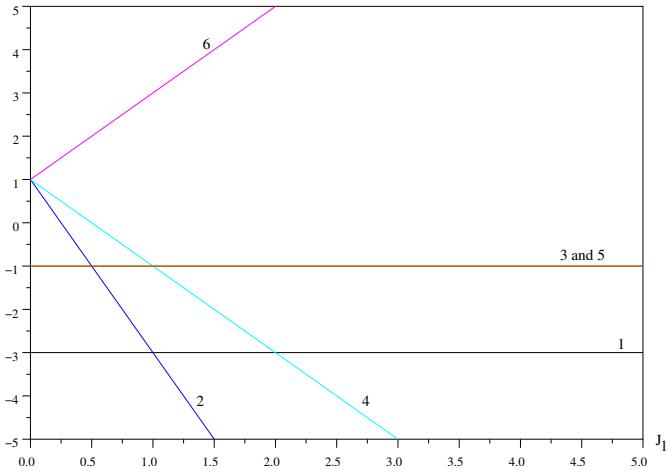

Figure 4.2: Evolution of the six eigenenergies of the Hamiltonian Eq. (4.12) with the strength parameter $J_l = J_c = \gamma_{tl} J_t$, $J_t = 1$. The numbers in the figure label the different states.

positive constant quantities. In the present case $H_0 = 0$ and the basis vectors are chosen as $|m_{1_1}, m_{1_2}, m_{2_1}, m_{2_2}\rangle$ where $m_{i_j} = +(1/2)$ or $-(1/2)$ is the projection of the spin 1/2 on the quantization axis at site i on the leg j. The subspace corresponding to $M_{tot} = 0$ where M_{tot} is the sum of the spin projections contains 6 states. The diagonalization for fixed J_t shows that eigenstates cross each other at specific values of γ_{tl} as shown in Fig.(4.2).

As an illustration of the fixed point property discussed above we consider the crossing point between the state labeled 2 and the degenerate states labeled 3 and 5 in Fig.(4.2). This is an exceptional point. The numerical results shown in Table 4.1 confirm that it is also a fixed point of the renormalization procedure induced by space truncation. As expected indeed J_t does not change when the size of Hilbert space is reduced from the initial dimension $n = N = 6$ to $n = 3$.

The three lowest eigenenenergies are conserved down to $n = 4$. For $n = 3$ the ground state and the second excited state energies are strongly affected. This is due to the fact that the fourth basis vector is strongly coupled to the first one, both being large components of the ground state wavefunction.

Now we extend the number of sites to $L = 6$ as an application which concerns a more

N	n	J_t	λ_1	λ_2	λ_3
6	6	20	-30	-10	-10
	5	20	-30	-10	-10
	4	20	-30	-10	-10
	3	20	-24.14	-10	4.14

Table 4.1: Behaviour of the three lowest eigenenergies corresponding to the model described by the quantum spin Hamiltonian given by Eq. (4.12) for $\gamma_{tl} = \gamma_c = 0.5$ and $J_t = 20$.

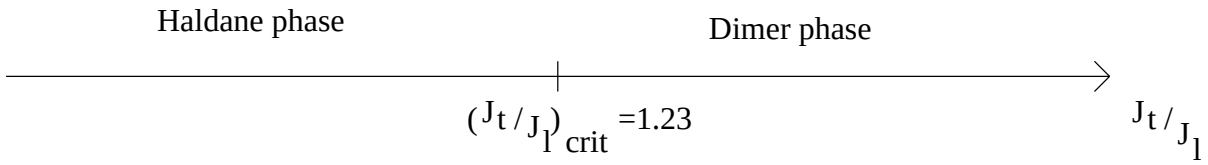

Figure 4.3: Phase diagram corresponding to the coupling parameters $J_t \neq J_l = J_c$. Here $L = 6$ sites, $(J_t/J_l)_{crit} \simeq 1.23$. For the phase diagram corresponding to $J_t \neq J_l \neq J_c$ see $FIG.$ 2 in reference [86].

realistic system described by the Hamiltonian $H^{(s,s)}$ given by Eq. (3.1) using an $SU(2)$-symmetry basis of states given below Eq. (3.2). Many studies of this type of systems have been done in different approaches to detect and localize a quantum phase transitions in the low energy spectrum, e.g. the first order transition from the rung dimer state [1] to the Haldane phase of the $S = 1$ chain[2] for $J_l = J_c$ (see Fig.(4.3)). Numerical methods like the Exact Diagonalization ($E.D.$) based on the computation of the ground and the first excited energy states in definite Hilbert spaces show in some cases critical values of coupling parameters corresponding to quantum phase transitions. These values depend on the size L of the system. One can mention two interesting analytical developments. The first one relies on the commutation relation between the components H_0 and H_1 of the Hamiltonian with one coupling parameter verifying $[H_0, H_1] = 0$. This corresponds to a Hamiltonian with two independent parts in which each of them describes a differ-

[1]The rung dimer state corresponds to $J_t > J_l, J_c$. In the *Dimer phase* the ground state is a singlet state in which the basis states are coupled to $\{S_i = 0, M_i = 0, i = 1, \ldots, L\}$ along the rungs, the ground state eigenvector is $|\Psi_g\rangle = |\Psi_{Dimer}\rangle = |S_1 M_1\rangle \bigotimes |S_2 M_2\rangle \ldots \bigotimes |S_i M_i\rangle \bigotimes \ldots \bigotimes |S_L M_L\rangle$.

[2]The isotropic $S = 1$ Heisenberg antiferromagnetic chain is an example of a system in the *Haldane phase*. In this phase, the ground and first excited state properties of the system are described by the Haldane's conjecture, see reference [61], page 22.

ent phase. A second interesting approach is the use of the spin wave theory to locate a first order quantum phase transition for specific values of J_i (see *Appendix D*). All these methods converge to the same values of critical coupling parameters. For instance a crossing between a rung dimer phase and a Haldane phase appears for $J_l = J_c$ when $(J_t/J_l)_{crit} \simeq 1.401$ in the case of an asymptotically large system [9, 28, 54, 55, 85]. The existence of a first order phase transition is analysed below to show how far our theory is able to localize it. The coupling constant $g = J_t$ is expected to stay constant at the level crossing point at which the transition takes place.

Several crossings between energy levels can be observed in Fig.(4.4-a) which shows the evolution of the energies of the four lowest states in the $M_{tot} = 0$ subspace as a function of $g = J_t$. The crossing between the ground state energy e_1 and the energy of the first excited state e_2 corresponds to $(J_t/J_l)_{crit} \simeq 1.23$ (see Fig.(4.3)).

The first test we performed corresponds to $J_t \geq 6$. Then the three lowest excited states corresponding to e_2, e_3, e_4 get rigorously degenerate which generates a continuous transition line [86]. Fixing $J_t = 10$ Fig.(4.4-b) shows the evolution of the four lowest states as a function of the size N of the Hilbert space following the algorithm described in *chapter* 3. The initial space dimension is $N = 924$. The stability of the spectrum is remarkable down to $N \leq 100$. This stability reflects in the constancy of J_t over the same dimensional range, see Fig.(4.4-c). For lower values of N deviations appear. They are due to inaccuracies inherent to the projection method as noted in the third remark of *subsection* 2.2.2. The limit of constancy of J_t indicates the minimum dimension of Hilbert space in which diagonalization will lead to the reproduction of the low energy part of the spectrum, i.e. the ground and first excited states. The behaviour of the spectrum shown here is observed for any value of $J_t \geq 6$, i. e. all along the degeneracy lines.

Fig.(4.4-d) shows the evolution of the entropy s per site defined in Eq. (3.7), at the fixed point $J_t = 5$ which corresponds in Fig.(4.4-a) to the crossing of the ground state e_1 with the first excited state e_2. Here $\{a_{1i}^{(N)}\}$ are the amplitudes of the components of

the ground state wavefunction developed on the basis of states $\{|\Phi_i>\}$ which span the space of dimension N. The step discontinuity signals the transition characterized by a strong change in the structure of the lowest state. The characteristic singularity observed at this value of J_t is conserved as long as the ground state keeps stable during the space reduction process.

At the exact location of the fixed point the instability of the spectrum is sizable and the coupling constant J_t at this crossing point stays constant over a smaller interval of values of N. A closer inspection shows that this instability might be related to a numerical difficulty in the renormalization of J_t. Indeed the coefficients of the algebraic second order equation which fixes Eq. (2.32) get accidentally vanishingly small at this place and consequently lead to strongly unprecise values of the roots of the equation. This corresponds to a pathological situation which may not be significative in the general case. Indeed, in the close neighbourhood of the fixed point, J_t stays stable over a much larger interval of values of N when $J_c = 3.8 \neq J_l$ (see Figs.(4.4-e) and (4.4-f)).

Fixed points in the SO(4)-symmetry framework

The reduction algorithm is next applied to the same system as above but described by the Hamiltonian $H^{(S,R)}$ given by Eq. (3.5) with a basis of states $\{|\Phi_i>\}$ written in the $SO(4)$ symmetry framework introduced in *subsection* 3.3.2. The spectrum given in Fig.(4.5-a) in the $M_{tot} = 0$ subspace is the same as in the case of the $SU(2)$ symmetry framework as it should be. However the behaviour of the numerically generated spectrum at different transition points behaves quite differently during the reduction procedure in Hilbert space.

At the crossing point between the ground state and the first excited state in the $M_{tot} = 0$ subspace which occurs at $J_t = 5$ (see Fig.(4.5-a)) the ground state energy e_1 and J_t remain stable all along the space dimension reduction procedure as seen in Fig.(4.5-b) and Fig.(4.5-c) and this can be shown by the evolution of the coefficients a, b and c related to g through the $DRHS$ in Eq. (4.11), see Figs.(4.7). It is however lost for the first excited state with energy e_2 which moves abruptly and stays then again constant

generating successive plateaus over more or less large intervals in N, Fig.(4.5-b). This shows that $d\lambda_i/dx = 0$, $(i = 2, 3, 4)$ is indeed preserved by steps, but not necessarily λ_i which jumps by steps over finite intervals of space dimensions. The jumps in $\{\lambda_i\}$ may be related to the elimination of non negligible components of the wavefunction during the reduction process, to the behaviour of the reduction procedure which uses a projected wave function, and to the difficulty to follow the accurate value of the point of degeneracy which is determined within an accuracy interval of 10^{-5}.

Fig.(4.5-d) shows the behaviour of the ground state entropy per site s which behaves like in the $SU(2)$ scheme but is quantitatively smaller. This is due to the fact that the wavefunction amplitudes are less equally distributed here than in the $SU(2)$-scheme as mentioned above. Fig.(4.5-e) and Fig.(4.5-f) show the behaviour of the spectrum and coupling constant J_t in the close neighbourhood of the transition point. One observes that the evolution of the energies is smoother than at the transition point itself and the coupling constant increases slightly with decreasing N. Some curves in the figures are drawn with a finite width in order to facilitate the observation of the stepwise evolution of the corresponding quantities. The degeneracy of the states $(e_2 = e_3 = e_4)$ and the consequent constancy for $J_t \geq 6$ is observed. It corresponds to a transition line. As seen in Fig.(4.6-a) and Fig.(4.6-b), the constancy of these quantities during the reduction procedure is preserved over the whole range of space dimensions N, except for $\{e_i\}$s at small N. But the $\{e_i\}$s stay more and more constant up to the smallest values of N with increasing J_t, see Fig.(4.6-c) and Fig.(4.6-d). This can be explained by the fact that the wavefunctions gets more and more dominated by a small number of basis states with increasing J_t. Evidently the robustness of the spectrum is stronger in the present symmetry scheme than in the case of $SU(2)$.

4.4.3 Application of the reduction algorithm at avoided crossings

As already mentioned continuous transitions reduce to avoided crossings in finite systems. States get degenerate at complex values of this parameter. Generally, genuine transitions cannot be explicitly seen in numerically determined spectra of finite systems when the parameter get complex.

Fig.(4.8-a) shows the spectrum of the ladder for specific values of the coupling constants. One observes several possible avoided crossings which are rather close to each other in the interval $4 < J_t < 9$. The typical behaviour of the spectrum is shown in Fig.(4.6-b) for $J_t = 6.6891$. Fig.(4.6-c) gives a quantitative estimate of the energy fluctuations of excited states (see Eq. (3.6)).

The spectrum and J_t are relatively stable down to $N \simeq 200$. Stability is lost below this value. The same is true at other avoided crossing points. It may be that clearer signals can be observed for larger systems since then the gap at crossings gets smaller (it goes to zero for an infinite system) and hence leads to a reduced imaginary part of the coupling constant.

Remarks:

- In the present calculations the system has open boundary conditions. For L odd the entropy shows the same characteristic discontinuity as observed for first order transitions in Fig.(4.4-d) and (4.5-d) at the transition point. For L even the discontinuity goes over to a finite peak which reminds an avoided crossing in a finite size system and a sign for a continuous transition. Therefore, we did not choose to study the system for J_t in the neighbourhood of 5 because the graph of the ground and first excited states cross each other or not depending on the parity of L contrary to $J_t = 6.891$ in which the second and third excited states do not show this effect. This shows that a naive interpretation of observables in finite systems can lead to

erroneous interpretations of the order of a transition.

- A necessary condition to get a relevant analysis for a finite system is that the correlation length should be smaller than the size of the system. This puts limits on the possibility to select transitions in small systems.

- Expected crossings may not necessarily be sufficient to signalize the order of transitions in the limit of infinite systems. In this limit the order may effectively be different. This phenomenon has also been observed in classical systems see f.i. [68] and references therein.

4.5 Conclusion

We used an algorithm which aims to reduce the size of the Hilbert space of states describing strongly interacting systems. The reduction induces a renormalization of coupling constants which enter the Hamiltonians of the systems, here frustrated two-leg quantum spin ladders.

We applied the algorithm at the location and in the neighbourhood of level crossing points and lines, and in the vicinity of avoided crossings which can correspond to transitions in infinite systems [79]. The analysis has been pursued in two different symmetry-schemes. As it may be expected the behaviour of the spectrum and the renormalized coupling parameter depend on the symmetry framework. Indeed, the description of the system depends crucially on the details of the wavefunctions of the different energy states and their structure is different in different representations.

In the case of level crossings we showed that the renormalized coupling constant J_t may indeed be numerically stable over a large set of dimensions of Hilbert space where great unstabilities appear in the low excited states of energy. These clues can be a signal of the presence of a transition as predicted by the theoretical considerations developed in *section* 4.3. As an example one may mention the case of the degeneracy corresponding to

a first order transition between the Haldane and the dimer phase. Strong instabilities in the renormalized coupling parameter may appear due to accidental numerical pathologies as mentioned in *section* 4.4.2.

Avoided crossings have also been investigated. The crossing points are difficult to locate. It may be due to the fact that the level crossing point occurs for a complex coupling constant which is not detected in the present algorithm. The precise understanding of these points related to numerics requires further work.

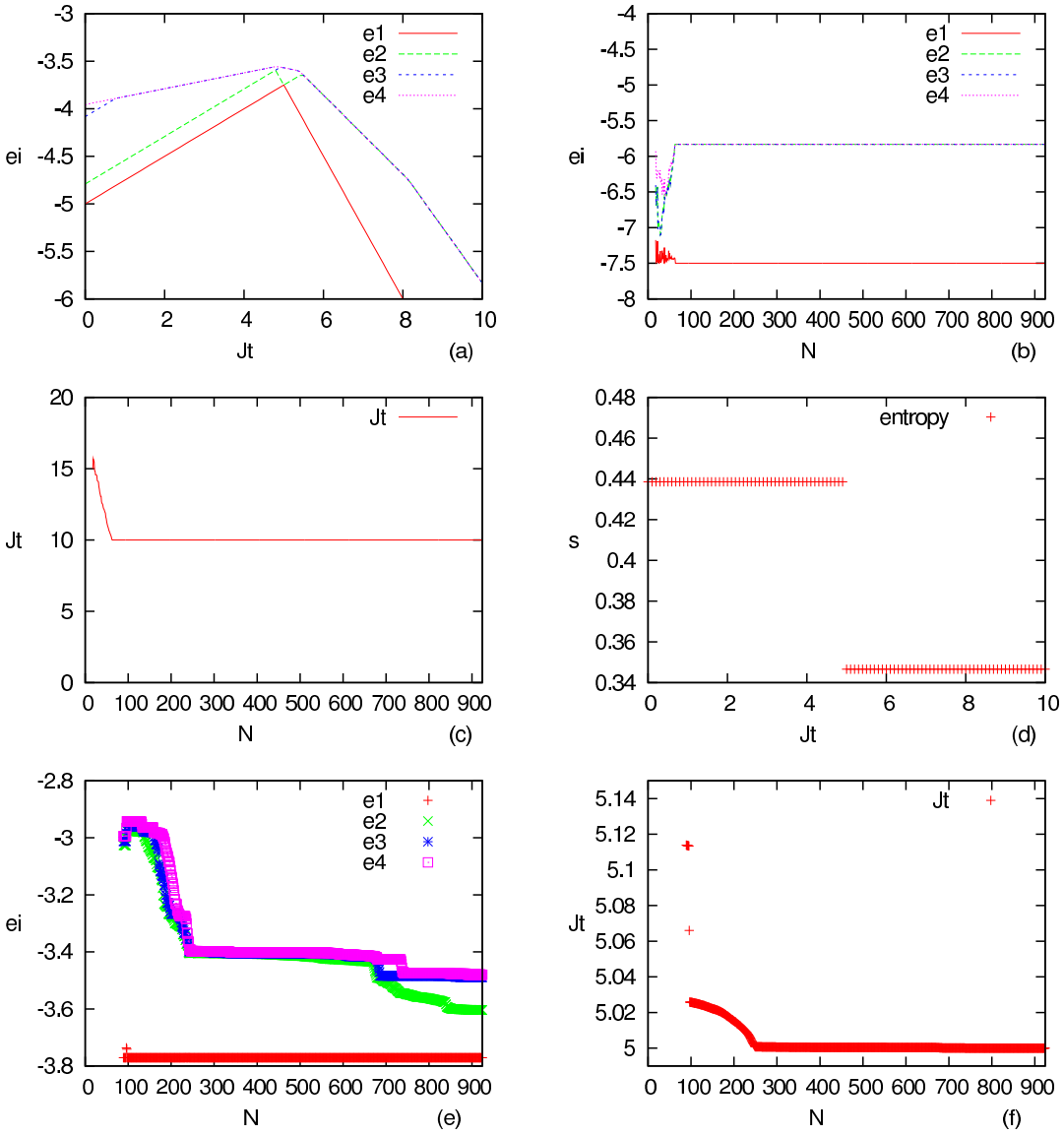

Figure 4.4: $SU(2)$-symmetry scheme. The $\{e_i, i = 1, 2, 3, 4\}$ are the energies per site of the ground and lowest excited states. N is the size of the Hilbert space, s the entropy of the ground state per site. The number of sites is $L = 6$ along a leg, $J_l = J_c \simeq 4.07$. (b) and (c) correspond to $J_t = 10$. Figs.(e) and (f) correspond to $J_c = 3.8 \neq J_l$ and $J_t = 5$. Broadened lines are drawn for the sake of readableness. See discussion in the text.

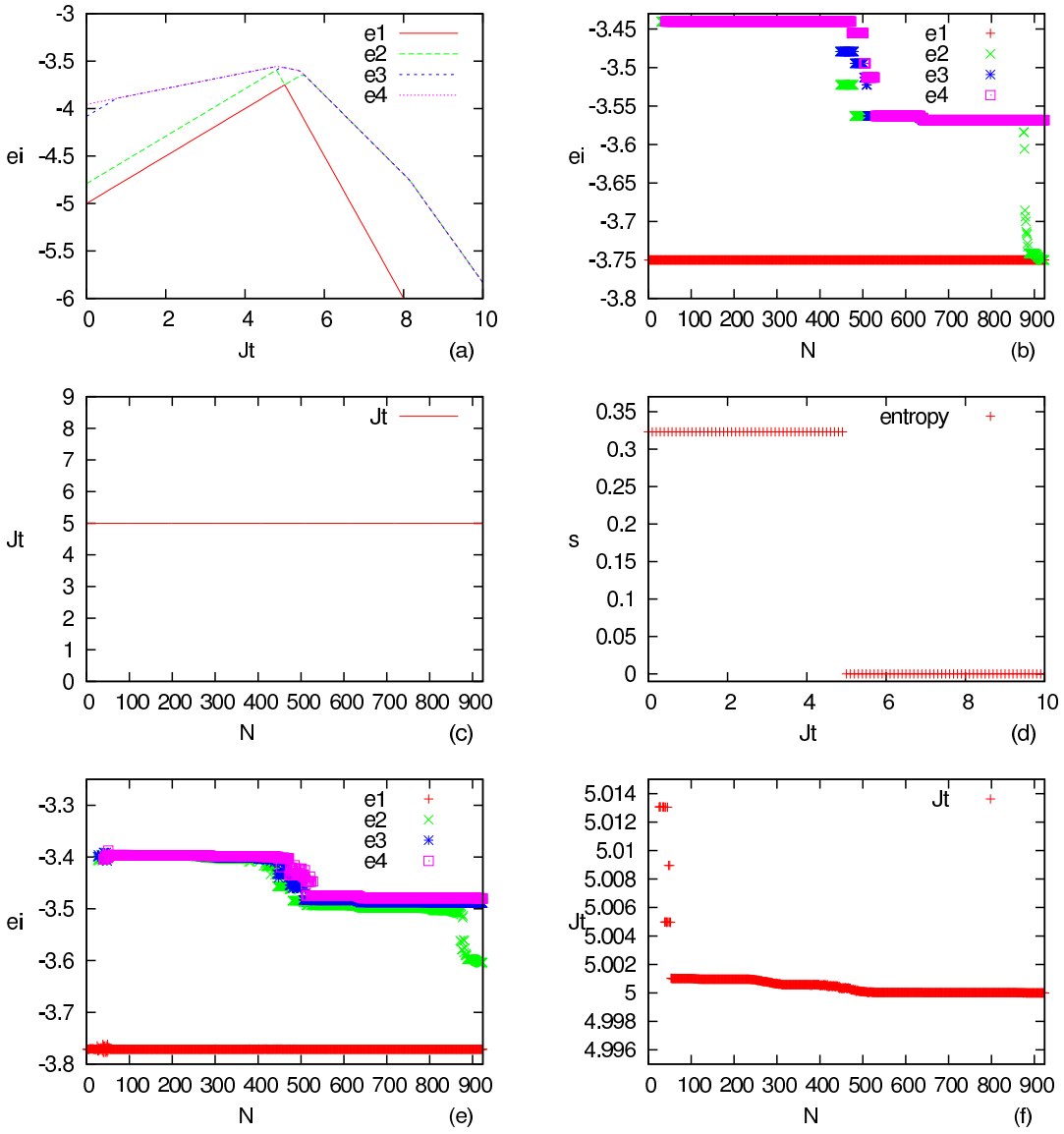

Figure 4.5: $SO(4)$-symmetry scheme. The $\{e_i, i = 1, 2, 3, 4\}$ are the energies per site of the ground and lowest excited states. N is the size of the Hilbert space, s the entropy of the ground state per site. The number of sites is $L = 6$ along the chain. (a) - (d): $J_l = J_c$. In (b) and (c) $J_t = 5$ (e) - (f): $J_t = 5$, $J_l \neq J_c$, $J_c = 3.8$. In both cases $J_t/J_l \simeq 1.23$. Broadened lines are drawn for the sake of readableness. See discussion in the text.

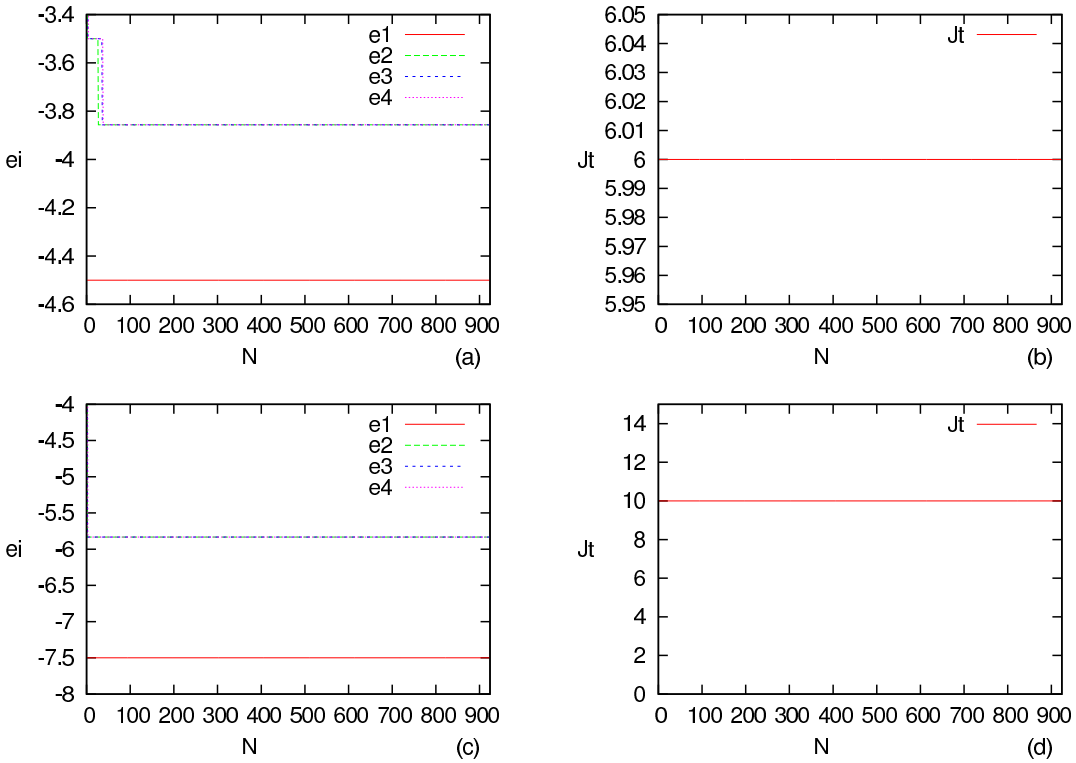

Figure 4.6: $SO(4)$-symmetry scheme. The $\{e_i, i = 1, 2, 3, 4\}$ are the energies of the ground and lowest excited states per site. The number of sites is $L = 6$ along the chain, $J_l = J_c \simeq 4.07$. (a) and (b) correspond to $J_t = 6$, (c) and (d) correspond to $J_t = 10$. See discussion in the text.

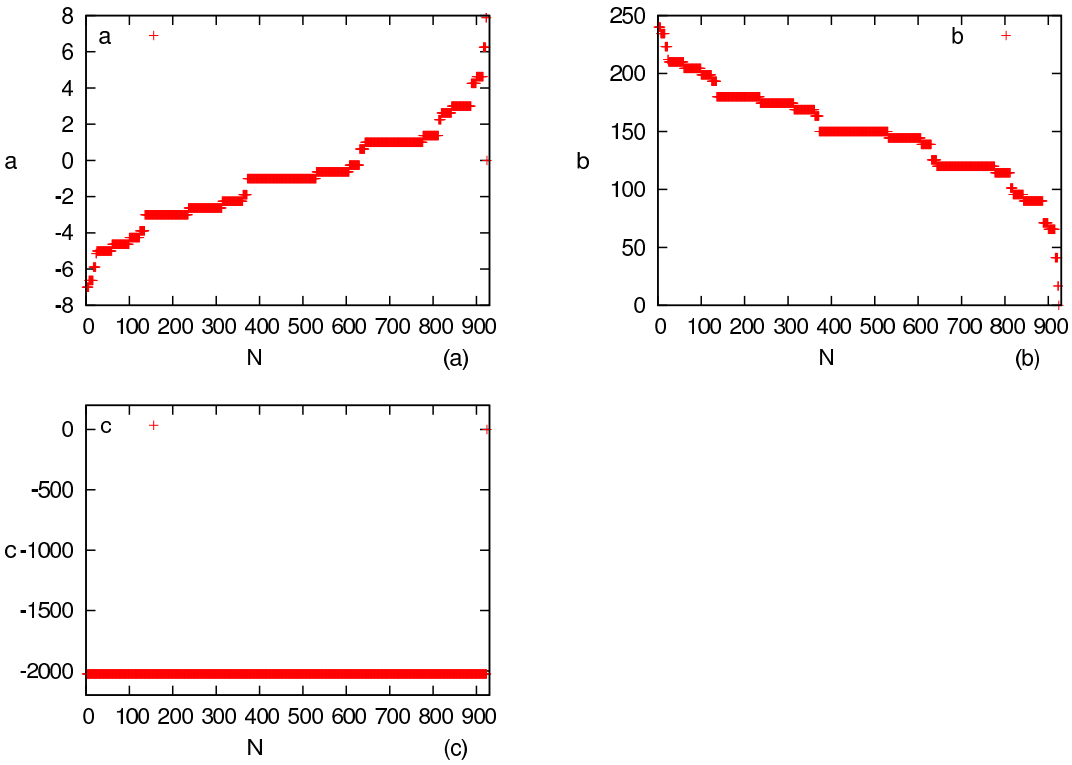

Figure 4.7: $SO(4)$-symmetry scheme. a, b and c are the coefficients related to g through the Eq. (4.11). N is the size of the Hilbert space. The number of sites is $L = 6$ sites, $J_t = 5$, $J_l = J_c \simeq 4.07$. See discussion in the text

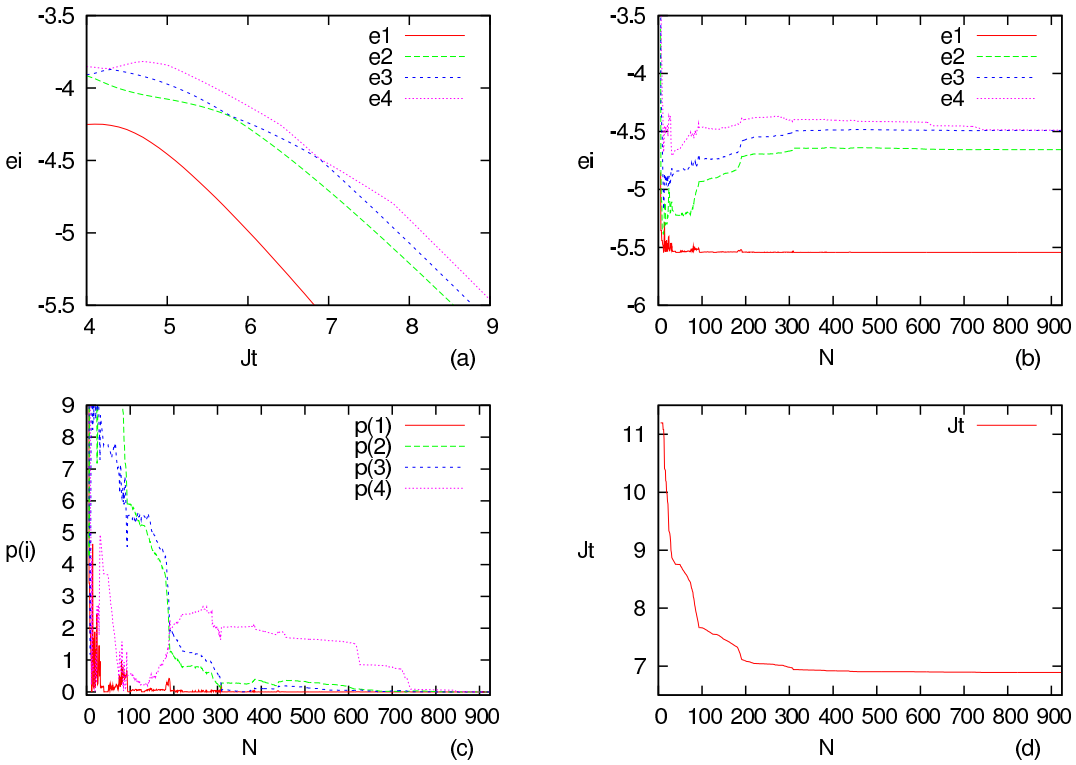

Figure 4.8: $SU(2)$-symmetry scheme. The $\{e_i, i = 1, 2, 3, 4\}$ are the energies per site of the ground and excited states. N is the size of the Hilbert space. The number of sites is $L = 6$ sites, $J_t = 6.891$, $J_l = 5, J_c = 3$. See discussion in the text

Chapter 5

Numerical implementation

Contents

5.1 Introduction

In this chapter, we present some details about the numerical work related to the implementation of algorithms of the reduction procedure in Hilbert space. The improvement of a numerical code is realized by taking into account two important factors, the memory requirements and the *CPU* (Central Processing Unit) time. We will mention the possibility to improve the code used in order to determine the energies of the ground and low excited states of strongly correlated systems at $T = 0$.

5.2 Numerical code

The algorithm starts with the generation and the storing of the elements of the Hamiltonian matrix $H^{(N)}$ computed in defined Hilbert space $\mathcal{H}^{(N)}$ in two vectors. One contains the diagonal elements arranged in increasing order and the second the off-diagonal ones. Then we introduce the Lanczos technique which fixes the ground state energy and wavefunction [1] (see *Appendix E*). The reduction procedure begins with the computation of the renormalized coupling parameter $g^{(N-1)}$ of Eq. (2.32). The code fixes the new effective Hamiltonian $H^{(N-1)}$ in the reduced space $\mathcal{H}^{(N-1)}$ by eliminating the last line and column of the matrix $H^{(N)}$. The procedure is repeated down to a reduced dimension N_{min} in Hilbert space in which the low energy spectrum becomes unstable.

Practically, we use the Lanczos technique to compute and follow the evolution of the low energy spectrum in reduced Hilbert space down to a very small dimension n to understand how far the renormalization can compensate the elimination of the states under the criterion of the arrangement of the diagonal elements in increasing order. This part is developed in *chapter 3*.

An implementation of the code in such a way can lead to a large consuming time

[1] The packages used to arrange the diagonal elements of the matrix and to diagonalize the Lanczos matrix are the numerical recipes(Fortran version) [70] and eigensystem subroutine package *EISPACK (http://www.netlib.org/eispack/)*

(CPU time) and require a large memory space. Therefore, we add propositions which can contribute in further works to improve this code to be more efficient numerically in future developments.

The CPU time can be reduced during the application of the reduction procedure in Hilbert space by using first the linear dimensional reduction procedure in Hilbert space ($LDRHS$) which leads to a linear discrete flow equation, hence is quicker than $DRHS$ procedure. In some cases, it can give results close to the ones obtained by the $DRHS$ procedure. Secondly, we can use the Lanczos technique which computes correctly the ground state properties without re-orthogonalization (see *Appendix E*).

There remains an open question about the appropriate number of basis states dimension N_{min} defined in section 2.3 in which the reduction process should stop to diagonalize the reduced matrix exactly and lead to eigenvalues close to ones in the complete Hilbert space. During the reduction of Hilbert space one can use the properties of the ratio between relevant and irrelevant amplitudes of the ground state eigenvector, see Fig.(3.8) and the divergence of the slope of the renormalized coupling parameter $g^{(n)}$ to stop approximatively the reduction process.

During the test of the reduction procedure we use a large dimension m Lanczos matrix in order to compute the low eigenvalues and the ground state eigenvector (see *Appendix E*). This increases the number of Lanczos vectors which becomes a cumbersome problem to the memory. In principle, one needs just a small m to compute the energy and the eigenvector of the ground state.

Remarks

- We adapted the Lanczos technique to the code. During the reduction procedure of the Hamiltonian matrix the necessary dimension m to diagonalize the Lanczos matrix in the Krylov space [18, 50] can change (see remarks in *Appendix E*).

- One should mention that the reduction procedure for some coupling parameters can be efficient without sizable renormalization of the coupling parameter as it is the case where J_t large comparing to J_l close to J_c. But generally renormalization takes effect to maintain the low spectral energy. As a generic example see Fig.(5.1) as a comparison between the reduction procedure with and without renormalization in the $SU(2)$-symmetry scheme for specific values of the coupling constants, and $L = 9$ sites.

- The numerical tests in the SO(4)-symmetry scheme are limited in comparison to those carried out in the $SU(2)$-*scheme*. This is due to a numerical difficulty concerning the storage of the basis states in binary words which allows an automatic generalization of the code. Each effective site possesses a basic state $S_i = 1$ with three projections and $S_i = 0$ with one projection, hence four values are needed. In the $SU(2)$-symmetry scheme each site possesses a basic state $s_i = 1/2$ with two projections [53].

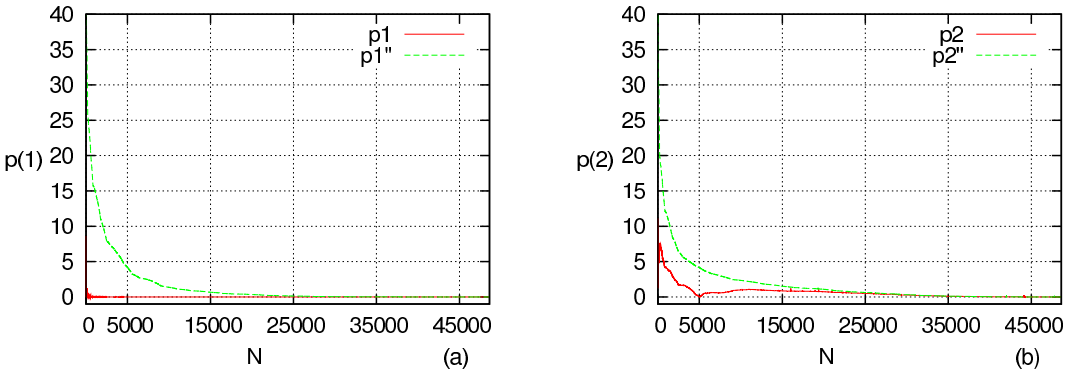

Figure 5.1: $SU(2)-$*symmetry scheme*. N is Hilbert space dimension. The $\{p(i), i = 1, 2\}$ are the accuracies of the ground and first excited states with renormalization see Eq. (3.6), and $\{p(i''), i = 1, 2\}$ are the accuracies of the ground and first excited states in the absence of renormalization. $L = 9$ sites along the chain. $J_t = 5.5$, $J_l = 5$, $J_c = 3$

Chapter 6

Conclusion and Outlook

Contents

6.1 Conclusion

In this work, we proposed an algorithm which generates a dimensional reduction procedure in Hilbert space with the purpose to study the low energy spectral properties of strongly interacting systems in reduced Hilbert space. We tested this method on two-leg frustrated antiferromagnetic quantum spin ladder systems for which perturbation approaches break down. We showed that the proposed algorithm allows for the determination of low energy spectral properties of such systems. We analysed the spectral energy properties for the system mentioned above in two symmetry-schemes, the $SU(2)$ and $SO(4)$ symmetries, for different coupling parameter values and we showed how far excited states can be faithfully reproduced in reduced space, down to a lower value N_{min} of Hilbert space where the reduction process should stop. At the dimension N_{min} the low eigenvalues keep quantitatively close to the ones in the whole space.

We noticed that in practice and generally speaking a meaningful truncation algorithm may not necessarily ground on the systematic elimination of those states whose diagonal matrix elements lie highest in energy. The physical low energy states are the states of interest. An importance sampling sorting out those states which have the strongest components on the physical low-lying states due to strong non-diagonal matrix elements should be kept in the final space of states. The symmetry and the way of arrangement of the matrix elements can help to improve the description of the physical low-lying state properties of a system in reduced Hilbert space. In this work, we chose to arrange the diagonal elements in increasing order and study how far the renormalization can maintain the low spectral energy for different domains of values of coupling parameters.

We showed that exceptional points which may appear in physical spectra are related to fixed points in Hilbert space which characterize the existence of phase transitions and correspond to values of coupling constants which keep constant during the reduction process.

We studied the effect of the reduction procedure in Hilbert space at level crossing points

in the spectrum of energy for real values and in the vicinity of avoided ones for complex values of the running coupling constant. Following the evolution of the coupling parameter and the low spectral of energy we noticed that at the level crossing points which corresponds to a degeneracy of state energies the coupling parameter stays constant down to a small dimension of Hilbert space. This remarkable stability can be explained by the fact that the ground state wavefunction is strongly dominated by a small number of states. The stability is larger in the case of an $SO(4)$-symmetry representation where the number of large components is reduced.

The present investigations show that first order transition points in quantum spin systems may be correlated with strong fluctuations in the energies of low-lying excited states. The presence of these points is predicted by theoretical considerations and signalized numerically in some specific cases by the constancy of the strength of the couplings which enter the Hamiltonian along the dimensional reduction procedure of Hilbert space. This is the case at least up to the point at which numerical stability gets lost. This may happen at different stages of the reduction procedure since it depends on the structure of the ground state wavefunction.

One should mention that the constancy of the strength of the coupling parameters during the reduction procedure is not always a sufficient numerical signal of the existence of a fixed point in Hilbert space. To clarify this point we comment the results concerning the cases of J_t greater than J_l and J_c. We may mention two cases, the first corresponds to J_t very large relatively to J_l and J_c and the second corresponds to J_t close to $J_l = J_c$. In both cases, the ground state of energy is dominated by dimer energies and for the same symmetry-scheme the structure of the ground state eigenvector is almost similar in the sense that the number of relevant-irrelevant amplitudes of the ground state eigenvector defined *in remarks in section* 3.6.2 is the same. In both cases we observe a strong stability in the coupling parameter and in the ground state energy. This is related to the mechanism of the reduction method. Indeed the ground state energy stability criterion and the property of the $g.s.$ at a fixed point may in some cases rely on the same fact

which is the constancy of the coupling strength parameter. Therefore, one should be careful about conclusions (indications) related to the degree of stability of the coupling parameter and the first excited of energy in the reduced Hilbert space. Another indication concerning this point can be given by the behaviour of the ground state entropy which may jump at the fixed point and may signal a level crossing.

Finally, one should investigate different domains of values of coupling parameters in the case where the conclusions cannot be drawn safely. This is so in the cases explained above in which one of them reflects the dimer structure of the ground state and the other which corresponds to a first order transition between the dimer and Haldane phase. Generally, it is difficult to know from the reduction procedure based on the knowledge of the ground state properties for which states one observes level crossings. This is the case f.i. for the transition line discussed in *chapter* 4. In spite of the difficulty to locate fixed points precisely the reduction procedure in some cases is able to show their existence and provides a signal for their relation with quantum phase transitions induced at exceptional points (EPs).

6.2 Outlook

Further points are worthwhile to be investigated:

- In the present approach the sequential reduction of space dimensions followed an energy criterion. It might be judicious to classify the sequence of states to be eliminated starting with those which have the smallest amplitude in the ground state wavefunction. The two procedures should however be correlated if not equivalent.

- It could be of interest to study the evolution of physical observables in reduced Hilbert states, f.i. the magnetization and correlation functions of quantum spin systems.

- We expect to extend the study to systems of higher space dimensions, f.i. $2d$ with magnetic field.
- The reduction concept can be extended to systems at finite temperature [71].

Appendix A

Counting the number of basis states in $SO(4)$ symmetry

In the present section, we give the expressions which fix the number of basis states for a fixed total projection M_{tot}. The states can be generated in different symmetry-schemes. Here we enumerate the number of states in the $SO(4)$ framework.

Let $\{\overrightarrow{s_i} = \overrightarrow{1/2}\}$ be the spins of the particles on sites i. Going from $SU(2) * SU(2)$ to $SO(4)$ by means of a local isomorphism [45], we replace $(\overrightarrow{s_{i1}}, \overrightarrow{s_{i2}})$ corresponding to dimers by $(\overrightarrow{S_i}, \overrightarrow{R_i})$ when the spin-operator $\overrightarrow{S_i} = \overrightarrow{1}$ generates the triplet states and the pseudospin-operator $\overrightarrow{R_i}$ the transition from a singlet to a triplet state.

We work out the arithmetic relations in the $SO(4)$ presentation which allow to get the number of states with a total projection of $M_{tot} = m$.

Consider the state

$$\underbrace{|\underbrace{1111111}_{l}000000000000>}_{L} = |\Phi_k\rangle,\ \{k = 1, \ldots, N\}$$

where the quantum number 1 corresponds to the triplet state $\{S_i = 1; i = 1, \ldots, l\}$ with the projection $\{M_i = +1, 0, -1\}$ and the quantum number 0 corresponds to the sin-

glet state $\{S_i = 0; i = 1, \ldots, (L-l)\}$ with the projection $\{M_i = 0\}$.

L : total number of sites corresponding to $SO(4)$ group.

l : number of sites of $S_i = 1$ with $m_i = +1, 0, -1$.

The number of states involved in the subspaces with fixed (m, L) is given by the following combinatorial expressions.

A.1 Even total projection m

.

Even number of sites L

l even

For $\{m = 0, 2, \ldots, L\}, L_{min} = 0$

$$\sum_{p=0}^{[\frac{L-m}{2}]} \sum_{q=0}^{p} \begin{pmatrix} L \\ p-q \end{pmatrix} \begin{pmatrix} L-(p-q) \\ (p-q)+m \end{pmatrix} \begin{pmatrix} L-(2p-2q)-m \\ 2q \end{pmatrix}$$

l odd

For $\{m = 0, 2, \ldots, L-2\}, L_{min} = 2$.

$$\sum_{p=0}^{[\frac{L-(2+m)}{2}]} \sum_{q=0}^{p} \begin{pmatrix} L \\ p-q \end{pmatrix} \begin{pmatrix} L-(p-q) \\ (p-q)+m \end{pmatrix} \begin{pmatrix} L-(2p-2q)-m \\ 2q+1 \end{pmatrix}$$

Odd number of sites L

l even

For $\{m = 0, 2, \ldots, L-1\}$, $L_{min} = 1$.

$$\sum_{p=0}^{[\frac{L-(1+m)}{2}]} \sum_{q=0}^{p} \begin{pmatrix} L \\ p-q \end{pmatrix} \begin{pmatrix} L-(p-q) \\ (p-q)+m \end{pmatrix} \begin{pmatrix} L-(2p-2q)-m \\ 2q \end{pmatrix}$$

l odd

For $\{m = 0, 2, \ldots, L-1\}$, $L_{min} = 1$.

$$\sum_{p=0}^{[\frac{L-(1+m)}{2}]} \sum_{q=0}^{p} \begin{pmatrix} L \\ p-q \end{pmatrix} \begin{pmatrix} L-(p-q) \\ (p-q)+m \end{pmatrix} \begin{pmatrix} L-(2p-2q)-m \\ 2q+1 \end{pmatrix}$$

A.2 Odd total projection m

.

Even number of sites L

l even

For $\{m = 1, 3, \ldots, L-1\}$, $L_{min} = 2$.

$$\sum_{p=0}^{[\frac{L-(1+m)}{2}]} \sum_{q=0}^{p} \begin{pmatrix} L \\ p-q \end{pmatrix} \begin{pmatrix} L-(p-q) \\ (p-q)+m \end{pmatrix} \begin{pmatrix} L-(2p-2q)-m \\ 2q+1 \end{pmatrix}$$

l odd

For $\{m = 1, 3, \ldots, L-1\}, L_{min} = 2$.

$$\sum_{p=0}^{[\frac{L-(1+m)}{2}]} \sum_{q=0}^{p} \begin{pmatrix} L \\ p-q \end{pmatrix} \begin{pmatrix} L-(p-q) \\ (p-q)+m \end{pmatrix} \begin{pmatrix} L-(2p-2q)-m \\ 2q \end{pmatrix}$$

Odd number of sites L

l even

For $m \in (1, 3, \ldots, L-1), L_{min} = 3$

$$\sum_{p=0}^{[\frac{L-(2+m)}{2}]} \sum_{q=0}^{p} \begin{pmatrix} L \\ p-q \end{pmatrix} \begin{pmatrix} L-(p-q) \\ (p-q)+m \end{pmatrix} \begin{pmatrix} L-(2p-2q)-m \\ 2q+1 \end{pmatrix}$$

l odd

For $\{m = 1, 3, \ldots, L-1\}, L_{min} = 1$.

$$\sum_{p=0}^{[\frac{L-m)}{2}]} \sum_{q=0}^{p} \begin{pmatrix} L \\ p-q \end{pmatrix} \begin{pmatrix} L-(p-q) \\ (p-q)+m \end{pmatrix} \begin{pmatrix} L-(2p-2q)-m \\ 2q \end{pmatrix}$$

l is related implicitly to the relations developed above through p and q.

For fixed L one gets the number of basis states for a fixed total projection $M_{tot} = m$ by summing the relations of l even and odd.

Appendix B

Effective Hamiltonian

The explicit form of H_{eff} of Eq. (2.16) can be obtained by using the properties of the projection operators P and Q.

We define the Hamiltonian H in Hilbert space of dimension $dim\mathcal{H}^{(\mathcal{N})} = N$

$$H^{(N)} = H_0 + V^{(N)} \tag{B.1}$$

with

$$V^{(N)} = \sum_{i=1}^{p} g_i^{(N)} H_i \tag{B.2}$$

p, $g_i^{(N)}$ and H_i are defined in *chapter* 2.

Define $PHQ = H_{PQ}$, $QHP = H_{QP}$, $PHP = H_{PP}$, $QHQ = H_{QQ}$ and then multiplies the Schroedinger equation, Eq. (2.3), by P and Q

$$(H_{PP} + H_{PQ})|\Psi_i\rangle = \lambda_i P|\Psi_i\rangle \tag{B.3}$$

and

$$(H_{QP} + H_{QQ})|\Psi_i\rangle = \lambda_i Q|\Psi_i\rangle \tag{B.4}$$

Developing Eq. (B.4) and using the property $Q^2 = Q$ one gets

$$Q(\lambda_i - H_{QQ})|\Psi_i\rangle = H_{QP}|\Psi_i\rangle \tag{B.5}$$

This implies that formally

$$Q = \frac{1}{\lambda_i - H_{QQ}} H_{QP} \tag{B.6}$$

Introducing Q in Eq. (B.3) and using the property that $Q^2 = Q$ and $P^2 = P$. One gets

$$(H_{PP} + H_{PQ}\frac{1}{\lambda_i - H_{QQ}} H_{QP})P|\Psi_i\rangle = \lambda_i P|\Psi_i\rangle \tag{B.7}$$

The l.h.s. corresponds to the effective Hamiltonian

$$H_{eff}(\lambda_i) = H_{PP} + H_{PQ}\frac{1}{\lambda_i - H_{QQ}} H_{QP} \tag{B.8}$$

If we choose a model Hamiltonian in which H_0 commutes with P and Q

$$[P, H_0] = [Q, H_0] = 0 \tag{B.9}$$

then

$$PH_0Q = QH_0P = 0 \tag{B.10}$$

Using Eq. (B.10), one obtains

$$QHQ = QH_0Q + QVQ = H_{0(QQ)} + V_{QQ} \tag{B.11}$$

$$PHP = PH_0P + PVP = H_{0(PP)} + V_{PP} \tag{B.12}$$

$$PHQ = PVQ = V_{PQ} \tag{B.13}$$

$$QHP = QVP = V_{QP} \tag{B.14}$$

which leads to the expression

$$H_{eff}(\lambda_i) = H_{0(PP)} + V_{PP} + V_{PQ}\frac{1}{\lambda_i - H_{0(QQ)} - V_{QQ}}V_{QP} \tag{B.15}$$

where Eq. (B.15) is used as a common expression in many fields of physics and adapted to perturbation expansions in terms of V.

If one normalizes the eigenstate $P|\Psi_i\rangle$ to 1

$$|C|^2\langle\ P\Psi_i|P\Psi_i\rangle = 1 \tag{B.16}$$

$$\text{hence } |C|^2 = \frac{1}{\langle\ P\Psi_i|P\Psi_i\rangle} \tag{B.17}$$

This implies that, the correct eigenvalues come out as

$$\lambda_i = |C|^2\langle\ P\Psi_i|H_{eff}|P\Psi_i\rangle \tag{B.18}$$

Appendix C

Flow equation in Hilbert space

The flow equation of the renormalized strength parameter g of Eq. (2.41) in $DRHS$ can be obtained for large dimension N in Hilbert space by going over from discrete Hilbert space $(k, k-1)$ to the continuum one $(x, x-dx)$. So, Eq. (2.32)

$$a^{(N-1)}g^{(N-1)^2} + b^{(N-1)}g^{(N-1)} + c^{(N-1)} = 0 \tag{C.1}$$

becomes

$$a(x-dx)g(x-dx)^2 + b(x-dx)g(x-dx) + c(x-dx) = 0 \tag{C.2}$$

when in the continuum Hilbert space x

$$a(x)g(x)^2 + b(x)g(x) + c(x) = 0 \tag{C.3}$$

We use Taylor formula in the first order to develop

$$g(x-dx) = g(x) - dx\frac{dg}{dx} \tag{C.4}$$

$$a(x-dx) = a(x) - dx\frac{da}{dx} \tag{C.5}$$

$$b(x-dx) = b(x) - dx\frac{db}{dx} \tag{C.6}$$

$$c(x-dx) = c(x) - dx\frac{dc}{dx} \tag{C.7}$$

$$\tag{C.8}$$

One neglects the developments beyond the first order in Eq.(C.2) and uses Eq.(C.3). One obtains

$$\frac{dg}{dx} = -\frac{1}{2a(x)g(x)+b(x)}(\frac{dc}{dx} + \frac{db}{dx}g(x) + \frac{da}{dx}g(x)^2) \tag{C.9}$$

Following the same development mentioned above, one can obtain the flow equation of the renormalized strength parameter g of Eq. (2.47) in $LDRHS$.

Appendix D

Spin wave theory

D.1 Introduction

In this appendix we show how for antiferromagnetic quantum spin systems like quantum spin ladders it is possible to use the spin wave theory as a tool to estimate the ratio between the coupling parameter values corresponding to a first order quantum phase transition [54, 55].

In 1952 *P. W. Anderson* developed the semi-classical spin wave approach for antiferromagnetic quantum spin systems which assumes that its ground state is not very different from the classical ground state. This approach is based on the assumption that the spins $\overrightarrow{s}$ are large. The lattice of dimension D is divided into two sublattices. The first sublattice contains the spins on the positive axis direction, here the z axis, and the second one contains the spins on the opposite direction [2].

In general, spin wave theory is based on the $SU(N)$ broken symmetry, f.i. $SU(2)$ symmetry. The expectation value of the spin vector operator $\overrightarrow{s}$ it reduced to at least one nonzero component f.i. s_z. The excitations are described by fluctuations of the spins about their expectation values [3, 52, 57].

It is our aim to compute the coupling parameters of a quantum spin ladder Hamilto-

nian at the first order quantum phase transition between the dimer phase and the Haldane phase at $J_l = J_c$.

D.2 Spin wave theory and quantum phase transition

Writing Eq. (3.1) in terms of vector operators $\overrightarrow{\sigma}_i = \overrightarrow{s}_{i1} + \overrightarrow{s}_{i2}$ along a dimer, where $s_{i_1} = s_{i_2} = 1/2$ one gets [54]

$$H = -2LJ_t\frac{3}{4} + J_t\sum_{i=1}^{L}\sigma_i^2 + 2J_l\sum_{i=1}^{L-1}\overrightarrow{\sigma}_i\overrightarrow{\sigma}_{i+1} \tag{D.1}$$

Apart from a constant, H describes a spin chain with nearest-neighbour interaction $2J_l$.

According to the selection rules the quantum number $|\sigma|$ takes the values 0 or 1. And, $\overrightarrow{\sigma_i}[i1, i2] = 0$.

Where $[i1, i2] = \frac{1}{\sqrt{2}}(|1/2_{i_1}, -1/2_{i_2}\rangle - |-1/2_{i_1}, 1/2_{i_2}\rangle)$ is the spin-1/2 dimer basis state.

Using the last relation, one notices directly that the dimer state $|\Psi_D\rangle = \prod_{i=1}^{L}[i1, i2]$ is an eigenstate of the spin ladder. If $J_t \to \infty$, $|\sigma| = 0$ the ground state energy of dimers goes over to: $E_D = \langle\Psi_D|H|\Psi_D\rangle = -\frac{3}{2}LJ_t$.

Hence, consequently

$$\langle\Psi_D|\sum_{i=1}^{L}\sigma_i^2 + 2(\frac{J_l}{J_t})\sum_{i=1}^{L-1}\overrightarrow{\sigma}_i\overrightarrow{\sigma}_{i+1}|\Psi_D\rangle = 0 \tag{D.2}$$

According to (D.1), the increase of J_l relatively to J_t leads to the generation of inter-

acting spin-1 chains dominated by the third term J_l with a ground state $|\Psi_g\rangle$.

Antiferromagnetic spin-σ chain systems have been under intensive scrutiny for a long time and have been studied by means of many different approaches. We assume here that the semi-classical spin wave theory applies to antiferromagnetic systems

$$\sigma_{zi} \cong +|\sigma| \; and \; \sigma_{zj} \cong -|\sigma| \tag{D.3}$$

where $j = i + 1$.

Considering the last term of Eq. (D.1) which is a spin-σ chain and using the assumption (D.3) leads to the ground state energy of the antiferromagnetic ($D = 1$) system

$$E_g = \langle\Psi_g|2J_l \sum_{i=1}^{L-1} \overrightarrow{\sigma}_i \overrightarrow{\sigma}_{i+1}|\Psi_g\rangle \cong -D(2J_l)L\sigma(\sigma+1) + 2D(2J_l)\sigma\sum_{\lambda}(1-\gamma_\lambda^2)^{1/2} \tag{D.4}$$

where γ_λ is a factor related to the symmetry of the crystalline network [24, 38].

In the continuum limit, L large, and $D = 1$ one can write

$$\sum_{\lambda}(1-\gamma_\lambda^2)^{1/2} = \frac{L}{2}I_{(D=1)} = \frac{L}{(2)}\frac{1}{(2\pi)}\int_{-\pi}^{\pi}|sin(\lambda)|d\lambda = \frac{L}{\pi} \tag{D.5}$$

Using the property (D.5), the Hamiltonian of Eq. (D.4) becomes

$$E_g \cong -(2J_l)L\sigma(\sigma+1) + 2(2J_l)\sigma\frac{L}{\pi} \tag{D.6}$$

The spin wave approach developed by Anderson gives at least a good approximation of the ground state energy of $D = 1$ Heisenberg systems with nearest neighbour interaction.

According to (D.1) one notices that the system goes over from a spin dimer system to a spin chain with decreasing J_t. Near the transition point there appears a competition between the dimer phase related to the spin dimer and the Haldane phase related to the spin chain. If one assumes that (D.2) keeps correct at the phase transition, the ground state energy is essentially the energy of dimer system. Then

$$\langle \sum_{i=1}^{L} \sigma_i^2 \rangle + 2(\frac{J_l}{J_t})_{crit} \langle \sum_{i=1}^{L-1} \overrightarrow{\sigma}_i \overrightarrow{\sigma}_{i+1} \rangle = 0$$

where the brackets stand for the average values of the corresponding operators.

$$L\sigma(\sigma+1) - 2(\frac{J_l}{J_t})_{crit} L\sigma(\sigma+1) + 2 \times 2(\frac{J_l}{J_t})_{crit} \sigma \frac{L}{\pi} = 0 \tag{D.7}$$

By using this method one obtains $(J_t)_{crit}$:

$$(\frac{J_l}{J_t})_{crit} = \frac{\pi}{2} \frac{1}{\pi - \frac{2}{\sigma+1}} \tag{D.8}$$

$|\sigma| = 1$ for a spin-1 chain. One finds that the transition between the dimer phase and the Haldane phase gives $(J_t/J_l)_{crit} = 1.363$ within 3% accuracy. The approach is valid for systems with higher dimensions D.

Appendix E

Lanczos algorithm

E.1 Introduction

Diagonalization of matrices is a cumbersome numerical problem. It is related to memory requirements and CPU (Central Processing Unit) time which asks for methods like Jacobi transformations, Householder reductions and others (see [70], *chapter* 11). One practical method is the *Lanczos algorithm* which is well adapted to the computation of extremal eigenvalues of large sparse matrices, see [18, 37, 50, 92] and references therein. Therefore, it is a powerful numerical tool for which we use to study quantum spin systems [48].

E.2 Lanczos technique

The Lanczos algorithm starts from an initial (randomly chosen) vector $|V_1\rangle$ of dimension N. After an orthogonal transformation of a matrix H of dimension N it generates a tridiagonal matrix, the Lanczos matrix, in a reduced space, the Krylov space $\mathcal{K} = \mathcal{E}(|V_1\rangle\ , H|V_1\rangle\ , \ldots, H^m|V_1\rangle\ , m \in [2, \ldots, N])$. The Lanczos matrix allows to compute the low state energies and wavefunctions in this space.

We exhibit now the steps which lead to a tridiagonal matrix by means of the basic (single-vector) Lanczos recursion from a real symmetric matrix H. Let $\{|\Phi_k\rangle\ , k = 1, \ldots, N\}$ be the basis states in which the elements of the matrix are computed.

The recursion starts by generating a random normalized vector $|V_1\rangle = \sum_{k=1}^{N} c_{1k}|\Phi_k\rangle$ in order to construct the diagonal and off-diagonal elements α_m and β_m of the tridiagonal matrix and its orthonormal basis states $\{|V_i\rangle = \sum_{k=1}^{N} c_{ik}|\Phi_k\rangle \, , i = 2, \ldots, m\}$. Acting on $|V_1\rangle$ with H leads to:

$$H|V_1\rangle = \alpha_1|V_1\rangle + \beta_1|V_2\rangle \tag{E.1}$$

and, the recursion relation

$$H|V_m\rangle = \beta_{m-1}|V_{m-1}\rangle + \alpha_m|V_m\rangle + \beta_m|V_{m+1}\rangle \tag{E.2}$$

where $m = \{2, \ldots, N\}$, $\beta_N = 0$, and $\langle V_i|V_j\rangle = \delta_{ij}$, with $i, j \in \{1, \ldots, m\}$.

The computation of the coefficients α_m, β_m, and $|V_{m+1}\rangle$ can be done by following the four steps :

1− $\alpha_m = \langle V_m|H|V_m\rangle$

2− $Y_m = \beta_m|V_{m+1}\rangle = H|V_m\rangle - \beta_{m-1}|V_{m-1}\rangle - \alpha_m|V_m\rangle$

3− $\beta_m = (Y_m \times Y_m)^{1/2}$

4− $|V_{m+1}\rangle = Y_m/\beta_m$

The efficiency of the Lanczos matrix stems from its ability to compute the extremal eigenvalues in the Krylov space for m states which is small relatively to the total number of states N. In order to work out the eigenvectors, one should project the Lanczos vectors

$\{|V_i\rangle\}$ back on the initial basis states $\{|\Phi_k\rangle\ , k = 1, \ldots, N\}$. For instance, the ground state eigenvector can be written

$$\begin{aligned} |\Psi_1\rangle &= \sum_{i=1}^{m} d_{1i}|V_i\rangle \\ &= \sum_{i=1}^{m}\sum_{k=1}^{N} d_{1i}c_{ik}|\Phi_k\rangle \end{aligned} \tag{E.3}$$

The disadvantage of the Lanczos technique comes from the rounding error problem which affects the orthogonality $|V_i\rangle$. In principle, the $|V_i\rangle$ are orthonormalized vectors, but because of the problem of numerical accuracy they loose their orthogonality which leads to spurious eigenvalues. One of possibilities to resolve this problem is the use of the Gram-Schmidt orthogonalization method which consists of a re-orthogonalization of each vector with respect to the previous ones. This approach keeps the Lanczos technique stable but requires memory storage capacity.

Remarks

- One should notice that the Lanczos technique gives good ground states eigenvalue and eigenvector even without re-orthogonalization.

- In some cases β_m coefficients can be equal to zero for $m < N$ in the Lanczos matrix and this is related to the original matrix structure. In this case, one should generate only the $(\alpha_{\{i=1,\ldots,m\}},\beta_{\{i=1,\ldots,m\}})$ and stop for $\beta_{\{m<N\}} = 0$ in order to diagonalize correctly the Lanczos matrix equivalent to the original matrix .

Appendix F

Tight-binding model

F.1 Introduction

We aim to show here a further test of the efficiency of the procedure which was described in *chapter* 2 by means of two tight-binding model examples. These models are described by symmetric matrices with non-zero elements on the diagonal and the symetrically located subdiagonals. This type of Hamiltonians describe systems like those encountered in atomic physics, semi-conductor physics and other,... [37, 76]. One starts from a full space spanned by states $\{|\varphi_i\rangle, i = 1, \ldots, N\}$ where the dimension N is the real space dimension equivalent to the number of sites in the system. The space dimensions are reduced by fixing the eigenvalue of the ground state λ_1 as described in *section* 2.3. Different values of N are considered as shown in tables F.1 and F.2.

F.2 Numerical application

a) Model 1

As a first application we consider a real symmetric tight-binding model which is generic for the description of many strongly correlated systems. Following the notations introduced above the Hamiltonian $H = H_0 + gH_1$ is degenerate and such that $H_0 = 0$. It possesses diagonal elements $\langle\varphi_i|H_1|\varphi_i\rangle = \beta$ and non-diagonal ones $\langle\varphi_i|H_1|\varphi_{i+1}\rangle = \langle\varphi_i|H_1|\varphi_{i-1}\rangle = \gamma$

which generate a coupling between nearest-neighbour states. By essence, a reduction of Hilbert space by means of perturbation expansions would be inefficient in this context, in particular when β and γ get large. Starting with an initial Hilbert space dimension N we apply the renormalization procedure to g starting from an initial value $g^{(N)}$. The evolution of the lowest eigenvalues and the flow of g are shown in Table F.1 for $g = 20$ and different values of N.

N	n	g	λ_1	λ_2	λ_3	λ_4	λ_5
50	50	20	0.038	0.15	0.34	0.60	0.94
	20	3.73	0.04	0.165	0.37	0.65	0.99
	10	1.11	0.045	0.176	0.38	0.65	0.95
100	100	20	0.010	0.038	0.087	0.15	0.24
	50	5.3	0.010	0.04	0.09	0.16	0.25
	10	0.28	0.011	0.045	0.1	0.166	0.24
200	200	20	0.0024	0.01	0.022	0.04	0.06
	100	5.15	0.0025	0.01	0.022	0.04	0.06
	10	0.07	0.003	0.01	0.024	0.042	0.06

Table F.1: Evolution of the coupling constant and the 5 lowest eigenvalues of the tight-binding matrix described in the text. Here $\beta = 1$, $\gamma = 0.5$. N is the initial space dimension, λ_1 is the ground state energy, λ_2 to λ_5 the energies of the lowest excited states.

In order to quantify the quality of the spectrum we introduce the quantity

$$\Delta_i^{(N,n)} = |1 - \lambda_i^{(n)}/\lambda_i^{(N)}| \tag{F.1}$$

where n stands for the size of the truncated space and i for increasing eigenenergies starting from the ground state $i = 1$.

For $N = 100$ and $n = 20$: $\Delta_i^{(100,20)} = 0.097, 0.092, 0.082, 0.068, 0.051$, $i = 1$ to 5 respectively.

For $N = 100$ and $n = 10$: $\Delta_i^{(100,10)} = 0.19, 0.16, 0.12, 0.07, 0.01$, $i = 1$ to 5 respectively.

As expected the results show that the effect of the coupling strength between conserved and eliminated states during the reduction procedure gets the more sizable the smaller the reduced space. For fixed $n = N_{min}$ however, $\Delta_i^{(N,n)}$ keeps practically the same for any $N \geq 50$.

One observes also that the coupling parameter g decreases systematically and rather strongly with the dimensional decrease of space indicating that the coupling between the remaining states gets systematically weaker.

As expected further calculations show that the stability of the spectrum of low-lying states is the better the smaller the non-diagonal matrix elements.

b) Model 2

As a second application we consider a generalization of the preceding Hamiltonian which is generated by adding a coupling between next-nearest-neighbour states $\langle\varphi_i|H_1|\varphi_{i+2}\rangle = \langle\varphi_i|H_1|\varphi_{i-2}\rangle = \delta$. One expects that the further coupling to next-nearest states increases the correlation between states. The outcome of the diagonalization is shown in Table F.2 for different values of the initial space dimensions N. The stability of the lowest eigenvalues is preserved down to some minimal dimension n_{min} which depends on the value of N, n_{min}/N is the smaller the larger the choice of N.

Using $\Delta_i^{(N,n)}$ as in the previous example one finds the same general trends. For $N = 500$ down to $N = 50$ and fixed $n = 20$, $\Delta_1^{(N,n)} \sim 0.04$ and $\Delta_2^{(N,n)} \sim 0.09$.

In the cases $N = 200$ and $N = 500$ the eigenvalues $\lambda_3, \lambda_4, \lambda_5$ change and increase for $n \leq n_{min}$ with $70 < n_{min} < 100$. Due to the strong coupling of the degenerate eigenstates of $H_0 = 0$ the renormalization of g cannot counteract the effect induced by the elimination of states. The comparison of the behaviour of the eigenenergies in *model* 1 shows that this is the stronger the larger the number of non-diagonal matrix elements.

N	n	g	λ_1	λ_2	λ_3	λ_4	λ_5
50	50	20	-2.366	-2.360	-1.968	-1.942	-1.32
	30	21.8	-2.35	-2.30	-1.26	-1.08	0.53
	20	25.5	-2.27	-2.16	0.43	0.74	4.83
200	200	20	-2.491	-2.490	-2.464	-2.463	-2.42
	70	20.48	-2.49	-2.485	-2.27	-2.26	-1.91
	50	21.00	-2.485	-2.478	-2.067	-2.04	-1.38
	20	26.80	-2.39	-2.27	0.45	0.78	5.08
500	500	20	-2.50	-2.50	-2.49	-2.49	-2.49
	70	20.54	-2.495	-2.493	-2.28	-2.27	-1.92
	50	21.07	-2.49	-2.48	-2.07	-2.04	-1.38
	20	26.9	-2.39	-2.28	0.45	0.78	5.09

Table F.2: Evolution of the coupling constant and the 5 lowest eigenvalues of the generalised tight-binding matrix described in the text. Here $\beta = 1$, $\gamma = 0.5$, $\delta = 0.5$, N is the initial space dimension, n the dimension of the restricted spaces and g the running coupling constant.

As a consequence the truncation process should be stopped at n_{min} when quantitative effects are sizable. One may notice that n_{min} gets independent of N for some N_{min} as it is the case in *model* 1. The present numerical investigations concern systems in which the states $\{|\varphi_i\rangle,\ i = 1, \cdots, N\}$ are degenerate and strongly coupled to each other, either directly or indirectly. The strong coupling is also seen through the fact that the ground state energy does not completely stabilize when the initial dimension of the Hilbert space N increases from 50 to 500 as seen in Tables F.1 and F.2.

Finally one should notice that the spectra of these systems can be obtained analytically [76]. Here the two models are analysed by using Open Boundary Conditions (OBC). Periodic Boundary Conditions (PBC) can change their low spectral properties during the reduction procedure.

List of Figures

List of Tables

Bibliography

[1] P. W. Anderson. The Resonating Valence Bond State in La_2CuO_4 and Superconductivity. *Science*, 235:1196, 1987.

[2] P. W. Anderson. An Approximate Quantum Theory of the Antiferromagnetic Ground State. *Phys. Rev.*, 86(5):694, June 1, 1952.

[3] Assa Auerbach. *Interacting Electrons and Quantum Magnetism.* Springer-Verlag, 1994.

[4] Roi Baer and Martin Head-Gordon. Energy renormalization-group method for electronic structure of large systems. *Phys.Rev. B*, 58:15296, 1998.

[5] K. W. Becker, A. Huebsch, and T. Sommer. *Phys.Rev. B66*, page 235115, 2002.

[6] M. Bhattacharya and C. Raman. Detecting Level Crossings without Looking at the Spectrum. *Phys. Rev. Lett.*, 97:140405, october 2006.

[7] C. Bloch and J. Horowitz. *Nucl. Phys.*, 8:91, 1958.

[8] Arno Bohm. *Quantum mechanics Foundations and Applications.* Springer edition, 1993. Page 213.

[9] Indrani Bose. The physical basis of integrable spin models. Special Issue on integrable systems, Proceedings of the Indian National Science Academy, cond-mat/0208039.

[10] B. H. Brandow. Linked-cluster expansions for the nuclear many-body problem. *Rev. Mod. Phys.*, 39:771, 1967.

[11] D. C. Cabra and M. D. Grynberg. Magnetization plateaux in dimerized spin-ladder arrays. *Phys. Rev. B*, 62(1):337, 2000.

[12] Enrico Carlon and Ferenc Iglói. Density profiles, Casimir amplitudes, and critical exponents in the two-dimensional Potts model: A density-matrix renormalization study. *Phys. Rev. B*, 57:7877–7886, 1998.

[13] Pavel Cejnar, Stefan Heinze, and Jan Dobes. Thermodynamic analogy for quantum phase transitions at zero temperature. *Phys. Rev. C*, 71:011304, 2005. Rapid communications.

[14] Pavel Cejnar and Jan Jolie. Quantum phase transitions studied within the interacting boson model. *Phys. Rev. E*, 61(6):6237, 2000.

[15] Jose Cervero and Rodriguez Alberto. Absorption in atomic wires. *Physical Review A*, 70:052705, 2004.

[16] Claude Cohen-Tanoudji, Jacques Dupont-Roc, and Gilbert Grynberg. *Processus d'interactions entre photons et atomes*. 1988.

[17] R. J. Creswick, H. A. Farach, and C. P. Poole. *Introduction to renormalization group methods in physics*. John Wiley and Sons. ISBN 0-471-60013-X.

[18] Jane K. Cullum and Ralph A. Willoughby. *Lanczos Algorithms for Large Symmetric Eigenvalue Computations, Vol. I: Theory, Classics in Applied Mathematics*. siam, 1985.

[19] E. Dagotto and T. M. Rice. Surprises on the Way from One- to Two- Dimensional Quantum Magnets:The Ladder Materials. *Science*, 271:618–623, 1996.

[20] Elbio Dagotto. Experiments on ladders reveal a complex interplay between a spin-gapped normal state and superconductivity. *Rep. Prog. Phys.*, 62:1525–1571, February 1999.

[21] Thiago R. de Oliveira, Gustavo Rigolin, Marcos C. de Oliveira, and Eduardo Miranda. Multipartite entanglement signature of quantum phase transitions. *Phys. Rev. Lett.*, 97:170401, 2006.

[22] C. Dembowski and al. Experimental Observation of the Topological Structure of Exceptional Points. *Phys. Rev. Lett.*, 86(5):787, January 2001.

[23] Oleg Derzhko, Johannes Richter, Andreas Honecker, and Heinz-Jürgen Schmidt. Universal properties of highly frustrated quantum magnets in strong magnetic fields. arxiv:cond-mat/0612281.

[24] Hung T. Diep. *Physique de la Matière Condensée*. Dunod edition, 2003. Paris.

[25] J. Eisert. Computational Difficulty of Global Variations in the Density Matrix Renormalization Group. *Physical Review Letters*, 97:260501, 2006.

[26] H. Feshbach. Unified Theory of Nuclear Reactions. *Annals of Physics*, 5:357–390, 1958.

[27] H. Feshbach. *Nuclear Spectroscopy part B*, 1960. Academic Press.

[28] Martin P. Gelfand. Linked-tetrahedra spin chain: Exact ground state and excitations. *Phys. Rev. B*, 43:8644, 1991.

[29] D. W. Heiss and H. L. Harney. The chirality of exceptional points. *Eur. Phys. J. D*, 17:149–151, 2001.

[30] W. D. Heiss. Exceptional points of a Hamiltonian and Phase Transitions. *Z. Phys. A-Atomic Nuclei*, 329:133–138, 1988.

[31] W. D. Heiss. Phases of wave functions and level repulsion. *Eur. Phys. J. D*, 7:1–4, 1999.

[32] W. D. Heiss. Repulsion of resonance states and exceptional points. *Phys. Rev. E*, 61(1):929, 2000.

[33] W. D. Heiss. Exceptional points-their universal occurence and their physical significance. *Czechoslovak Journal of physics*, 54(10):1091, 2004.

[34] W. D. Heiss, M. Müller, and I. Rotter. Collectivity, phase transitions, and exceptional points in open quantum systems. *Phys. Rev. E*, 58(3):2894, 1998.

[35] W. D. Heiss and A. L. Sannino. Avoided level crossing and exceptional points. *J. Phys. A:Math. Gen.*, 23:1167–1178, 1990.

[36] W. D. Heiss and W. H. Steeb. Avoided level crossings and Riemann sheet structure. *J. Math. Phys.*, 32(11):3003, November 1991.

[37] M. Henkel. *Conformal invariance and critical phenomena*. Springer verlag edition, 1999.

[38] A. Herpin. *Théorie du Magnétisme*. Institut national des sciences et Techniques nucléaires, Saclay edition, 1968.

[39] B. K. Jennings. Projection operator formalisms and the nuclear shell model. *Europhys. Lett.*, 72:211–215, 2005.

[40] T. Kato. *Perturbation Theory for Linear Operators*. Springer, Verlag, Berlin, 1966.

[41] Tarek Khalil and Jean Richert. Application of a renormalization algorithm in Hilbert space to the study of many-body quantum systems. *quant-ph/0606056*.

[42] Tarek Khalil and Jean Richert. An application of renormalization in Hilbert space at phase transition points in strongly interacting systems. *quant-ph/0610262*.

[43] Tarek Khalil and Jean Richert. Renormalization and fixed points in Hilbert space. *J. Phys. A: Math. Gen.*, 37:4851–4860, April 2004.

[44] K. Kikoin, Y. Avishai, and M. N. Kiselev. Dynamical symmetries in nanophysics. arXiv:cond-mat/0407063.

[45] K. Kikoin, Y. Avishai, and M.N. Kiselev. Explicit and hidden symmetries in quantum dots and quantum ladders. Talk given at NATO conference MQO (Bled, Slovenia, 7-10 September 2003), arXiv:cond-mat/0309606.

[46] M. N. Kiselev, K. Kikoin, and L. W. Molenkamp. Resonance kondo tunneling through a double quantum dot at finite bias. *Phys.Rev.B*, (68):155323, 2003.

[47] J. K. Korbicz and M. Lewenstein. Group-theoretical approach to entanglement. *Phys.Rev. A*, 74:022318, 2006.

[48] N. Laflorencie and D. Poilblanc. Simulations of pure and doped low-dimensional spin-1/2 gapped systems. *Lect. Notes Phys.*, 645:227–252, 2004.

[49] L. D. Landau and E. M. Lifshitz. *Statistical Physics*. Pergamon, oxford edition, 1980.

[50] Patrick Lascaux and Raymond Théodor. *Analyse numérique matricielle appliquée à l'art de l'ingénieur 2*. Dunod, Paris edition, 2000.

[51] Ö. Legeza and J. Sólyom. Two-site entropy and quantum phase transitions in low-dimensional models. *Phys. Rev. Lett.*, 96:116401, 2006. cond-mat/0511081.

[52] C. Lhuillier. *Frustrated Quantum Magnets in 2d: from Néel phases to Spin Liquids*. PITP-Les Houches Summer School, Quantum Magnetism, June 6-23, 2006 [1]

[53] H. Q. Lin. Exact diagonalization of quantum-spin models. *Phys. Rev. B*, 42(10):6561, 1990.

[54] H. Q. Lin, J. L. shen, and H. Y. Shik. Exactly soluble quantum spin models on a double layers: The net spin model. *Phys. Rev. B*, 66:184402, 2002.

[55] Hai-Qing Lin and J. L. Shen. Exact Ground States and Excited States of Net Spin Models. *Journal of the Phys. Soc. of Japan*, 69(3):878–882, March 2000.

[56] G. Mahler and al. *Quantum Networks. Dynamics of Open Nanostructures*. Springer edition.

[57] Norberto Majlis. *The Quantum Theory of Magnetism*. World scientific edition, 2000.

[58] Jean-Paul Malrieu and Nathalie Guihéry. Real-space renormalization group with effective interactions. *Phys.Rev. B*, 63:085110, 2001.

[1] http://pitp.physics.ubc.ca/upcoming/leshouches/archives.html?

[59] A. L. Malvezzi. An introduction to numerical methods in low-dimensional quantum systems. *Braz. J. Phys.*, 33:55–72, 2003. cond-mat/0304375.

[60] D. Richard Mattuck. *A Guide to Feynman Diagrams in the Many-Body systems.* Dover.

[61] Hans-Jürgen Mikeska and Alexei K. Kolezhuk. One-dimensional magnetism. In *Lect. Notes Phys.*, volume 645, pages 1–83, 2004.

[62] Colin J. Morningstar and Weinstein Marvin. Contractor renormalization group technology and exact Hamiltonian real-space renormalization group transformations. *Phys. Rev. D*, 54(6):4131, september 1996.

[63] N. Nagaosa. *Quantum Field Theory in Strongly Correlated Electronic Systems.* Springer edition. page 73.

[64] J. Von Neumann and E. Wigner. *Physik. Zeitschr*, 30:465, 1929. English translation in : R.S. Knox and A. Gold, Symmetry in the solid state(W. A. Benjamin, New York, 1964).

[65] Michael A. Nielsen and Isaac L. Chaung. *Quantum Computation and Quantum Information.* Cambridge edition.

[66] Kiyomi Okamoto and Kiyohide Nomura. Fluid-dimer critical point in S=1/2 antiferromagnetic Heisenberg chain with next nearest neighbor interactions. *PHYSICS LETTERS A*, 169:433–437, 1992.

[67] J. Piekarewicz and J. R. Shepard. Plaquette basis for the study of Heisenberg ladders. *Pys. Rev. B*, 56(9):5366, september 1997.

[68] M. Pleimling and A. Hüller. *J. Stat. Phys.*, 104(5/6):971–989, 2001.

[69] Janos Polonyi. Renormalization group in quantum mechanics. *Annals of Physics*, 252:300–328, 1996. arxiv:hep-th/9409004.

[70] William H. Press, Brian P. Flannery, Saul A. Teukolsky, and William T. Vetterling. *Numerical Recipes*. Cambridge University Press edition. The Art of Scientific Computing (Fortran Version).

[71] Jean Richert. A Renormalization Approach to Effective Interactions in Hilbert Space. *quant-ph/0209119*.

[72] Jean Richert. A variational approach to the low energy properties of even-legged d-dimensional quantum spin systems. *cond-mat/0510343*.

[73] Lewis H. Ryder. *Quantum Field Theory*. Cambridge university Press edition, 2001.

[74] S. Sachdev. *Quantum Phase Transitions*. Cambridge University Press, 1999.

[75] S. Sachdev. Quantum criticality: Competing ground states in low dimensions. *Science*, 288:475, 21 April 2000. Review.

[76] Bernard Sapoval and Claudine Hermann. *Physique des semi-conducteurs*. ellipses edition.

[77] T. H. Schucan and H. A. Weidenmüller. Perturbation Theory for the Effective Interaction in Nuclei. *Ann. Phys. (N.Y.)*, 76:483, 1973.

[78] T. D. Schultz, D. C. Mattis, and E. H. Lieb. Two-Dimensional Ising Model as a Soluble Problem of Many Fermions. *Rev. Mod. Phys.*, 36:856 – 871, 1964.

[79] Ralf Schützhold and Gernot Schaller. Adiabatic quantum algorithm as quantum phase transitions: First versus second order. *Phys. Rev. A*, 74(060304(R)), 2006.

[80] Valentin V. Sokolov, B. Alex Brown, and Vladimir Zelevinsky. Invariant correlational entropy and complexity of quantum states. *Phys. Rev. E*, 58(1):56, 1998.

[81] D. R. Tilley and J. Tilley. *Superfluidity and Superconductivity*. Institut of Physics Publishing, third edition, 1990.

[82] T. Vekua, D.C. Cabra, A. Dobry, C. Gazza, and D. Poilblanc. Magnetization plateaux induced by a coupling to the lattice. *Phys. Rev. Lett.*, 96:117205, 2006. arxiv:cond-mat/0511368.

[83] G. Vidal. Entanglement renormalization. *arxiv:cond-mat/0512165*.

[84] Alexander Volya and Vladimir Zelevinsky. Invariant correlational entropy as a signature of quantum phase transitions in nuclei. *Phys.Lett. B*, 574:27–34, 2003. nucl-th/0307028.

[85] Xiaoqun Wang. Low-lying energy properties of a frustrated antiferromagnetic spin-$\frac{1}{2}$ ladder. *Mod. Phys. Lett.*, B14:327, 2000. cond-mat/9803290.

[86] Zheng Weihong, V. Kotov, and J. Oitmaa. Two-chain spin ladder with frustrating second-neighbor interactions. *Phys. Rev. B*, 57:11439, 1998.

[87] S. R. White and R. M. Noack. Real-space quantum renormalization groups. *Phys. Rev. Lett.*, 68:3487, 1992.

[88] Steven R. White. Density matrix formulation for quantum renormalization groups. *Phys. Rev. Lett.*, 69:2863, 1992.

[89] Steven R. White. Density-matrix algorithms for quantum renormalization groups. *Phys. Rev. B*, 48(14):10345, october 1993.

[90] Steven R. White and David A. Huse. Numerical renormalization-group study of low-lying eigenstates of the antiferromagnetic S=1 Heisenberg chain. *Phys. Rev. B*, 48(6):3844, 1993.

[91] Steven R. White and D. J. Scalapino. Hole and pair structures in the t-j model. *Phys. Rev. B*, 55:6504–6517, 1997.

[92] R. R. Whitehead et al. *Advances in Nuclear Physics*, volume 9. Baranger-Vogt.

[93] K. G. Wilson. The renormalization group: Critical phenomena and the Kondo problem. *Rev. Mod. Phys.*, 47:773, 1975.

[94] L. A. Wu, M. S. Sarandy, and Lindar D. A. Quantum phase transitions and bipartite entanglement. *Phys. Rev. Lett.*, 93:250404, 2004.

[95] Y. Xian. Rigorous results on a first-order phase transition in antiferromagnetic spin-1/2 coupled chains. *Phys. Rev. B*, 52(17):12485, 1 november 1995.

[96] E. A. Yuzbashyan, B. L. Altshuler, and B. S. Shastry. The origin of degeneracies and crossings in the 1d hubbard model. *J. Phys. A: Math. Gen.*, 35(34):7525–7547, 30 August 2002.

[97] Miloslav Znojil. Linear representation of energy-dependent hamiltonians. *Physics Letters A*, 326:70–76, 2004. arxiv:quant-ph/0403223.